Basics of CT and CBCT

Marc Kachelrieß
marc.kachelriess@dkfz.de

German Cancer Research Center (DKFZ)
Heidelberg, Germany
www.dkfz.de/ct

dkfz. DEUTSCHES KREBSFORSCHUNGSZENTRUM IN DER HELMHOLTZ-GEMEINSCHAFT

Detector Technology

Clinical CT Detector Module

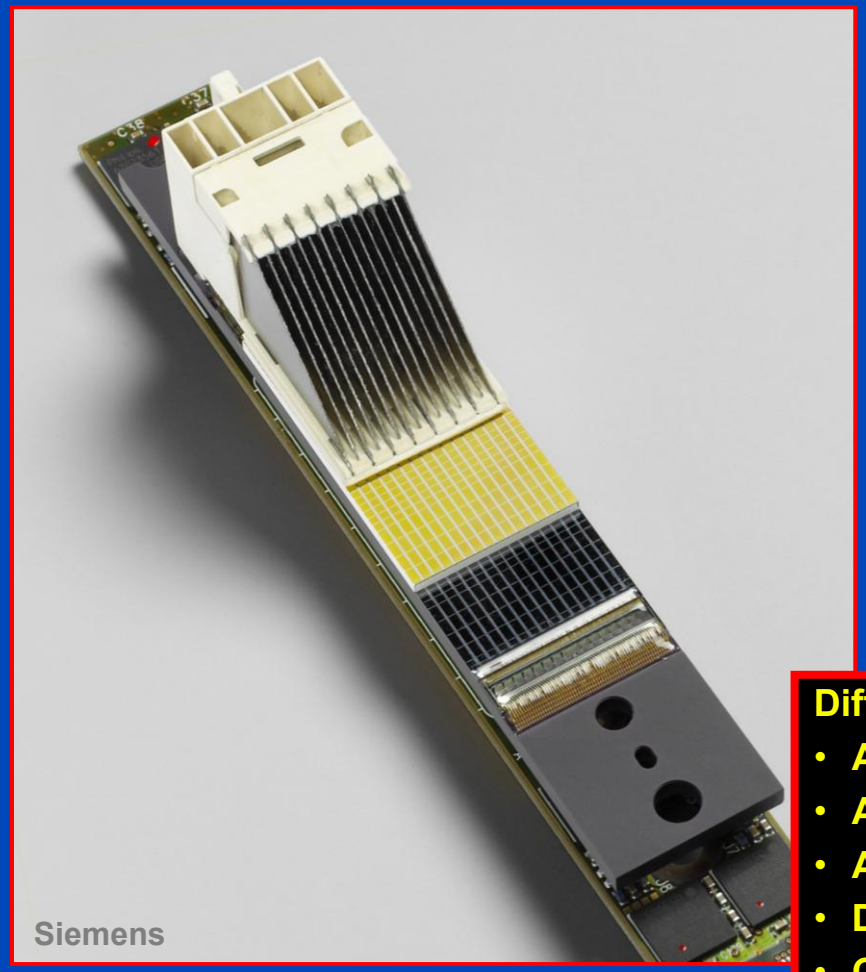

Siemens

Flat Detector (e.g. 40 × 30 cm)

Varex

Differences in:

- Absorption efficiency
- Afterglow
- Anti scatter grid
- Dynamic range
- Cross-talk
- Framerate
- …

dkfz.

Canon Aquilion ONE Genesis

GE Revolution Apex

Philips Spectral CT 7500

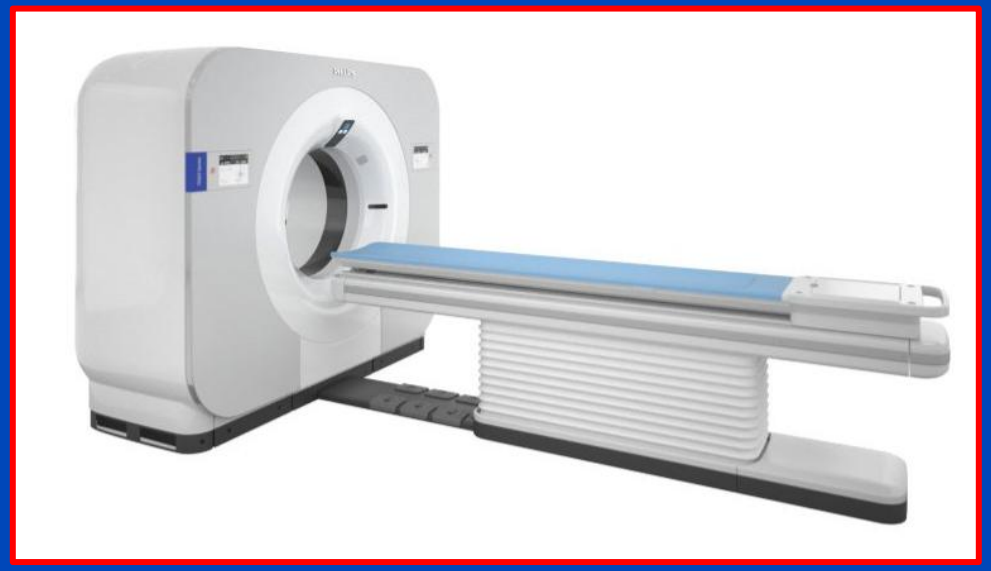

Siemens Naeotom Alpha

What does CT Measure?

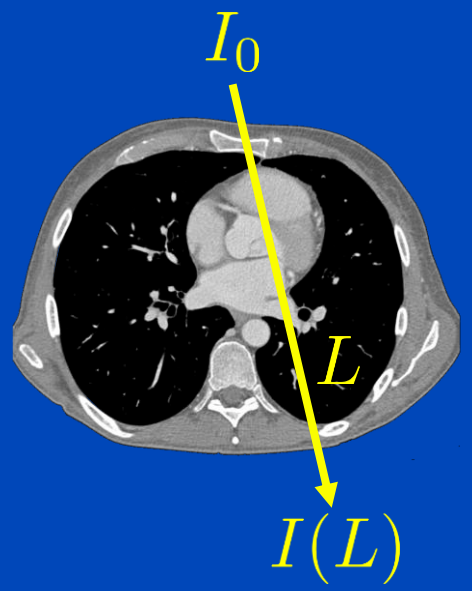

- X-rays are generated in an x-ray tube.
- The polychromatic radiation is attenuated in the patient. X-ray photon attenuation is dominated by the photo and the Compton effect.
- Detectors measure the x-ray intensity after the rays have passed through the patient along several lines *L*.
- The log intensity is the so-called x-ray transform:

$$q(L) = -\ln \frac{I(L)}{I_0} = -\ln \int dE\, w(E) e^{-\int dL \mu(\boldsymbol{r}, E)}$$

- Often, the follwing monochromatic approximation is used:

$$q(L) \approx p(L) = \int dL \mu(\boldsymbol{r}, E_{\text{eff}})$$

Energy-Dependence of X-Ray Spectra and Attenuation Coefficients

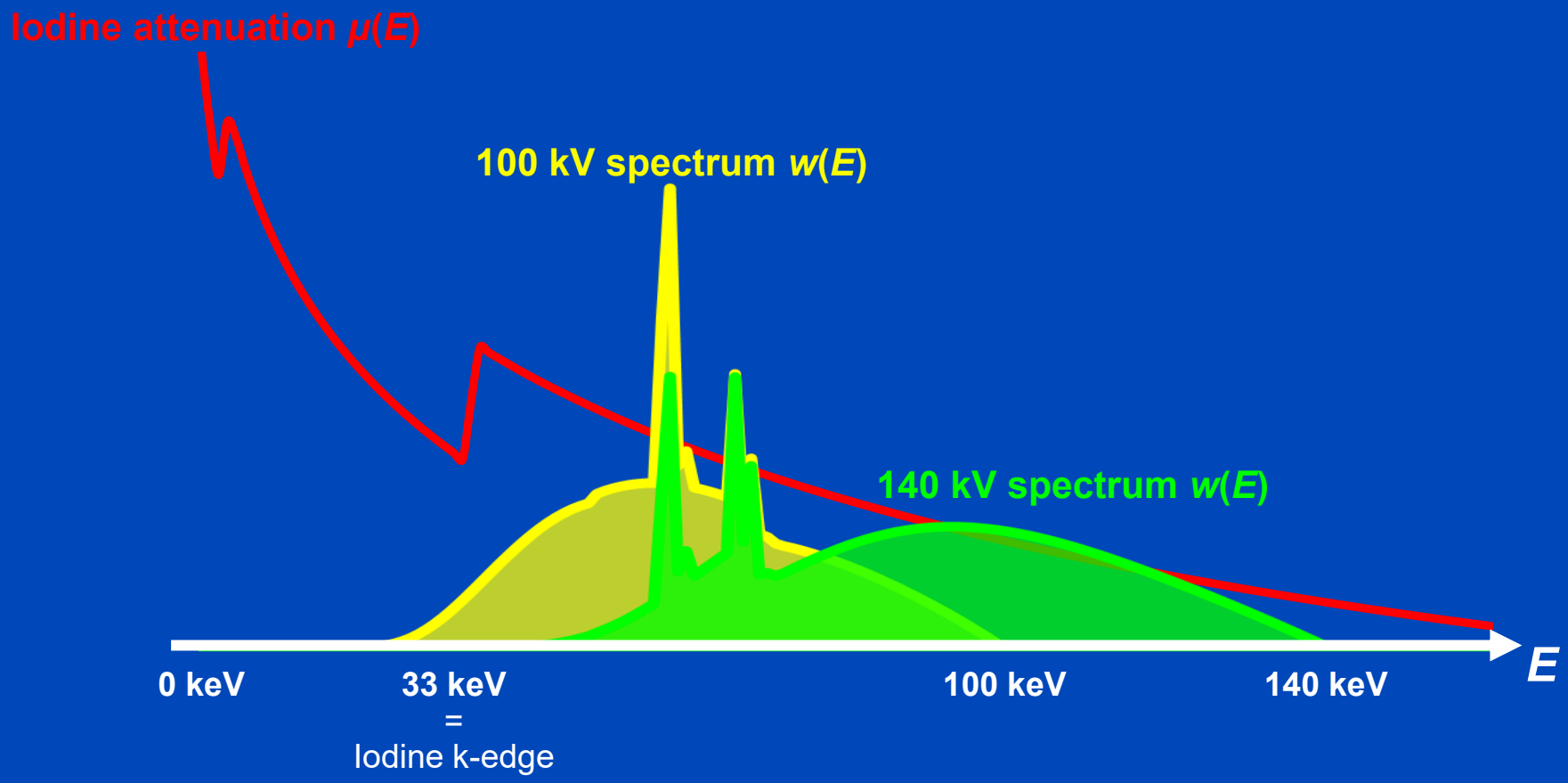

$w_{100\,\mathrm{kV}}(E)$

$w_{140\,\mathrm{kV}}(E)$

$\mu_{\mathrm{Iodine}}(E)$

100 kV and 140 kV EI spectra as seen after having passed 32 cm of water.

dkfz.

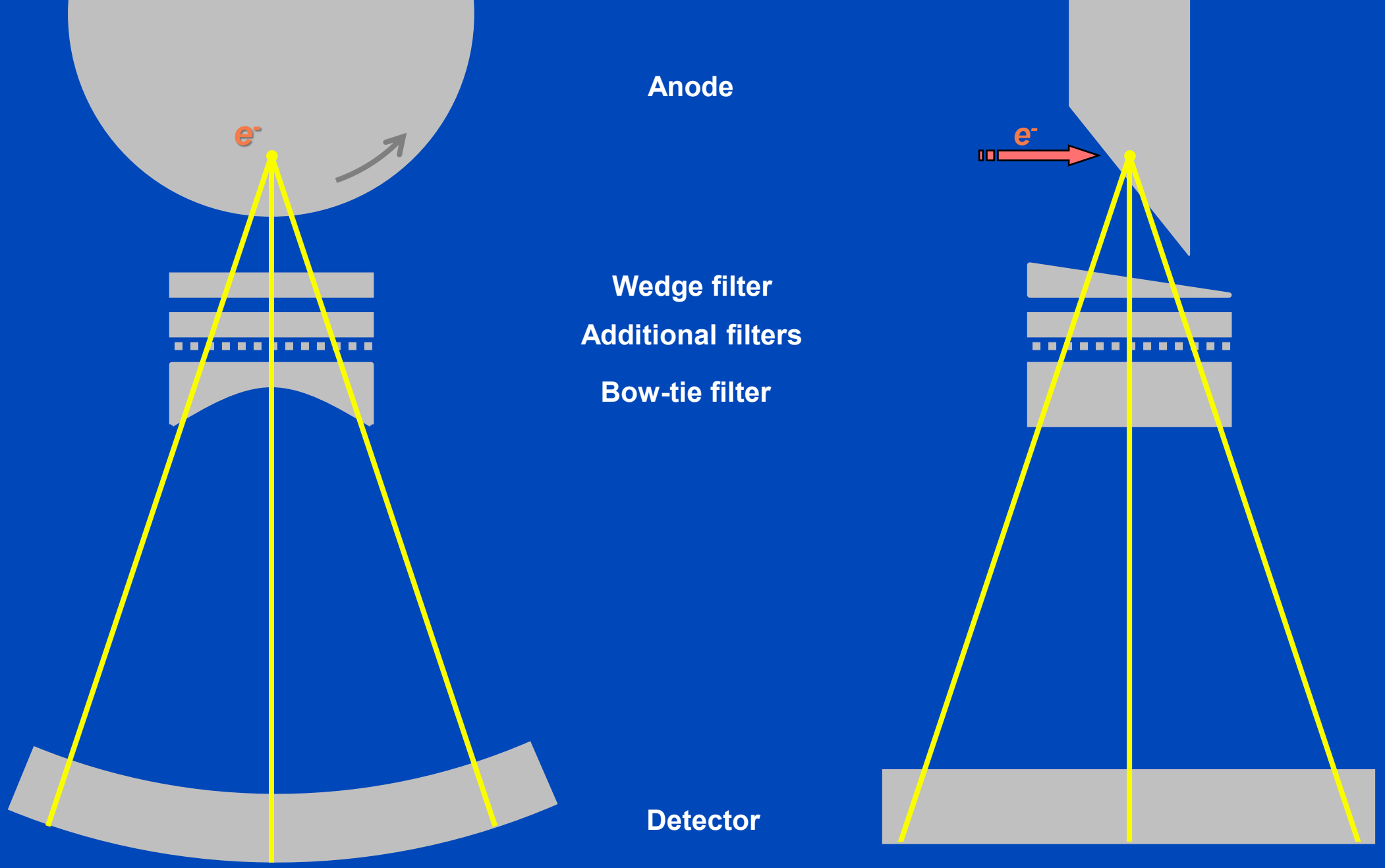

Figure not drawn to scale. Type and order of prefiltration may differ from scanner to scanner.
Depending on the selected protocol filters are changed automatically (e.g. small bowtie for pediatric scans).

dkfz.

Heel Effect

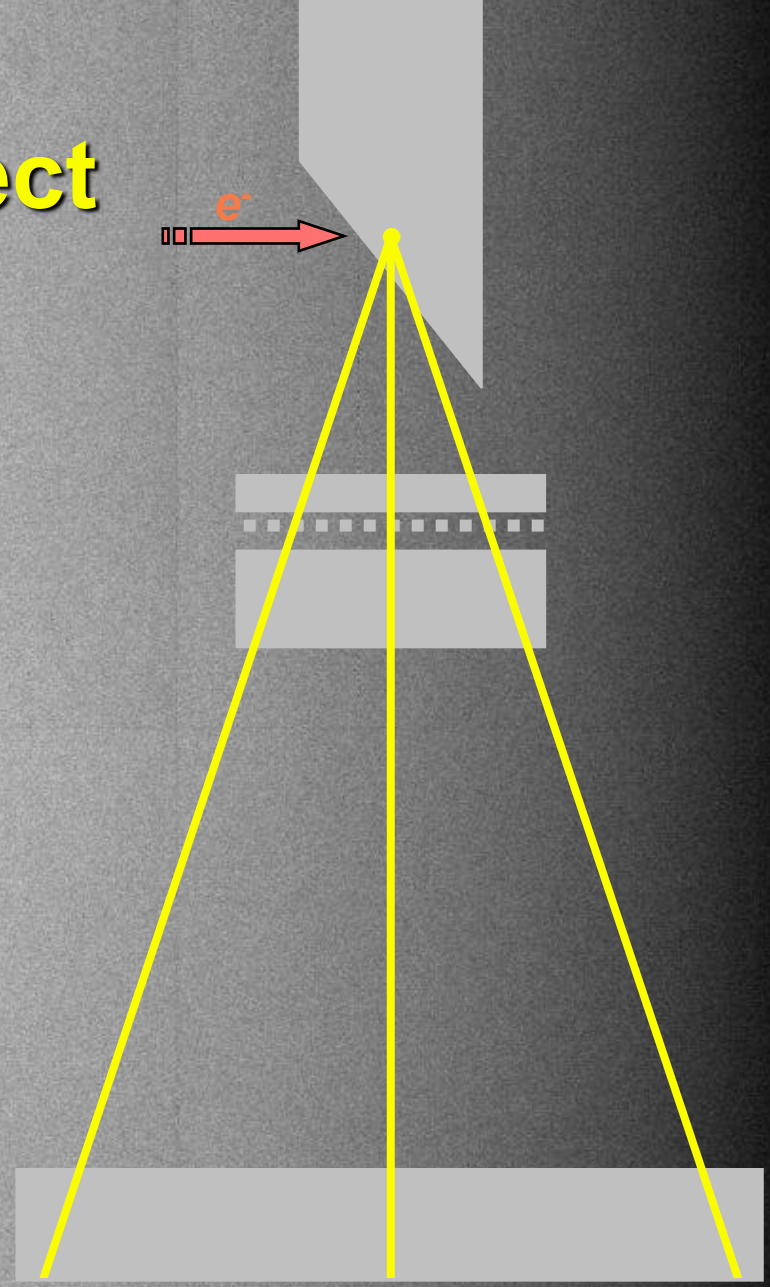

Offset-corrected image (40 kV, 1.39 mA, 23 ms, Ziehm Imaging CMOS)

120 kV + 0 mm water with and without prefilter

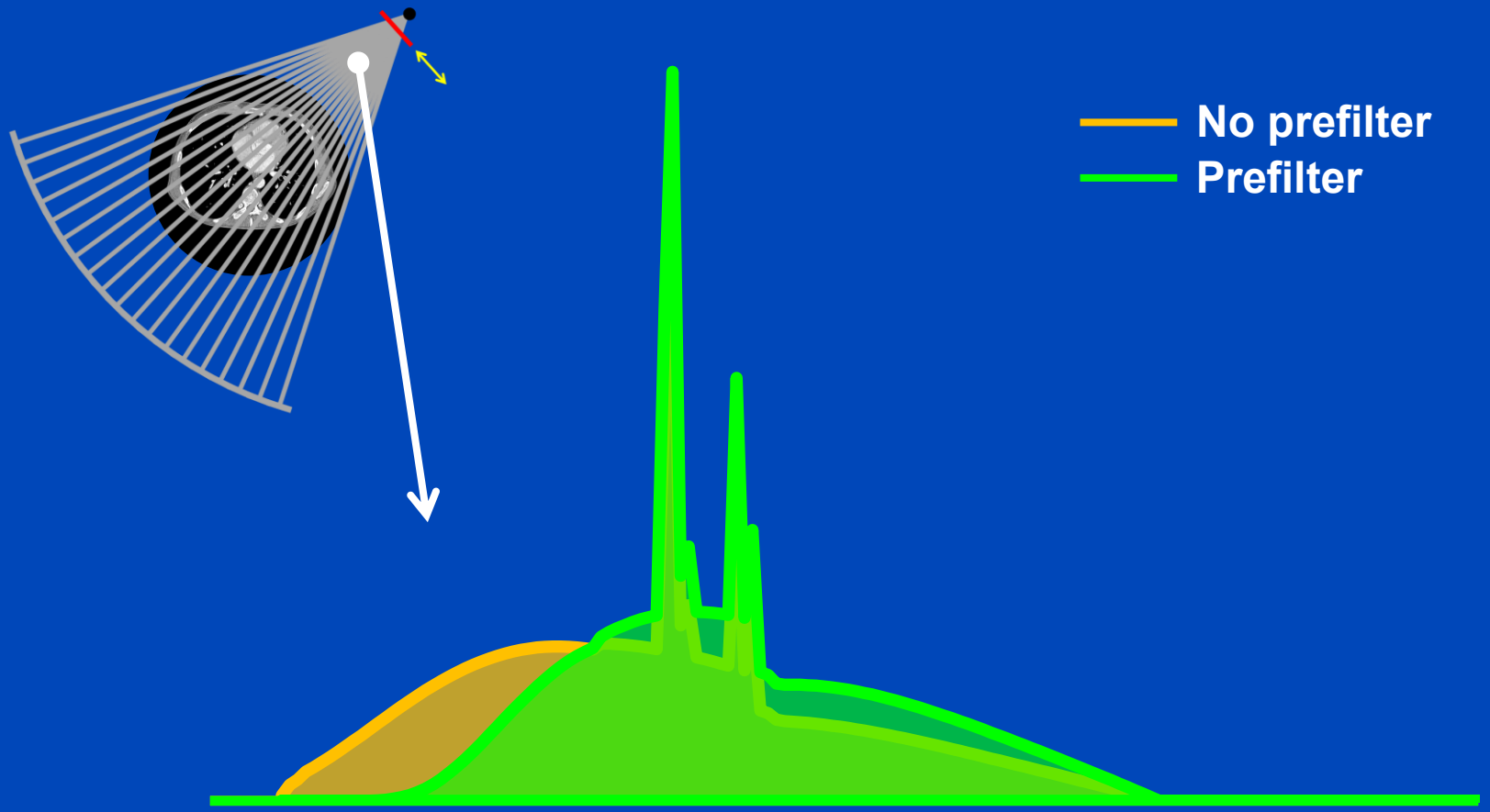

120 kV + 320 mm water with and without prefilter

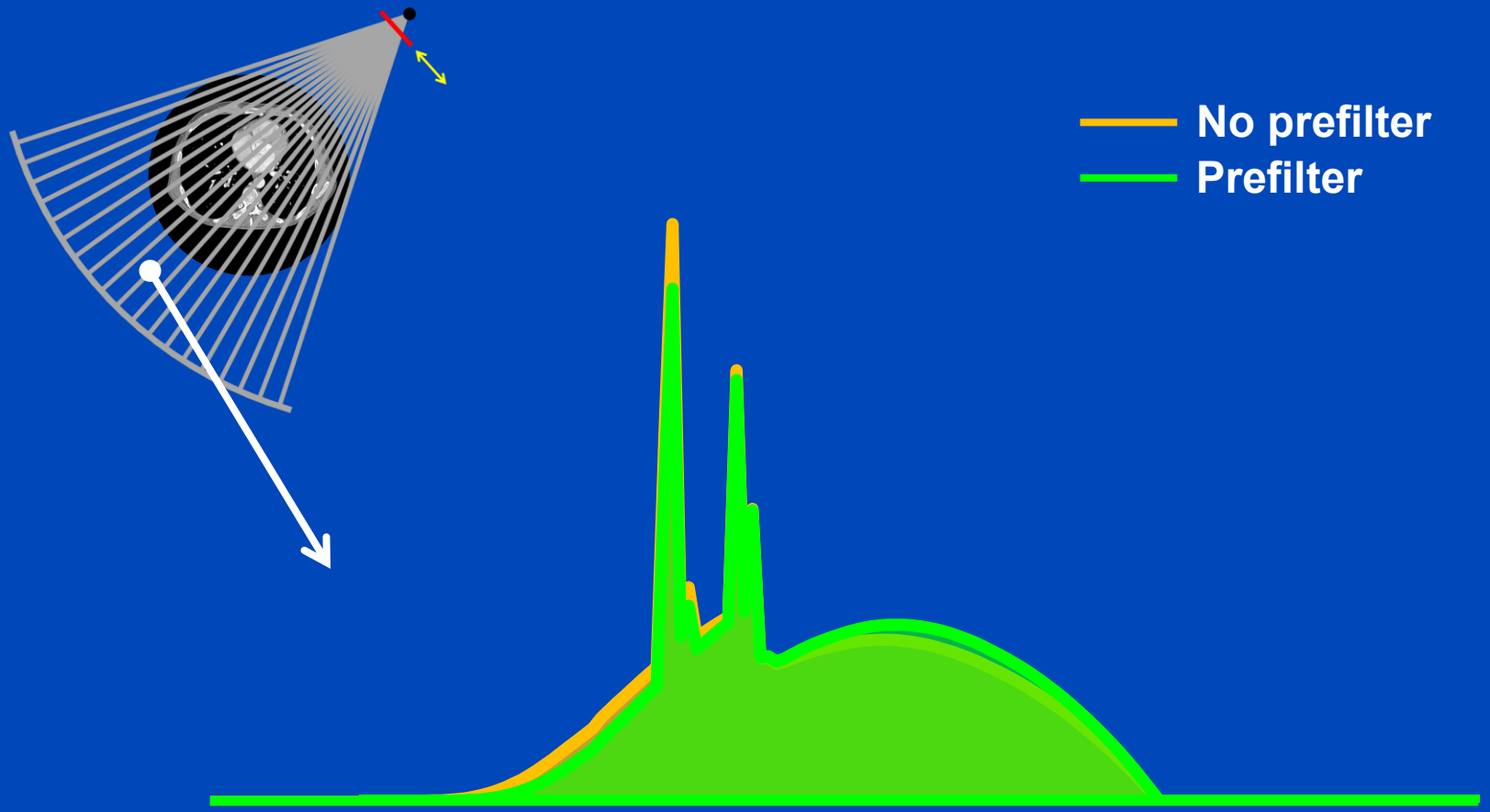

Task- and Patient-Specific (i.e. Removable) Prefilters in Use Today

- 0.4 and 0.7 mm Sn for Siemens` Naeotom Alpha.Peak and Alpha.Pro
- 0.4 mm Sn for Siemens` Naeotom Alpha.Prime
- 0.6 mm Sn for Siemens` Somatom Force, Edge Plus, go.Top and Definition Edge
- 0.4 mm Sn for Siemens` Somatom Flash, Drive, go.Now, go.Up, go.all, and pro.Pulse
- 0.4 mm and 0.7 mm Sn for Siemens` Somatom X.cite
- ≈ 0.5 mm Ag for Canon`s Aquilion ONE Prism Edition
- ≈ 1 mm Cu "for scout scans" in GE's Revolution Apex systems

In the energy range of clinical CT and with objects similar to patients we find that 0.5 mm Ag ≈ 0.6 mm Sn ≈ 2.0 mm Cu.

Cu: $Z = 29$, $\rho = 8.92$ g/cm^3, $E_K = 8.98$ keV. **Ag:** $Z = 47$, $\rho = 10.49$ g/cm^3, $E_K = 25.5$ keV. **Sn:** $Z = 50$, $\rho = 7.31$ g/cm^3 , $E_K = 29.2$ keV.

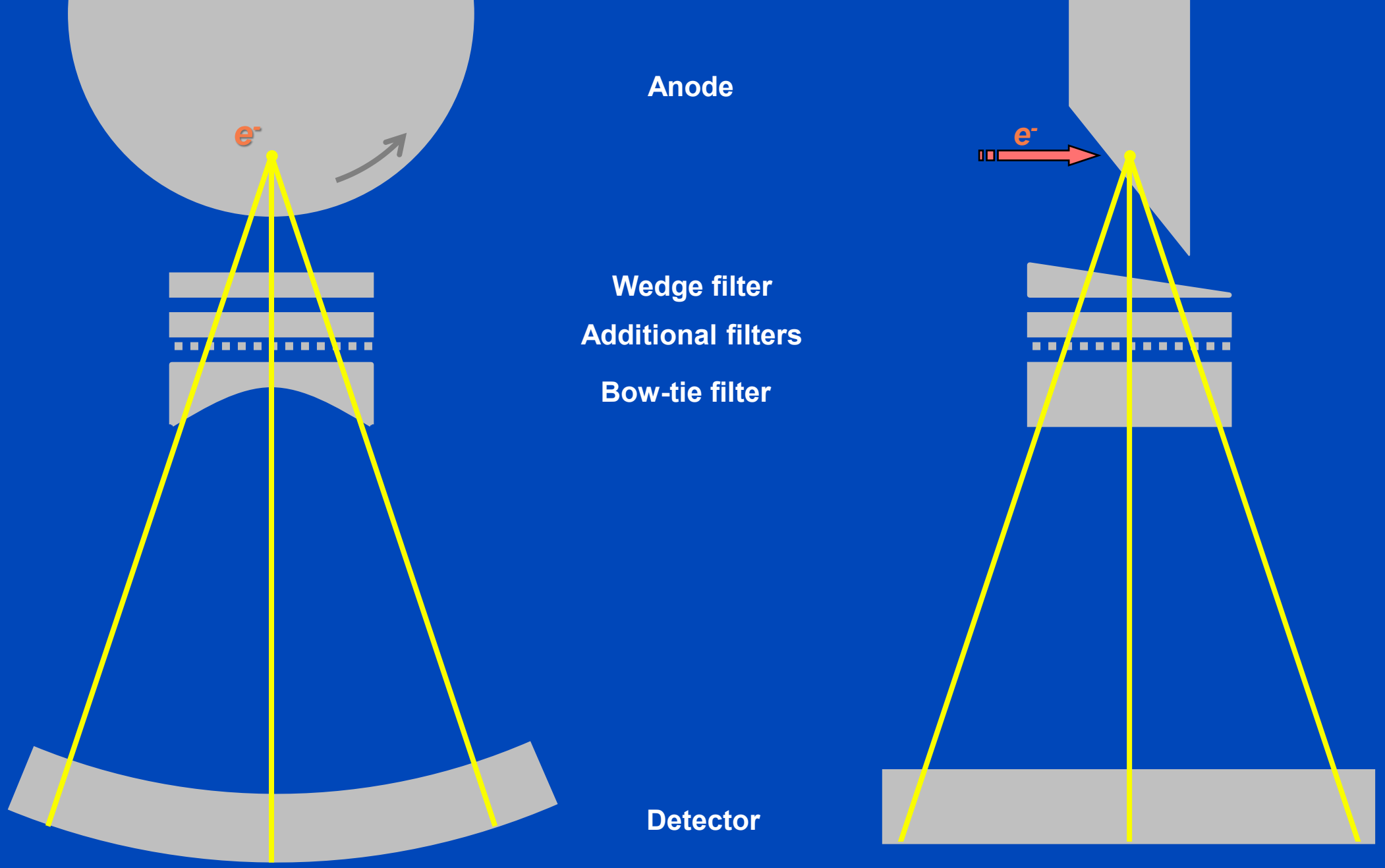

Figure not drawn to scale. Type and order of prefiltration may differ from scanner to scanner.
Depending on the selected protocol filters are changed automatically (e.g. small bowtie for pediatric scans).

dkfz.

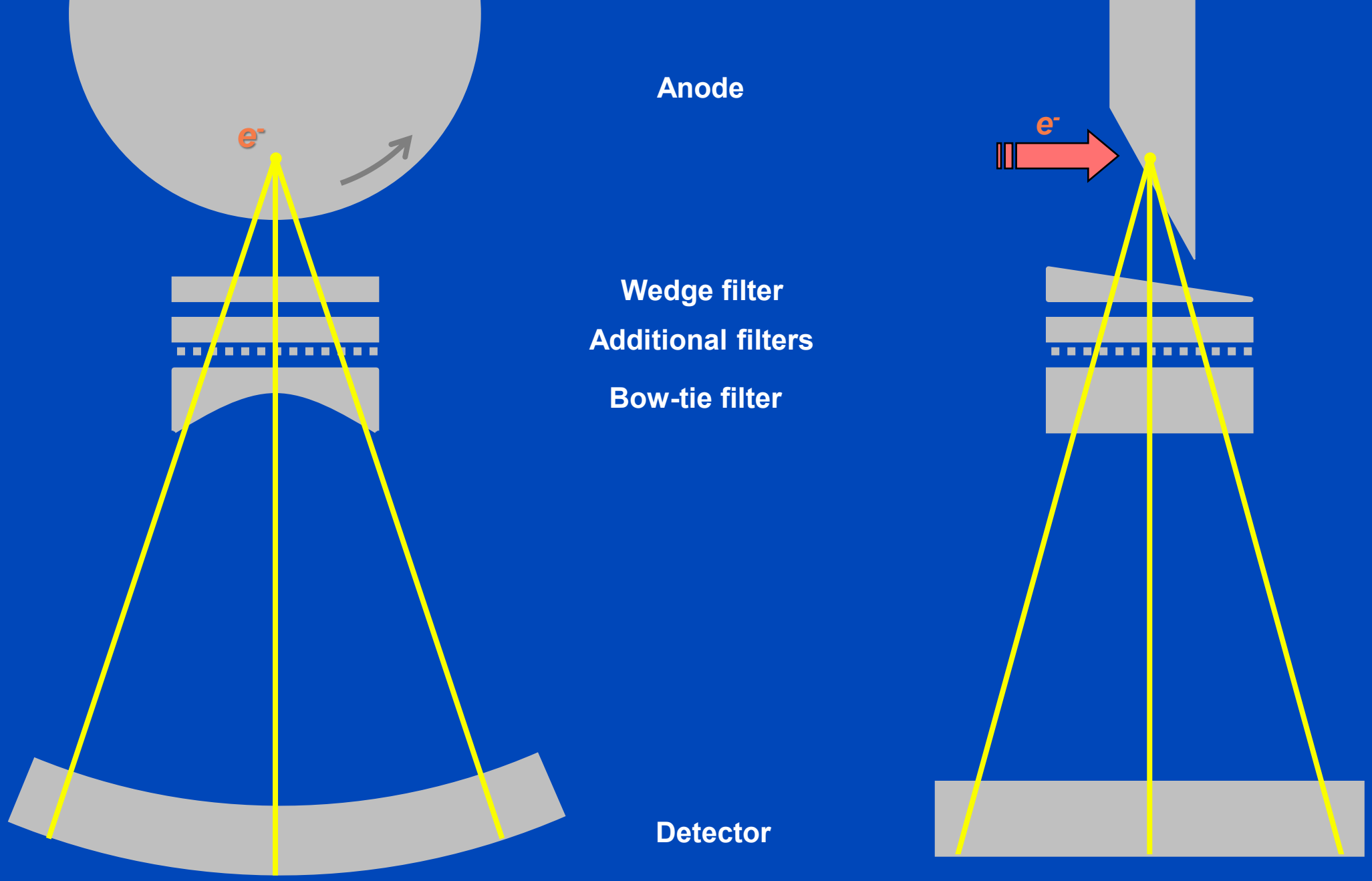

Figure not drawn to scale. Type and order of prefiltration may differ from scanner to scanner.
Depending on the selected protocol filters are changed automatically (e.g. small bowtie for pediatric scans).

dkfz.

Narrow Cone
=
High Tube Power

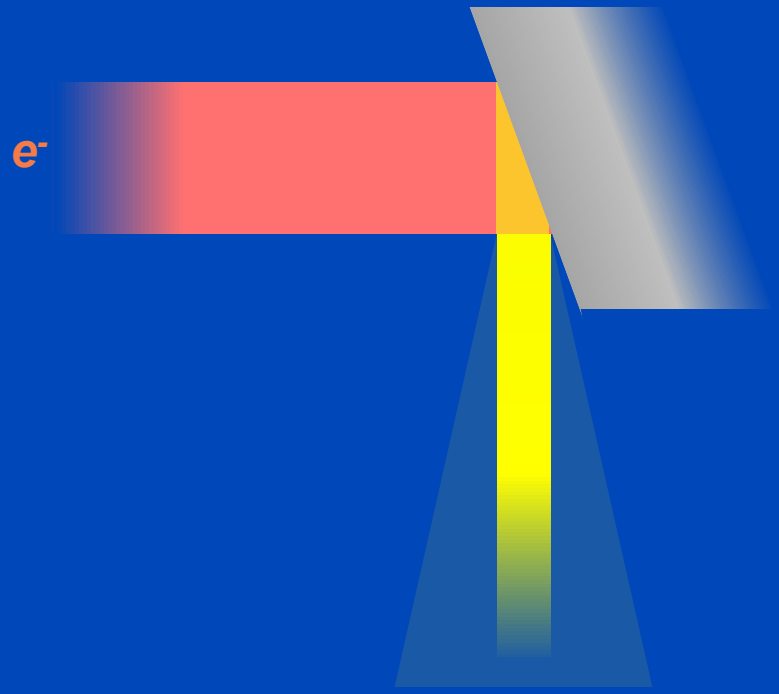

Wide Cone
=
Low Tube Power

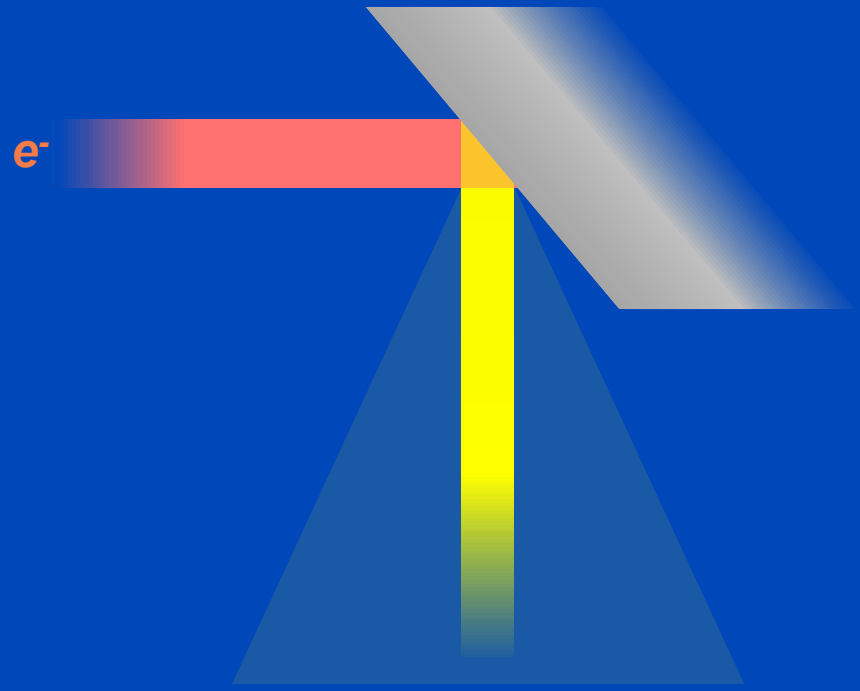

… at the same spatial resolution

Onset of target melting (rule of thumb)[1]: 1 W/µm

[1] D.E. Grider, A. Writh, and P.K. Ausburn. Electron Beam Melting in Microfocus X-Ray Tubes. J. Phys. D: Appl. Phys 19:2281-2292, 1986

dkfz.

What is Displayed?

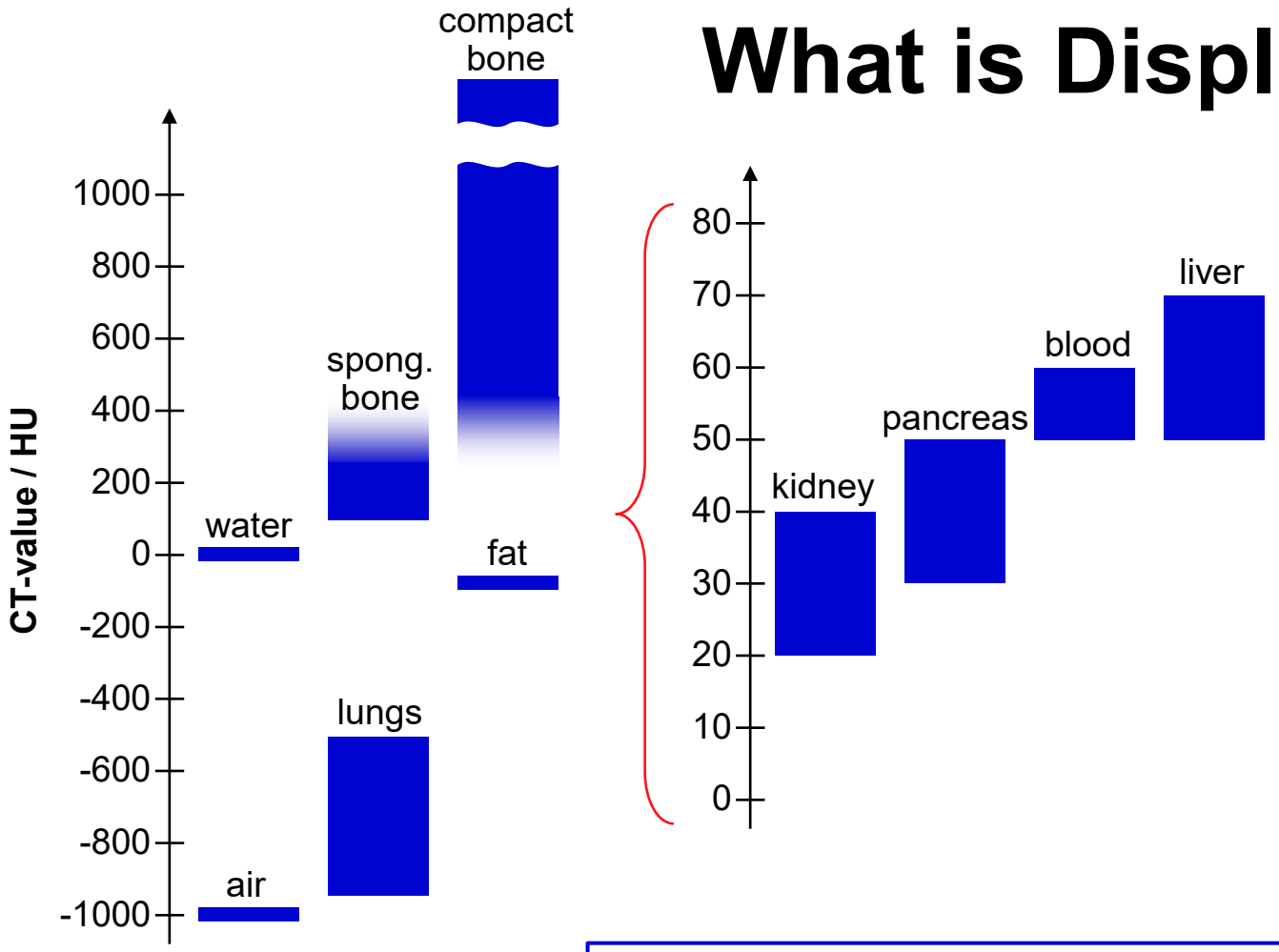

$$CT(\boldsymbol{r}) = \frac{\mu(\boldsymbol{r}) - \mu_{\mathrm{Water}}}{\mu_{\mathrm{Water}}} \cdot 1000\ \mathrm{HU}$$

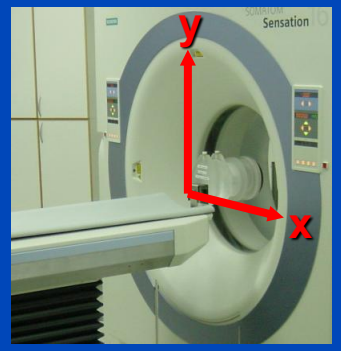

Fan-Beam Geometry (transaxial / in-plane / x-y-plane)

x-ray tube

field of measurement (FOM) and object

detector

y
x

In the order of 1000 detector channels are available per detector row.

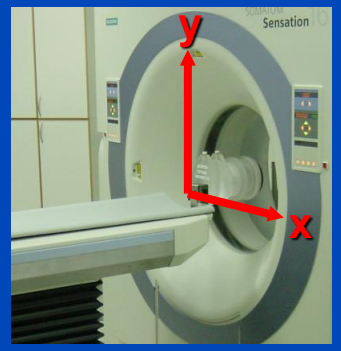

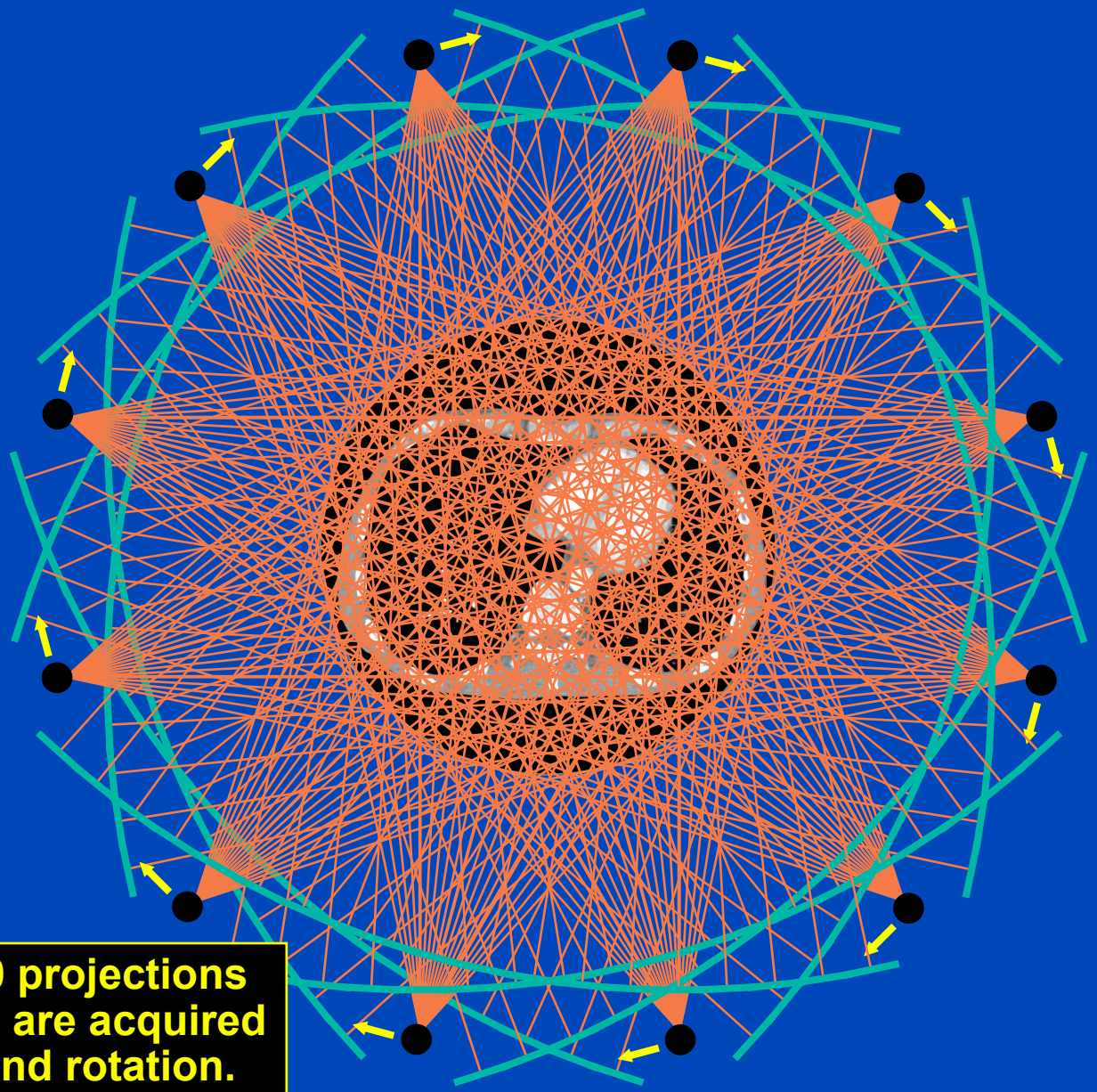

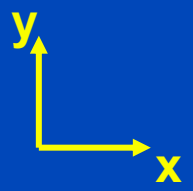

In the order of 1000 projections with 1000 channels are acquired per detector slice and rotation.

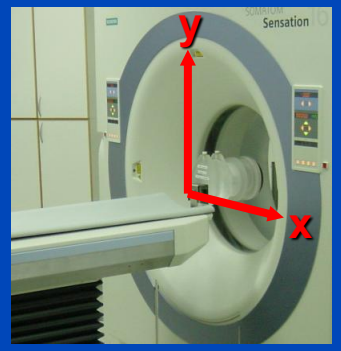

Data Completeness

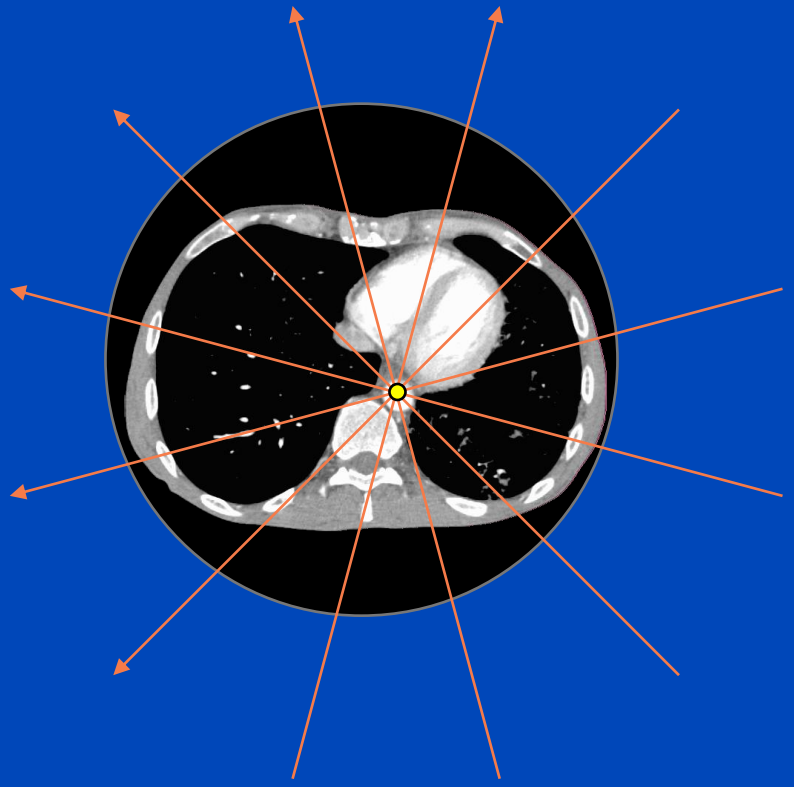

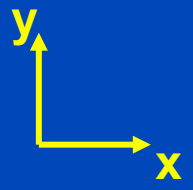

Each object point must be viewed by an angular interval of 180° or more. Otherwise image reconstruction is not possible.

Axial Geometry (z-Direction)

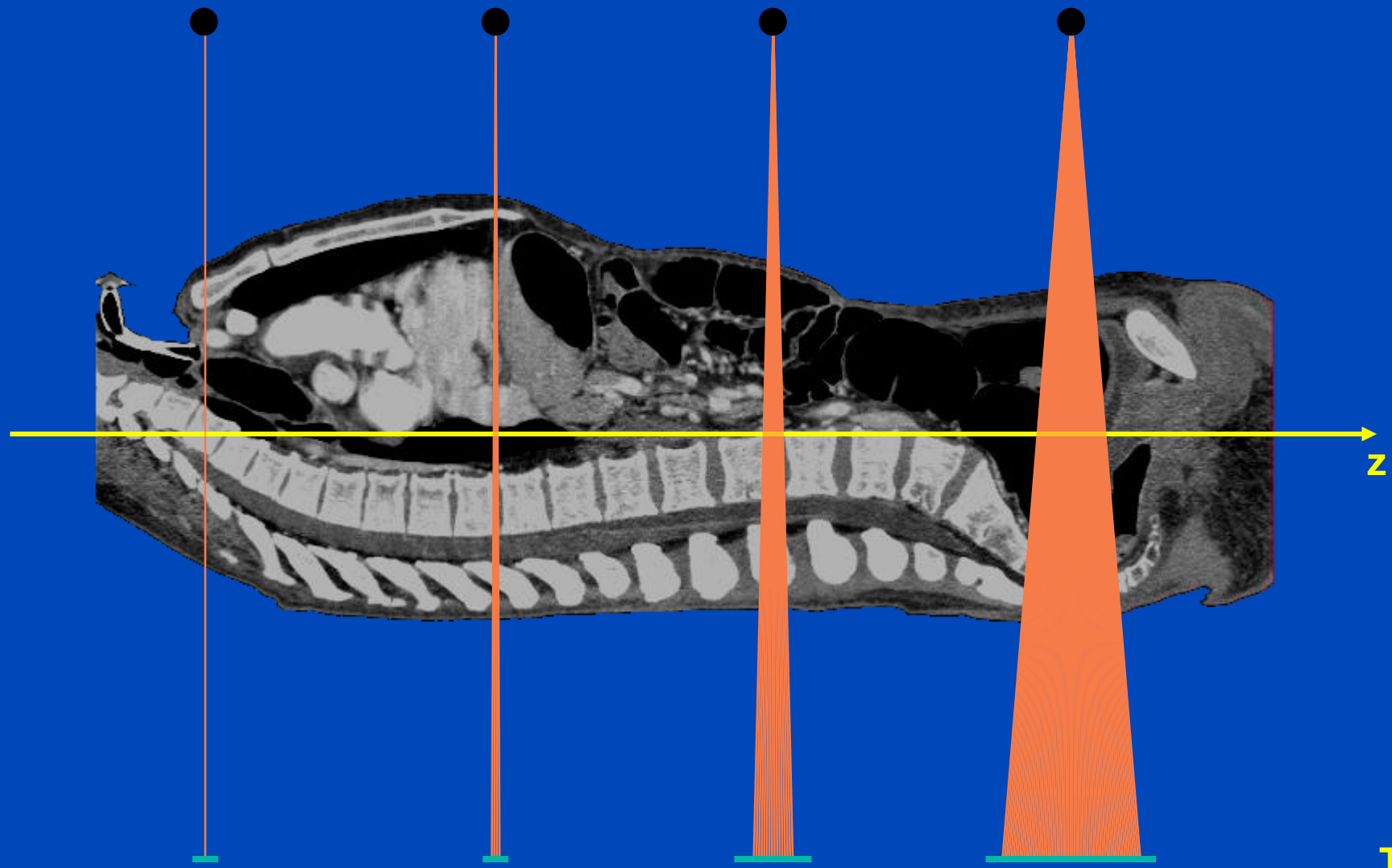

y
z

<1998: *M*=1

1998: *M*=4

2002: *M*=16

2006: *M*=64

Today:
up to *M*=320

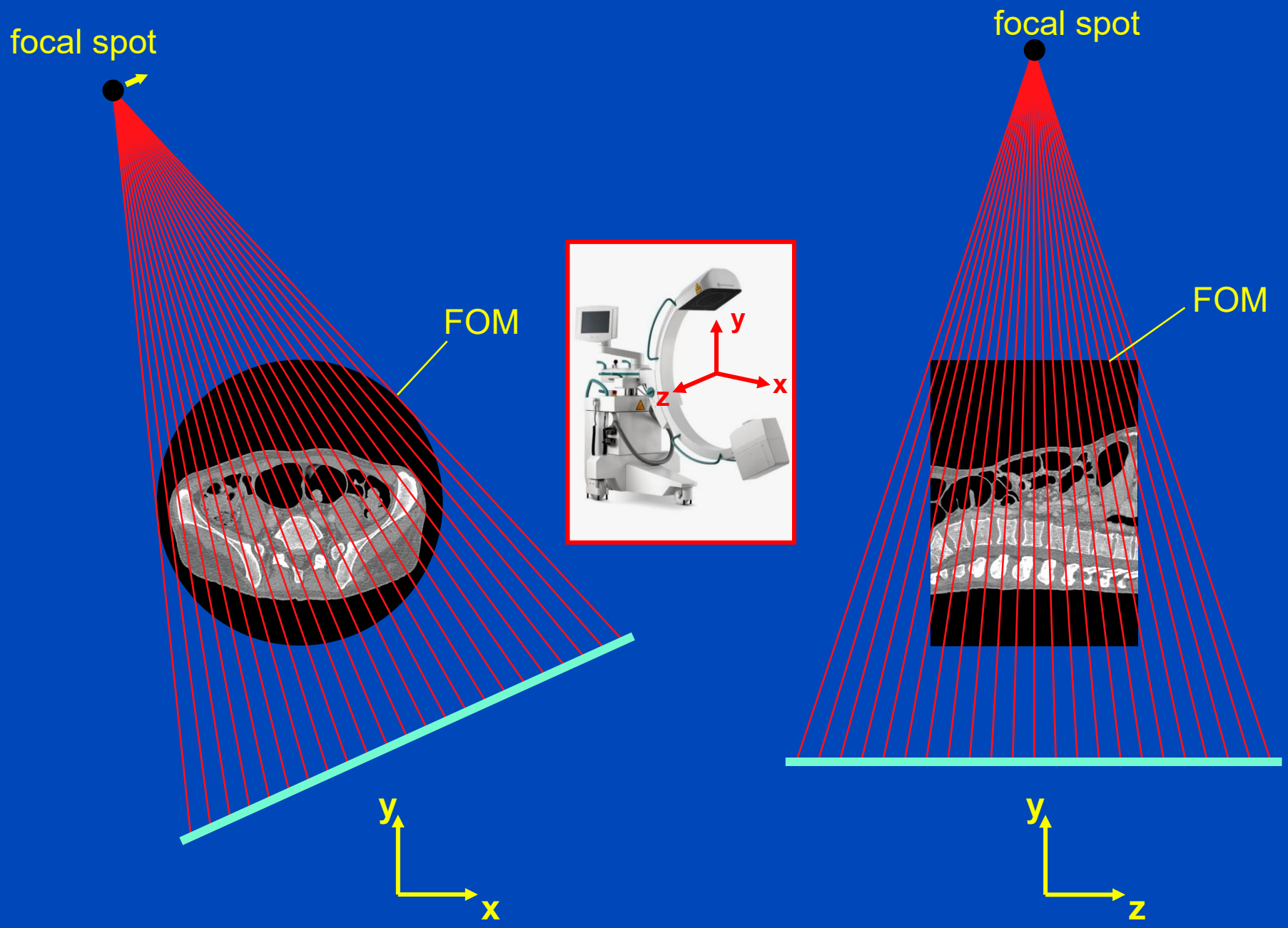

Detector: 1000×1000 to 4000×4000 elements, typically

dkfz.

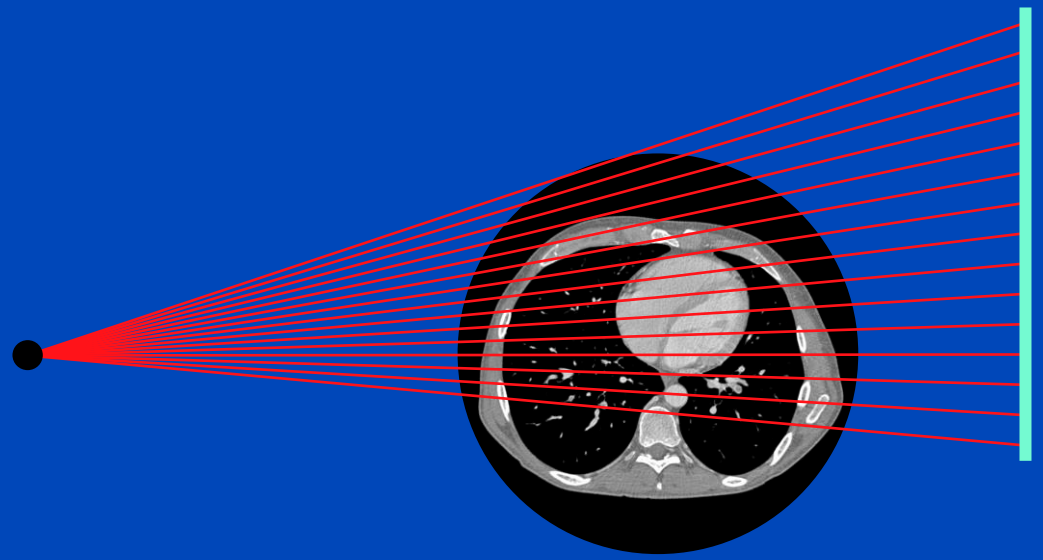

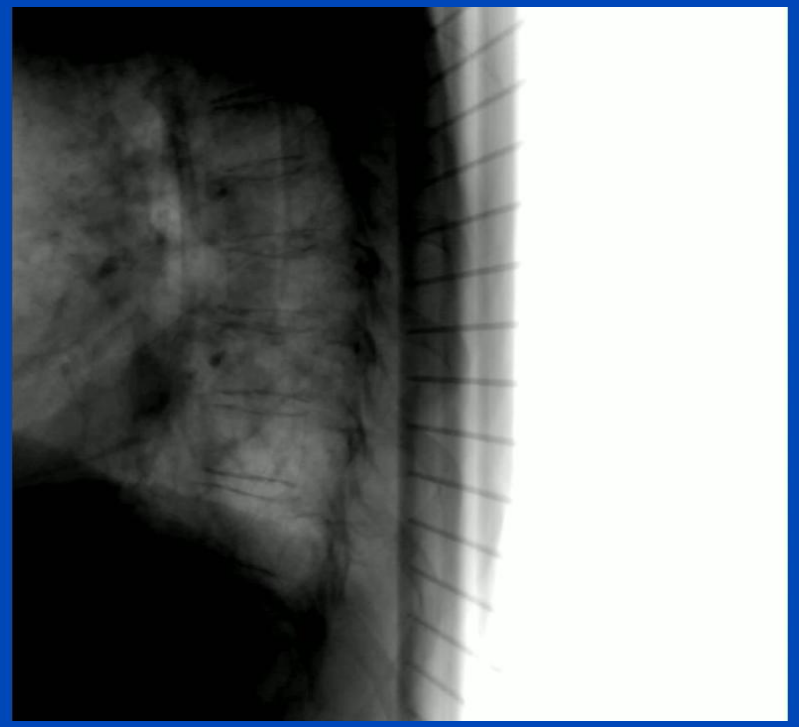

Rotate-Plus-Shift[1] (RPS) Trajectory

J. Kuntz, L. Ritschl, C. Fleischmann, M. Knaup, and M. Kachelrieß.
The Rotate-Plus-Shift C-Arm Trajectory (Parts I and II). MedPhys 2016.

AMERICAN ASSOCIATION of PHYSICISTS IN MEDICINE

Congratulations

This paper received the Sylvia&Moses Greenfield Award for the best scientific paper on imaging in Medical Physics in 2016.

dkfz.

EQUIPMENT TECHNOLOGY

Canon Aquilion ONE Vision

GE Revolution CT

Philips IQon Spectral CT

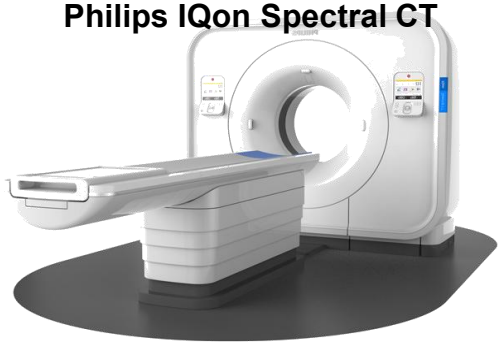

Siemens Naeotom Alpha

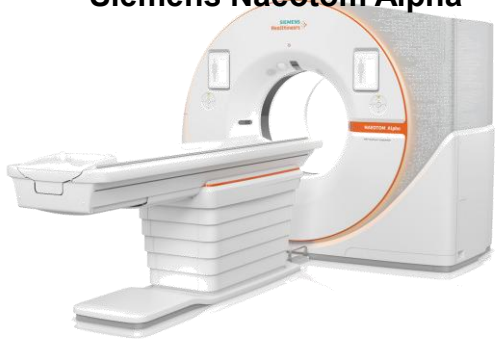

In-plane resolution: 0.2 … 0.7 mm

Nominal slice thickness: S = 0.2 … 1.5 mm

Tube (max. values): 120 kW, 150 kV, 1300 mA

Effective tube current: mAs_{eff} = 10 mAs … 1000 mAs

Rotation time: T_{rot} = 0.25 … 0.5 s

Simultaneously acquired slices: M = 16 … 320

Table increment per rotation: d = 1 … 183 mm

Scan speed: up to 73 cm/s

Temporal resolution: 50 … 250 ms

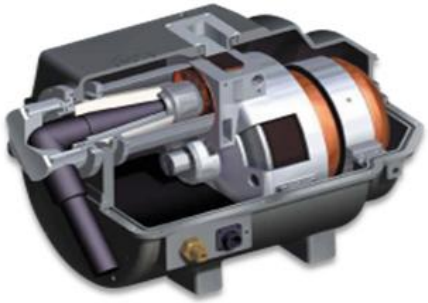

Canon Megacool Vi

GE Performix HDw

Philips iMRC

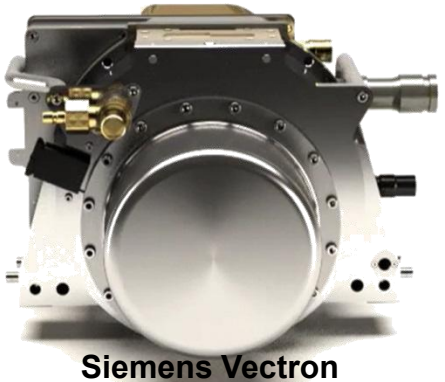

Siemens Vectron

Demands on the Mechanical Design

- Continuous data acquisition (spiral, fluoro, dynamic, …)
- Able to withstand very fast rotation
  - Centrifugal acceleration at 550 mm with 0.5 s: a = 9 g
  - with 0.4 s: a = 14 g
  - with 0.3 s: a = 25 g
  - with 0.2 s: a = 55 g
- Mechanical accuracy better than 0.1 mm
- Compact and robust design
- Short installation times
- Long service intervals
- Low cost

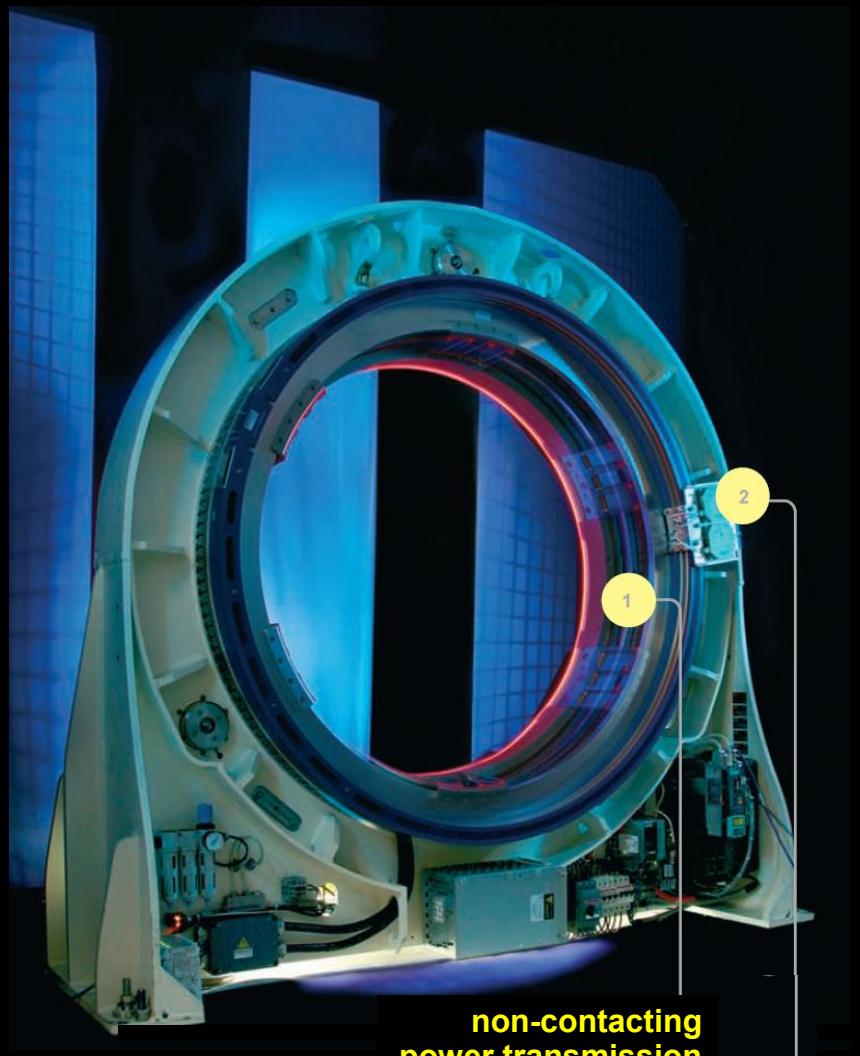

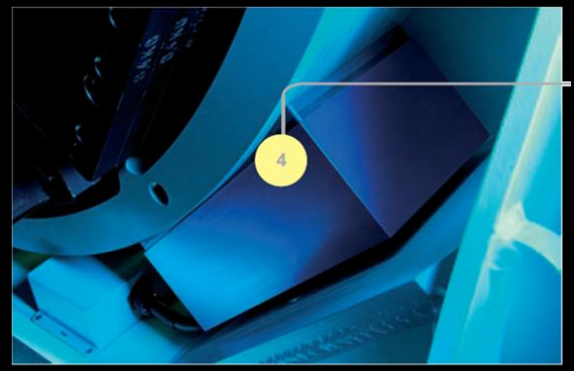

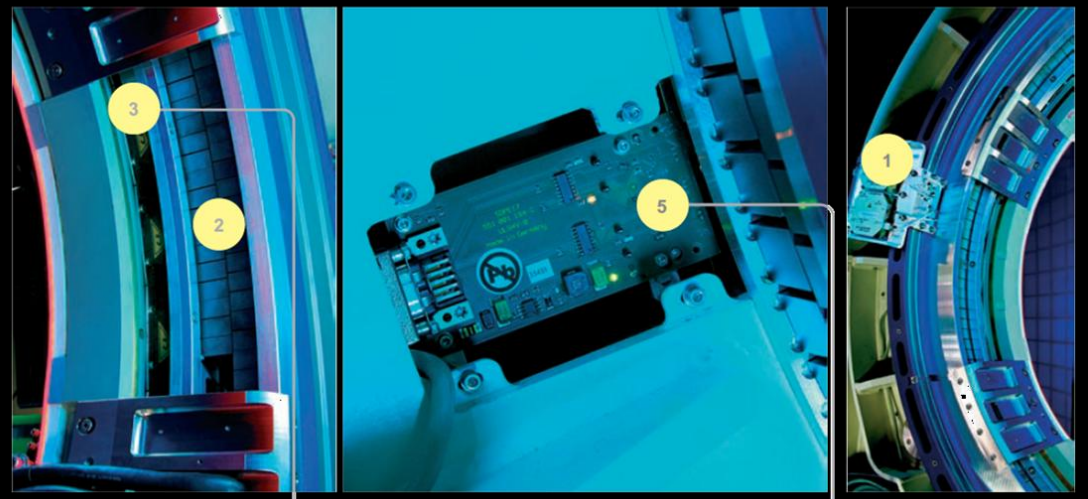

Data courtesy of Schleifring GmbH, Fürstenfeldbruck, Germany
and of rsna2011.rsna.org/exbData/1678/docs/Gantry_Subsystem.pdf

dkfz.

Demands on X-Ray Sources

- Tube voltages from 70 to 150 kV in steps of 10 kV
- High instantaneous power levels (typ. 50 to 120 kW)
- High tube currents at low kV (good for Iodine contrast)
- High continuous power levels (typ. > 5 kW)
- High cooling rates (typ. about 25 kW ≈ 1 MHU/min*)
- High tube current variation (low inertia)
- Must withstand centrifugal forces
  - Centrifugal acceleration at 550 mm with 0.5 s: a = 9 g
  - with 0.4 s: a = 14 g
  - with 0.3 s: a = 25 g
  - with 0.2 s: a = 55 g
- Compact and robust design
- Long service intervals
  - Ball bearings cannot be lubricated and wear out early
  - Liquid bearings to be preferred (also due to good heat conduction)

* 1 MHU = √2 MJ

Tube Technology

conventional tube
(rotating anode, helical wire emitter)

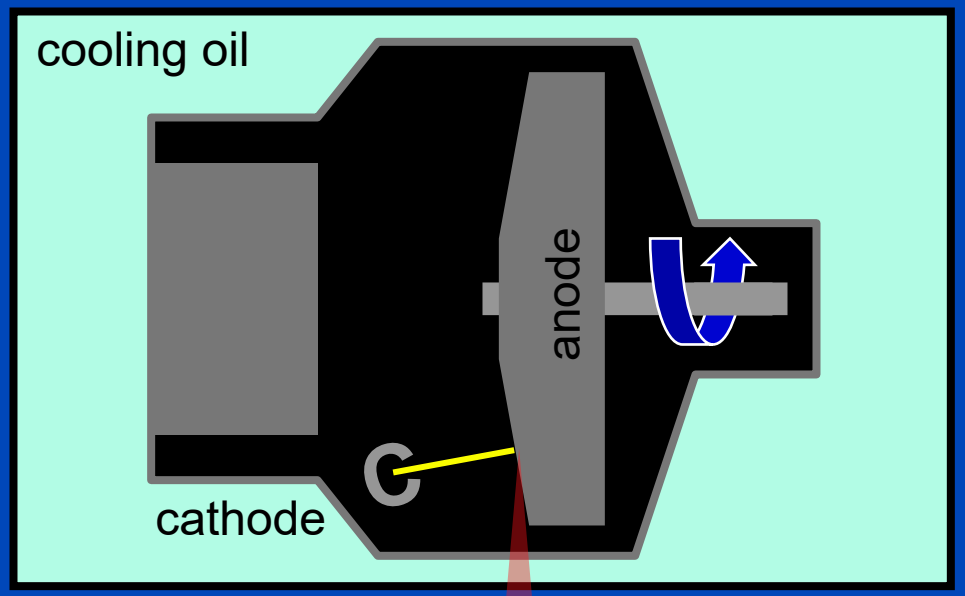

Photo courtesy of GE

Anode at high temperature (>> 1000 °C)

Radiative cooling ($\propto T^4$) is dominant

high performance tube
(rotating cathode, anode + envelope, flat emitter)

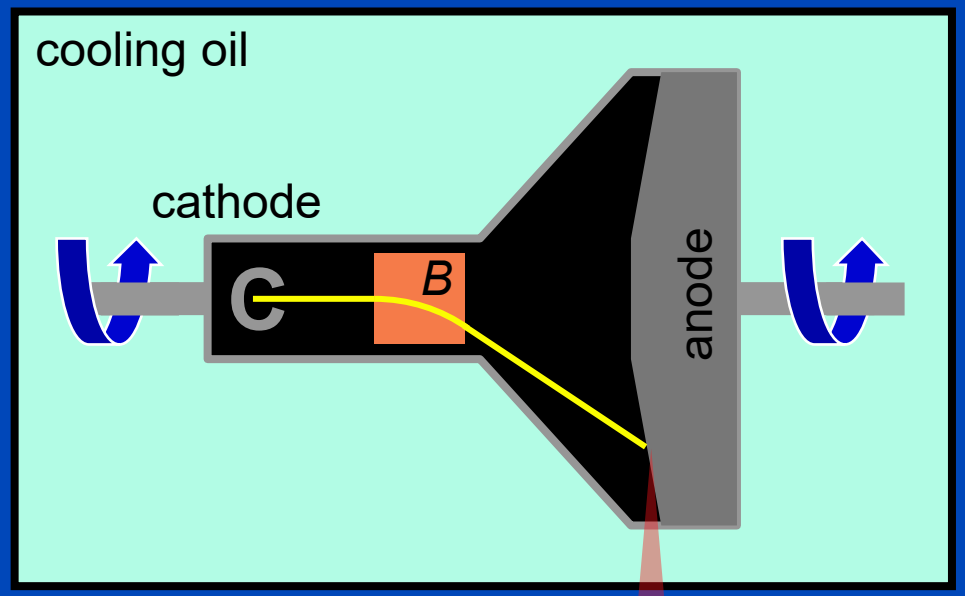

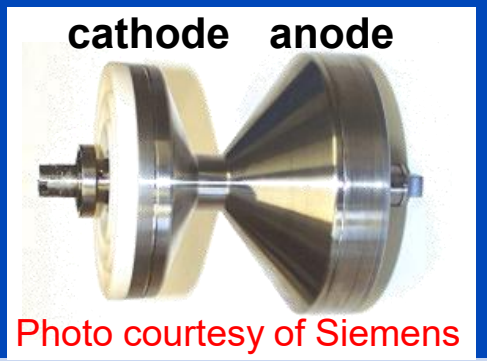

Photo courtesy of Siemens

Anode at low temperature (<< 1000 °C)

Conductive cooling ($\propto T$) is dominant

dkfz.

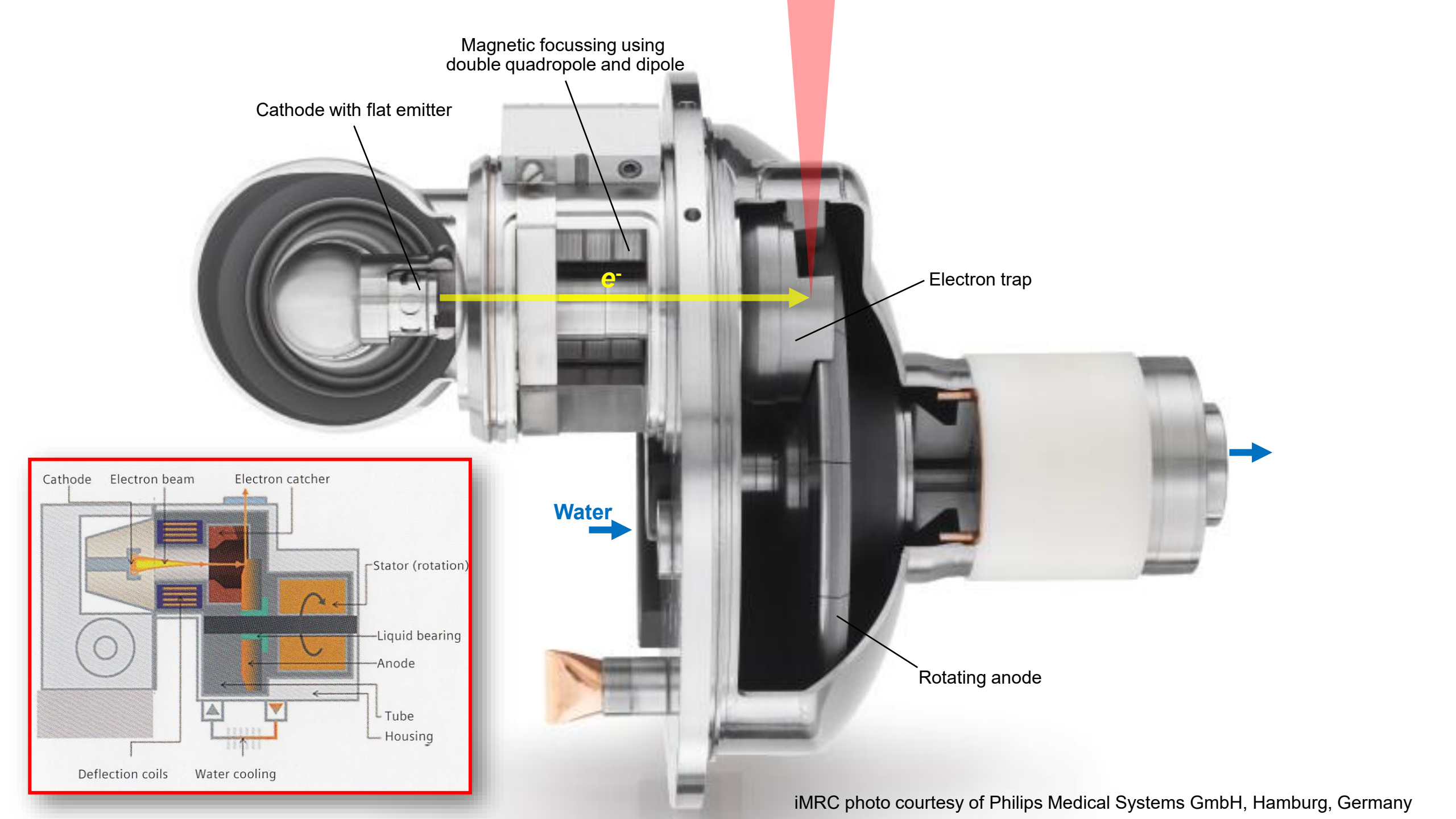

iMRC photo courtesy of Philips Medical Systems GmbH, Hamburg, Germany

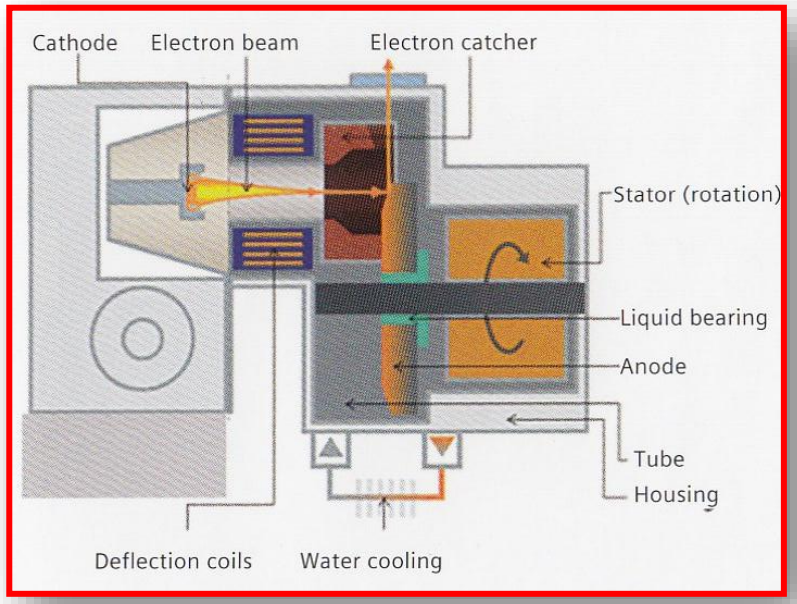

Liquid bearings
- “spiral” grooves (stationary)
- e.g. 10 µm GaInSn
- good heat conductivity
- nearly wear-free
- low vibration
- low noise

Graphite to store heat

iMRC photo courtesy of Philips Medical Systems GmbH, Hamburg, Germany

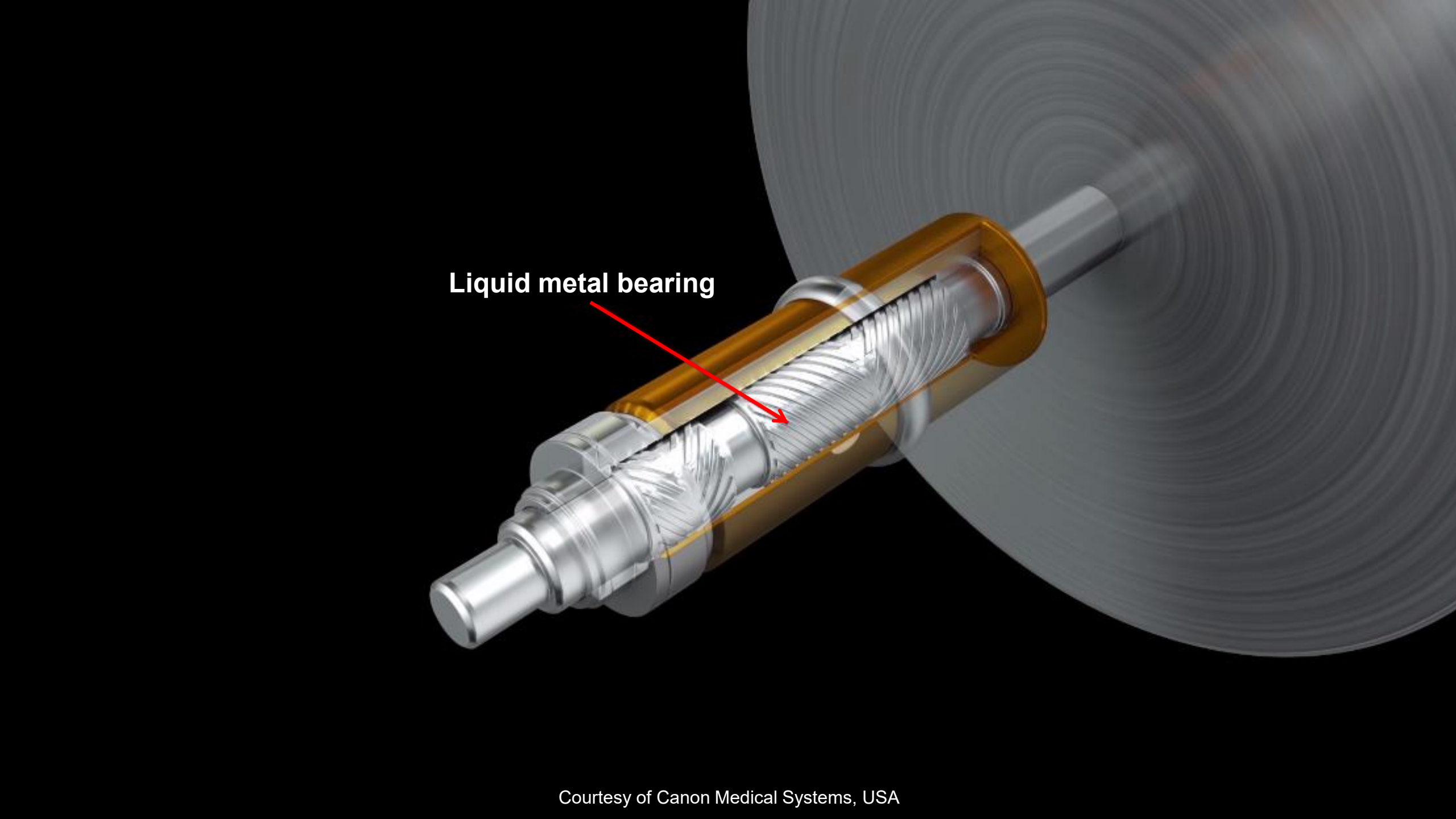

Courtesy of Canon Medical Systems, USA

Straton vs. Vectron at all kV

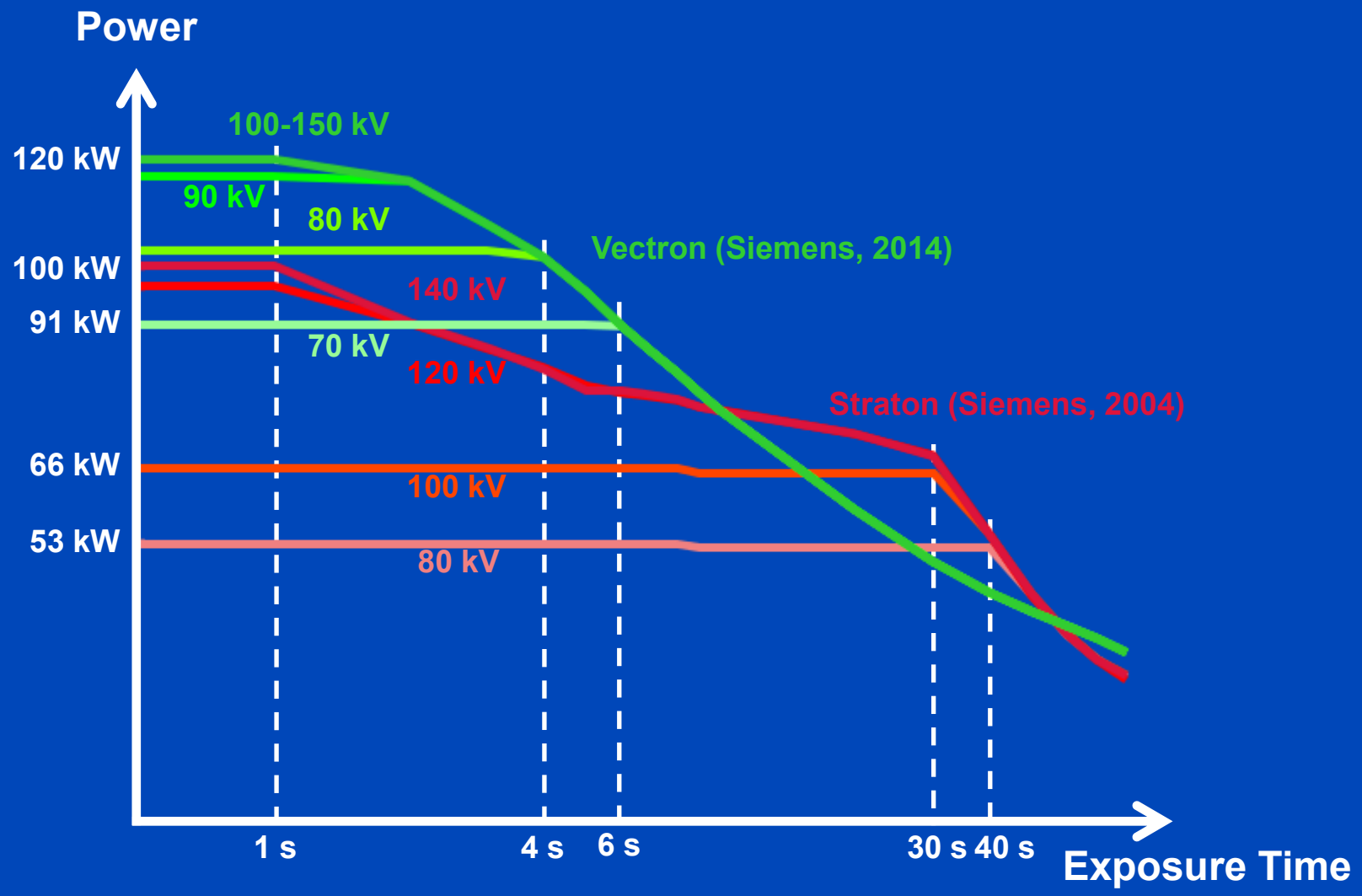

Tube Voltage 80 kV

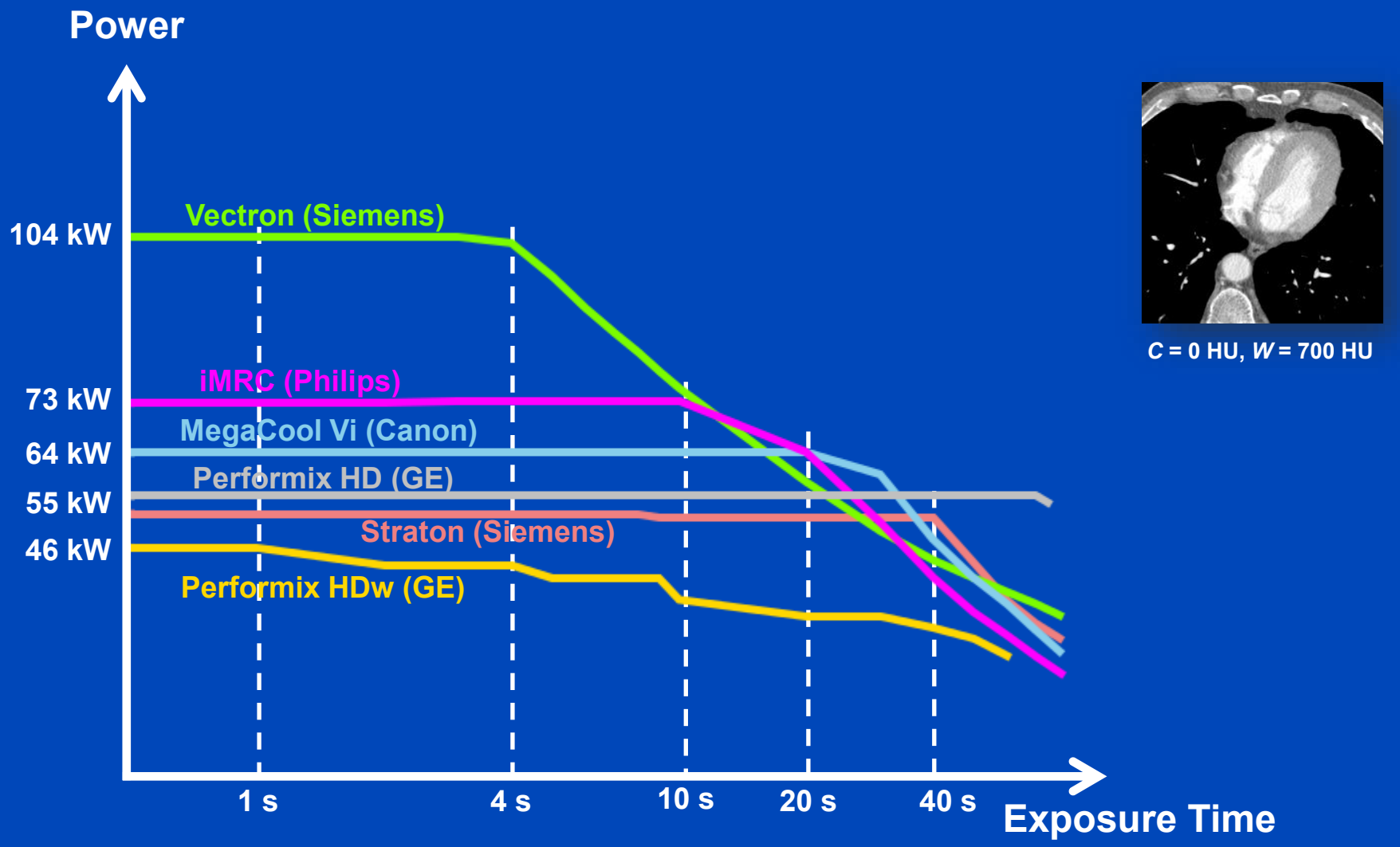

C = 0 HU, *W* = 700 HU

Tube Voltage 120 kV

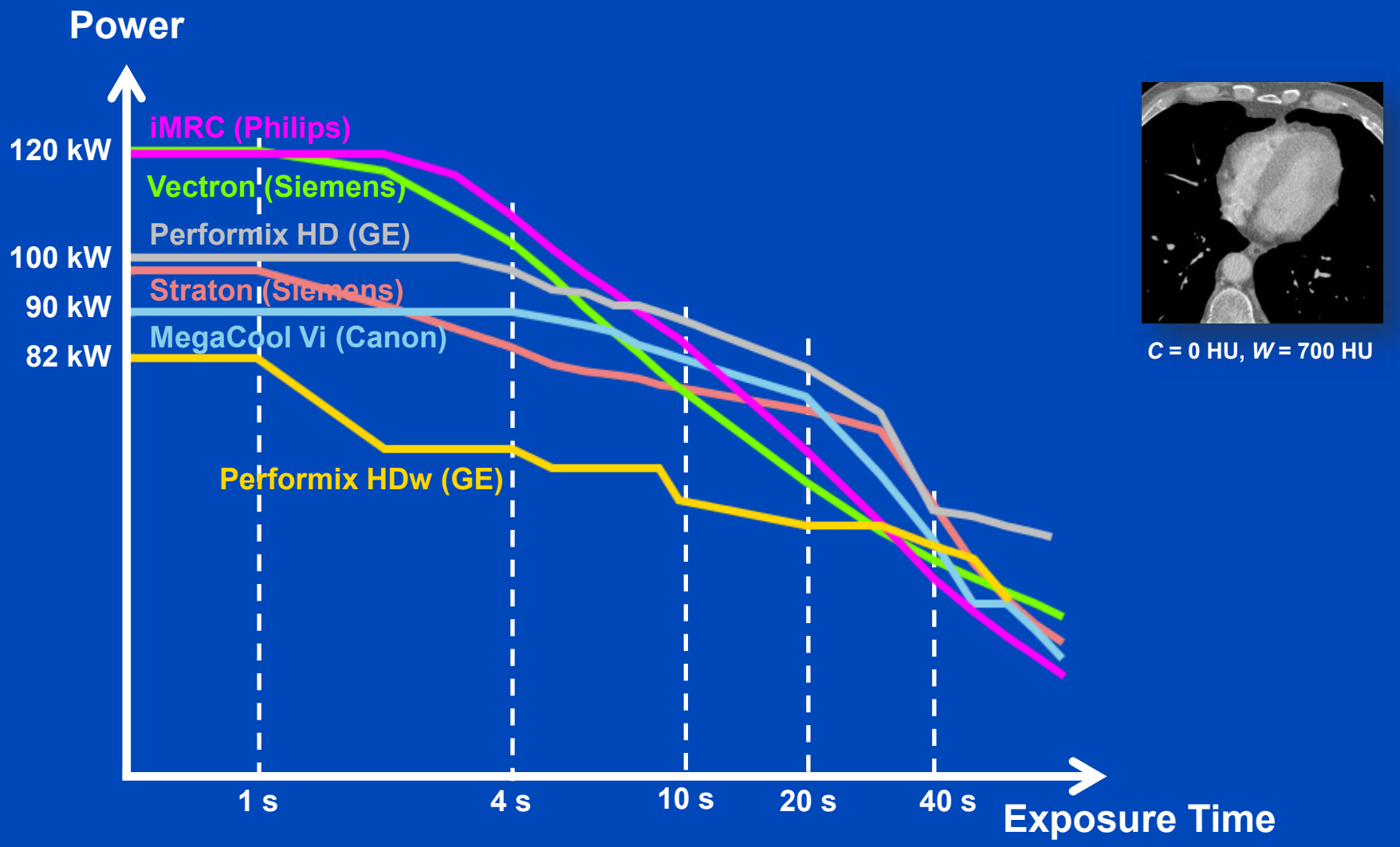

C = 0 HU, *W* = 700 HU

Narrow Cone = High Tube Power

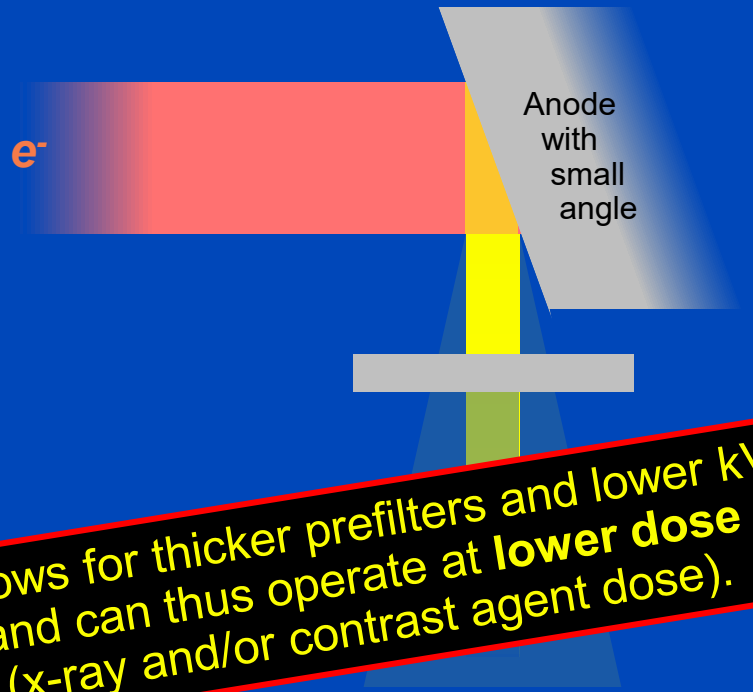

Allows for thicker prefilters and lower kV and can thus operate at **lower dose** (x-ray and/or contrast agent dose).

Wide Cone = Low Tube Power

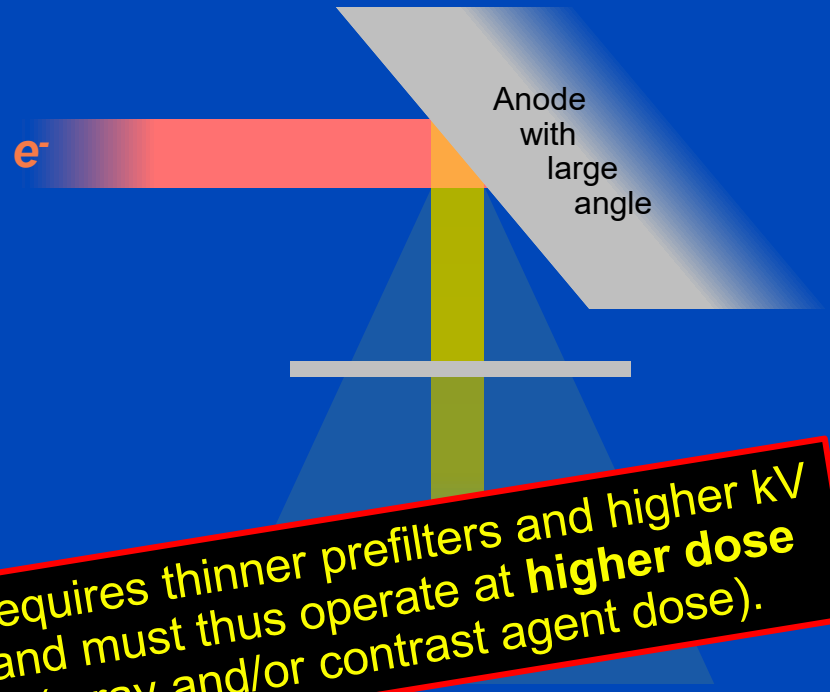

Requires thinner prefilters and higher kV and must thus operate at **higher dose** (x-ray and/or contrast agent dose).

… at the same spatial resolution

Onset of target melting (rule of thumb)[1]: 1 W/µm

[1] D.E. Grider, A. Writh, and P.K. Ausburn. Electron Beam Melting in Microfocus X-Ray Tubes. J. Phys. D: Appl. Phys 19:2281-2292, 1986

dkfz.

Demands on CT Detector Technology

- Available as multi-row arrays
- Very fast sampling (typ. 300 µs)
- Favourable temporal characteristics (decay time < 10 µs)
- High absorption efficiency
- High geometrical efficiency
- High count rate (up to 10^9 cps*)
- Adequate dynamic range (18 to 22 bit)
- Signal stability (better than 0.1%)

* in the order of 10^5 counts per reading and 10^4 readings per second

Detector Technology

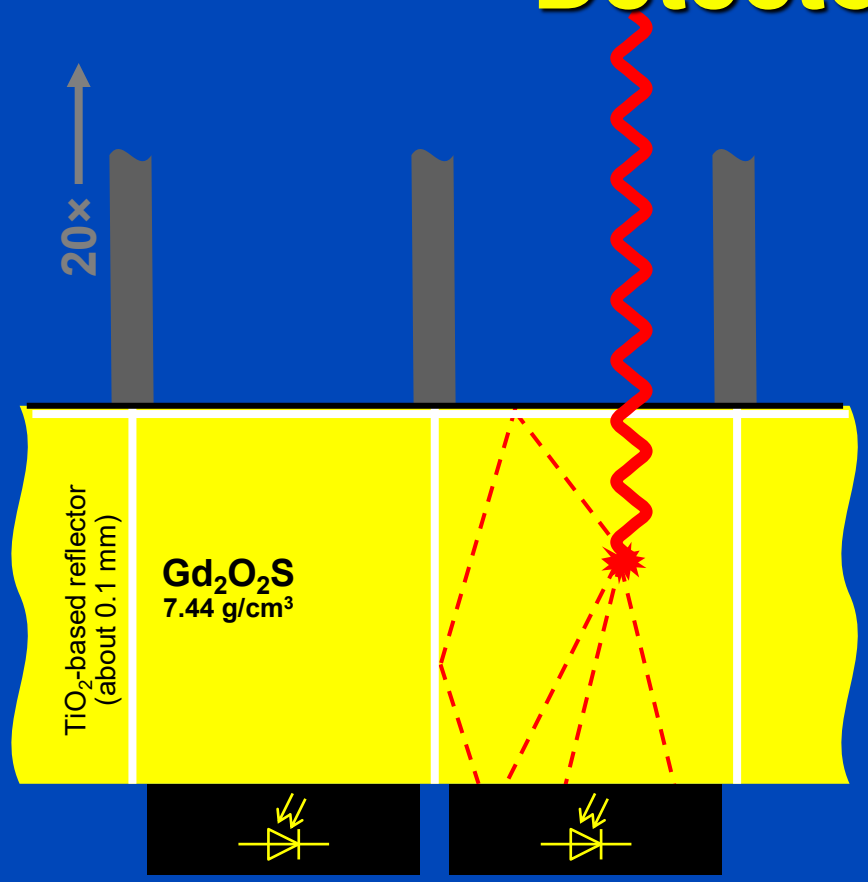

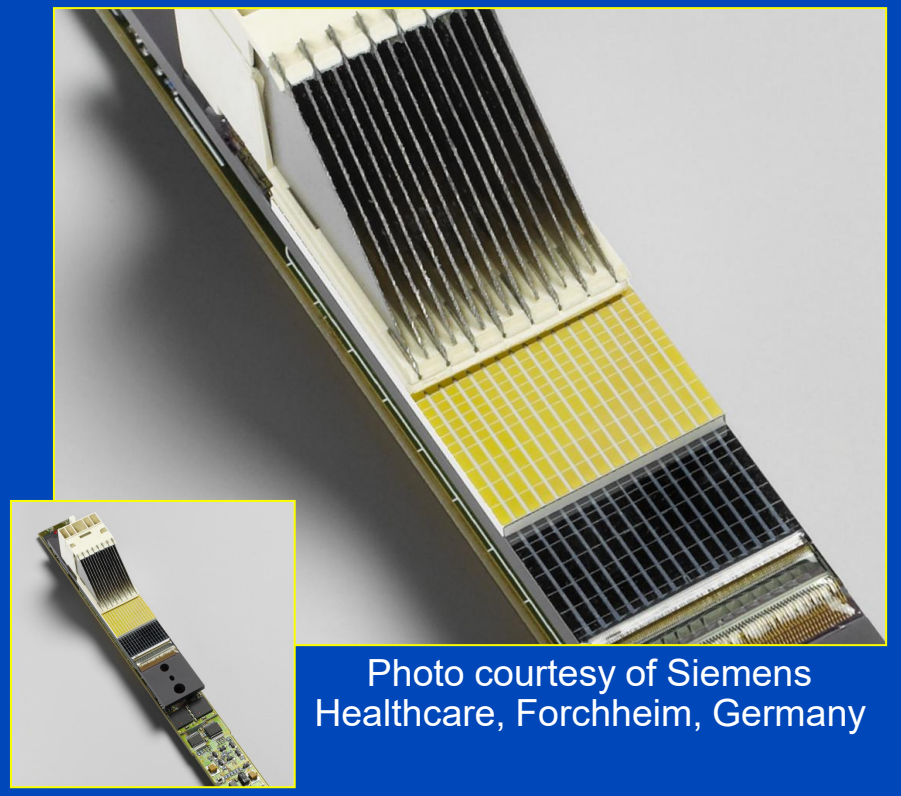

Photo courtesy of Siemens Healthcare, Forchheim, Germany

Clinical CT Detector

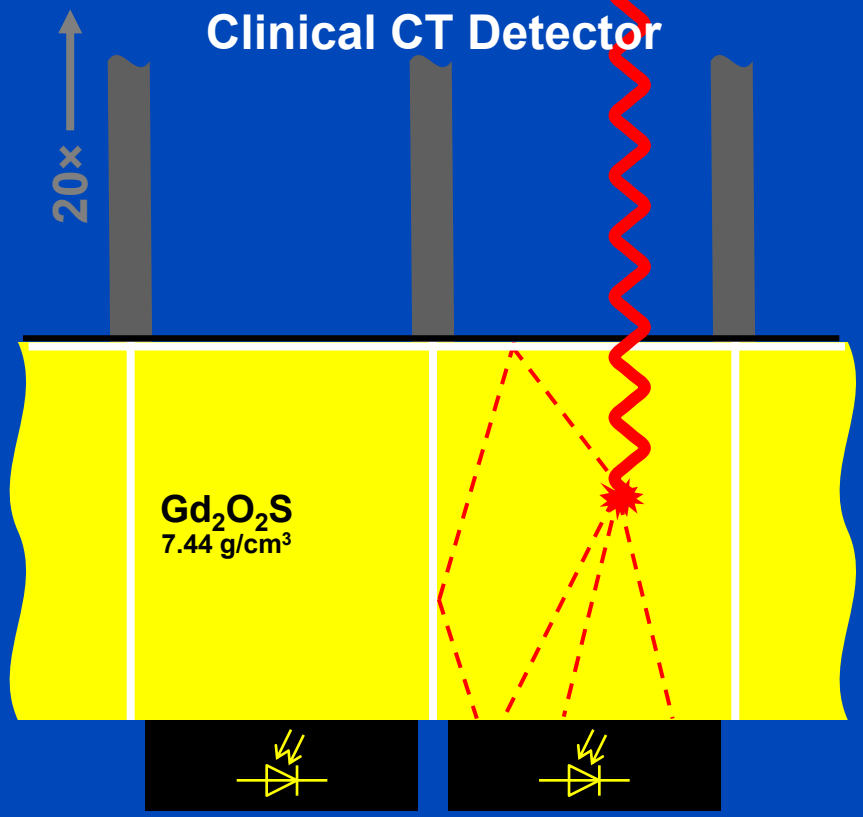

- Anti-scatter grids are aligned to the detector pixels
- Anti-scatter grids reject scattered radiation
- Detector pixels are of about 1 mm size
- Detector pixels are structured, reflective coating maximizes light usage and minimizes cross-talk
- Thick scintillators improve dose usage
- Gd_2O_2S is a high density scintillator with favourable decay times
- Individual electronics, fast read-out (e.g. 5 kHz)
- Very high dynamic range (10^7) can be realized

Flat Detector (CBCT)

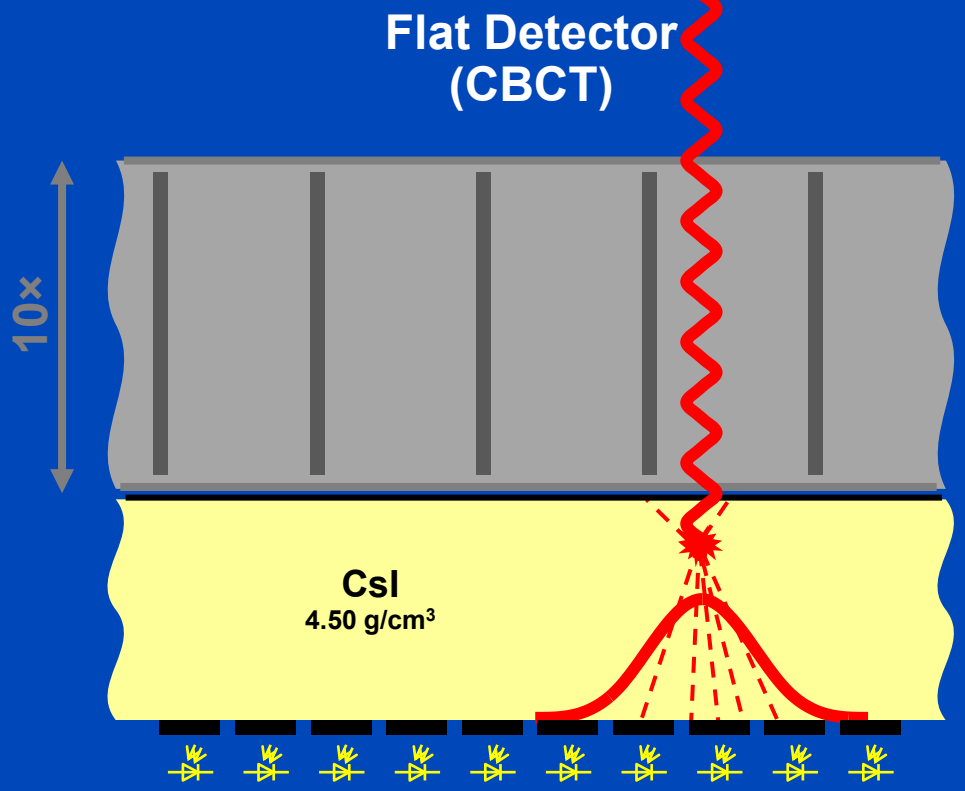

- Anti-scatter grids are not aligned to the detector pixels
- The benefit of anti-scatter grids is unclear
- Detector pixels are of about 0.1 to 0.2 mm size
- Detector pixels are unstructured, light scatters to neighboring pixels, there is significant cross-talk
- Thick scintillators decrease spatial resolution
- CsI grows columnar and suppresses light scatter to some extent
- Row-wise readout is rather slow (e.g. 25 Hz)
- Low dynamic range ($<10^3$), long read-out paths

Adaptive Array Technology 2002

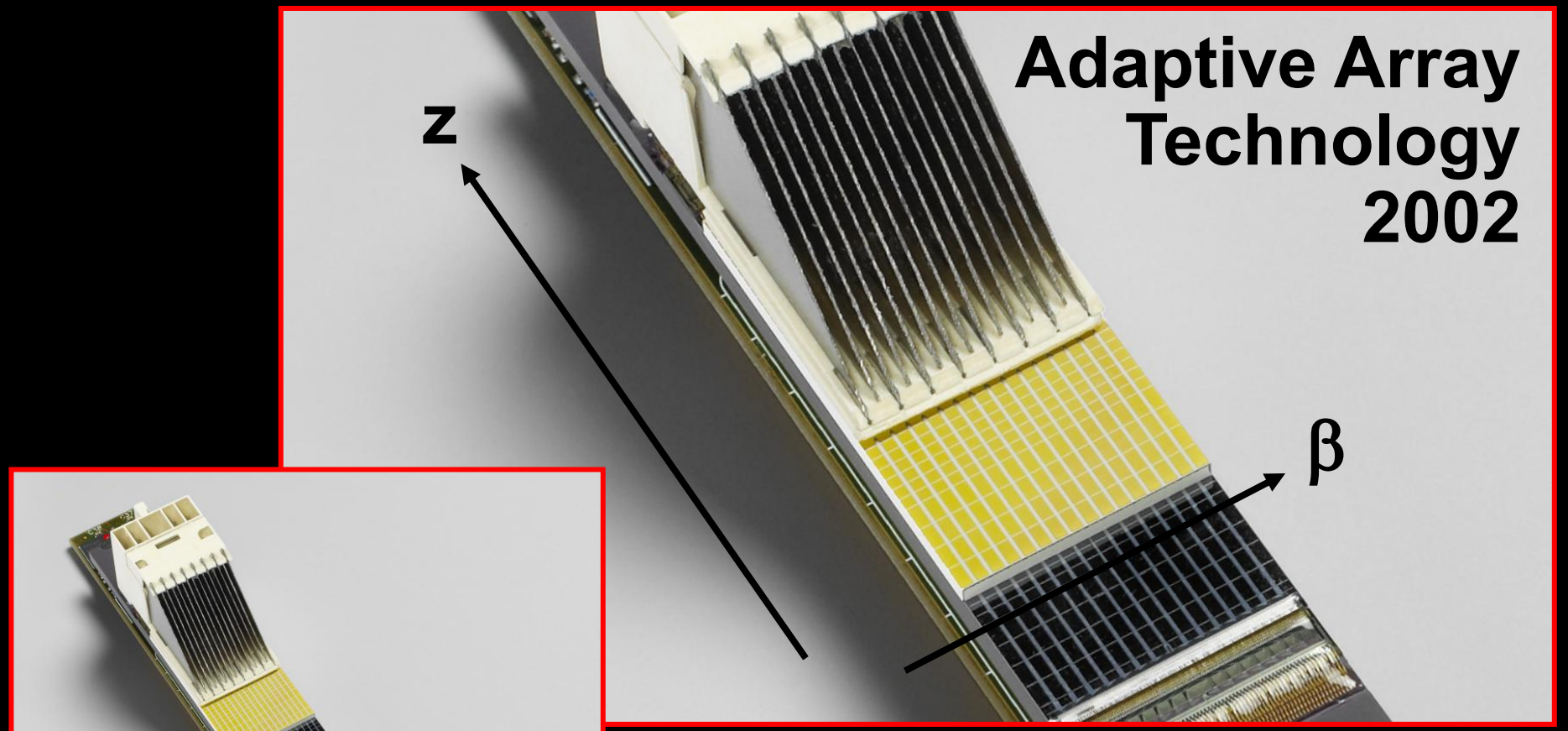

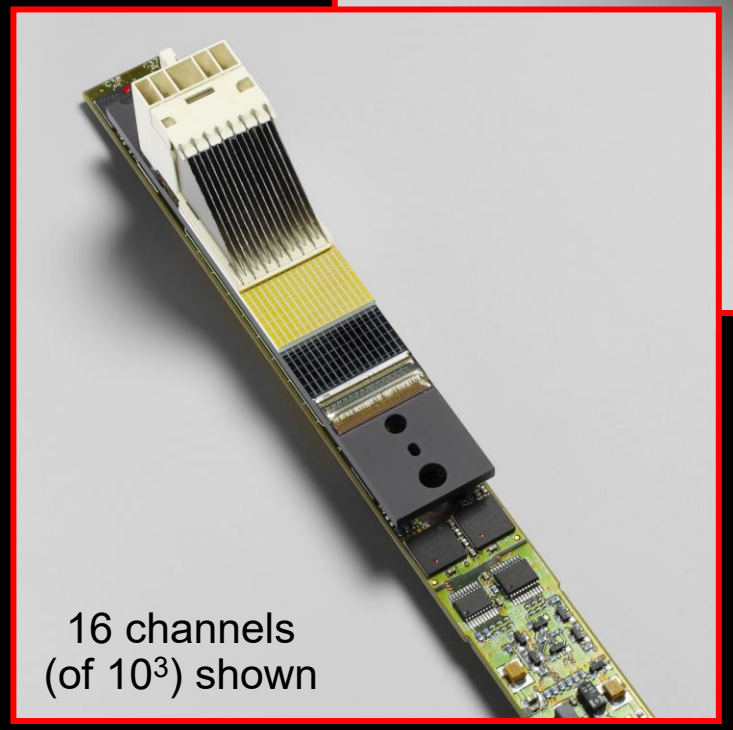

Photo courtesy of Siemens Healthcare, Forchheim, Germany

dkfz.

2007

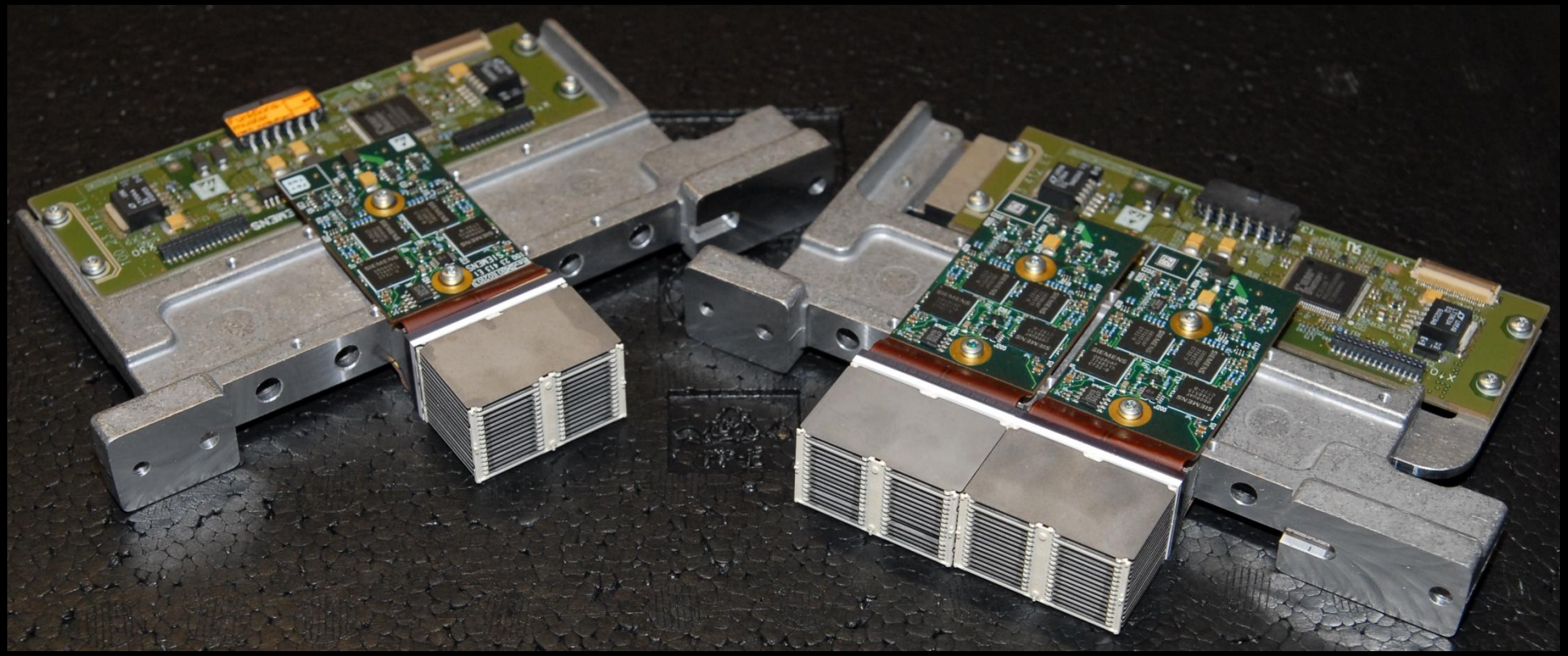

modular and 2D tileable, 1D anti-scatter grid,
modules arranged on the surface of a cylinder segment
(Photo courtesy by Siemens)

dkfz.

2007

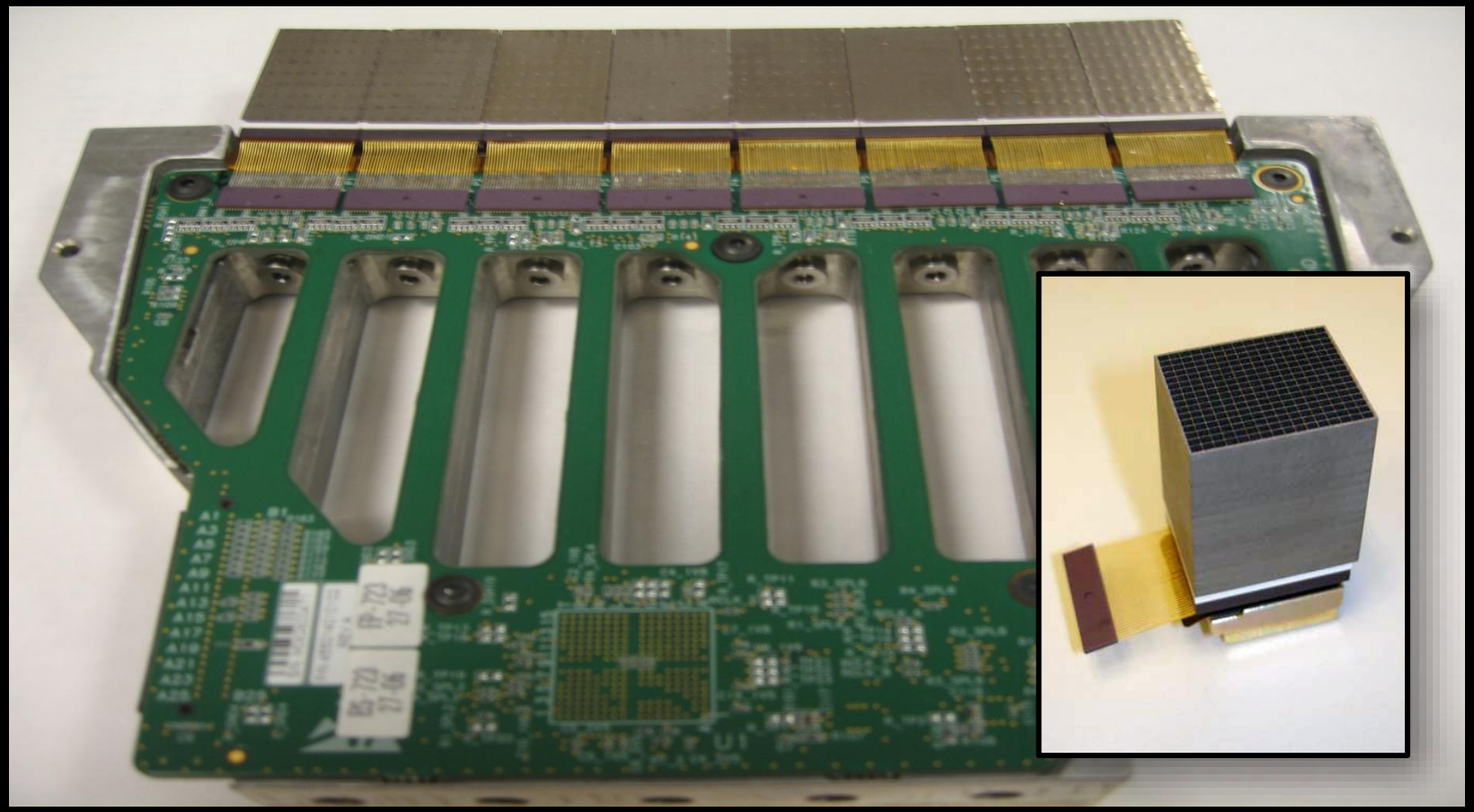

“Nano-panel detectors”, modular and 2D tileable, focussed 2D anti scatter grid
(Photo courtesy by Philips)

dkfz.

Fully Integrated Detector Electronics

- Electronics fully integrated into detector
- Very low electronic noise
- Less dose for infants, better images for obese

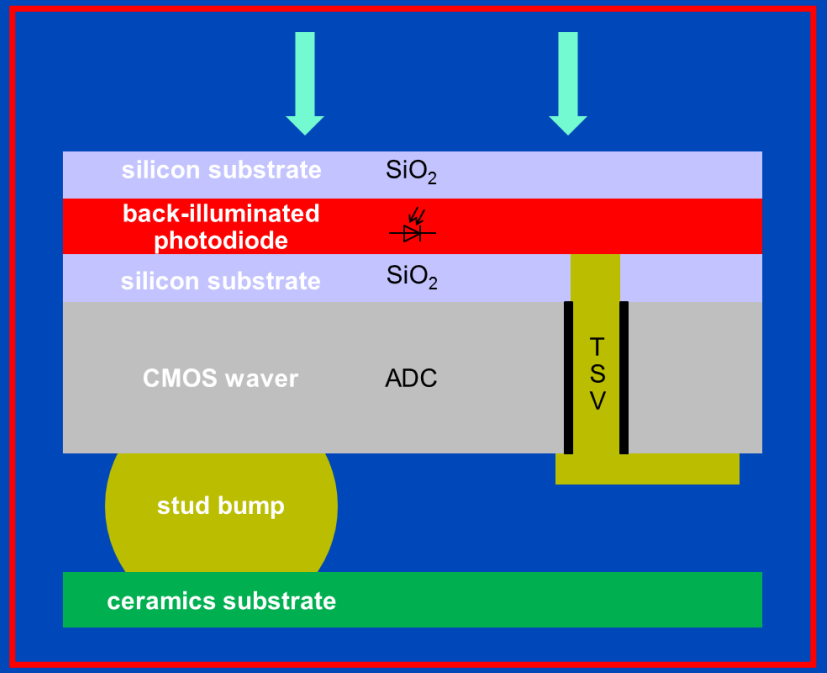

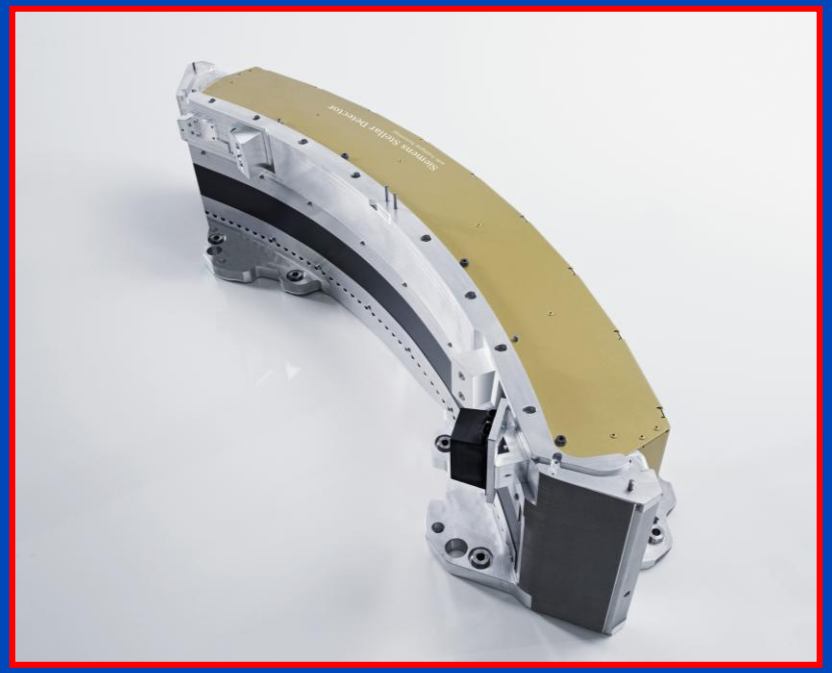

"Stellar detector", modular and 2D tileable, focussed 2D anti scatter grid. Photo courtesy by Siemens.

dkfz.

2012

“Stellar detector”, modular and 2D tileable, focussed 2D anti scatter grid. Photo courtesy by Siemens.

dkfz.

Ultra High Resolution Scans

- With energy-integrating detectors, UHR requires[1,2]
  - detector comb or detector grid
  - αFFS and/or zFFS
- Realizations
  - Somatom Flash and Force comb (0.61 mm → 0.33 mm)
  - Somatom Flash grid (0.61 mm → 0.33 mm and 0.56 mm → 0.53 mm)
- Dose loss
  - about 50% with comb (46% + penumbra for Flash or Force)
  - about 75% with grid (66% + penumbra for Flash)
- Dose penalty
  - about two-fold dose needed with comb
  - about three-fold dose needed with grid

Flash (0.7 mm × 0.8 mm focus)
- UHR: 1D comb
- zUHR: 2D grid

Force (0.4 mm × 0.5 mm focus)
- UHR: 1D comb
- sUHR: 1D comb + z-deconv

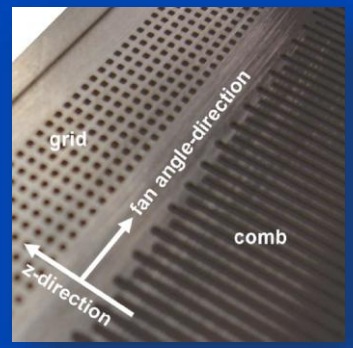

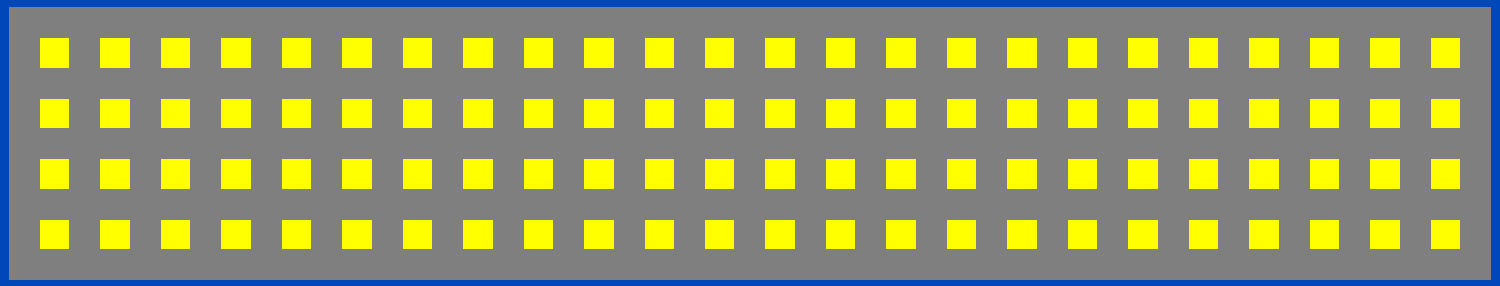

[1]Flohr et al. Novel ultrahigh resolution data acquisition and image reconstruction for multi-detector row CT. Med. Phys. 34(5):1712-1723, May 2007.
[2]Meyer et al. Initial results of a new generation DSCT system using only an in-plane comb filter for UHR temporal bone imaging. Eur Radiol 25:178-185, 2015.

dkfz.

Ultra High Resolution Scans

- Canon offers the Aquilion Precision, a system with dedicated ultra high resolution pixels
  - 0.25 mm pixel size at iso
  - 50% less septa thickness
  - 1792 channels
  - 160 detector rows
  - 1D anti scatter grid
  - 0.4 × 0.5 mm focal spot
  - 10800 rpm anode, liquid metal bearing
  - 512, 1024 or 2048 pixels per image
  - No need for post patient grid or comb: no dose penalty, small pixel effect can be utilized.

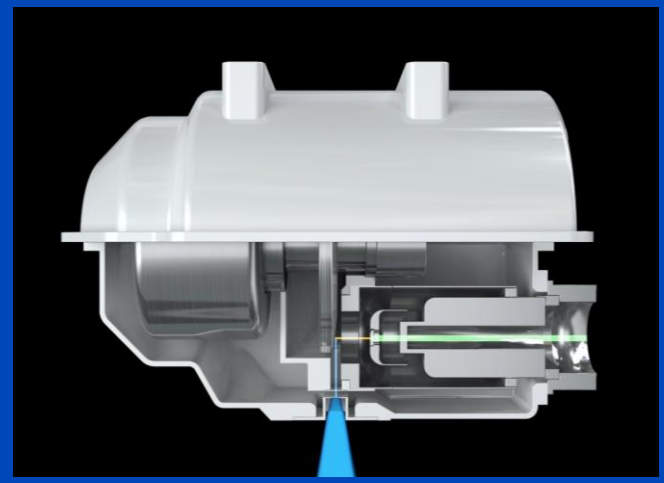

Image courtesy of Canon

dkfz.

Siemens Naeotom Alpha
The World‘s First Photon-Counting CT

- **Tubes**
  - tube A: 120 kW
  - tube B: 120 kW
  } ≈ ¼ MW
  - Focal spot size down to 181 µm
- **Detectors**
  - pixel size down to 150 µm
  - 288 detector rows
  - 2752 detector columns
- **Speed**
  - up to 4 rotations per second
  - up to 737 mm/s scan speed
  - down to 66 ms native temporal resolution
- **50 cm FOM**
- **Spectral**
  - VNC, VNCa (pure lumen), VMI

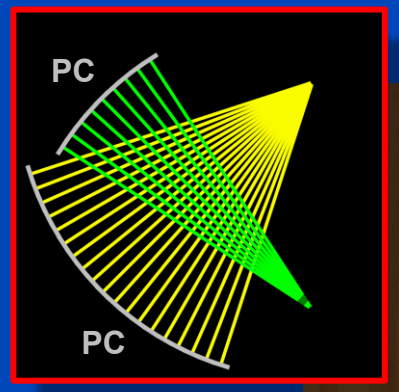

dkfz.

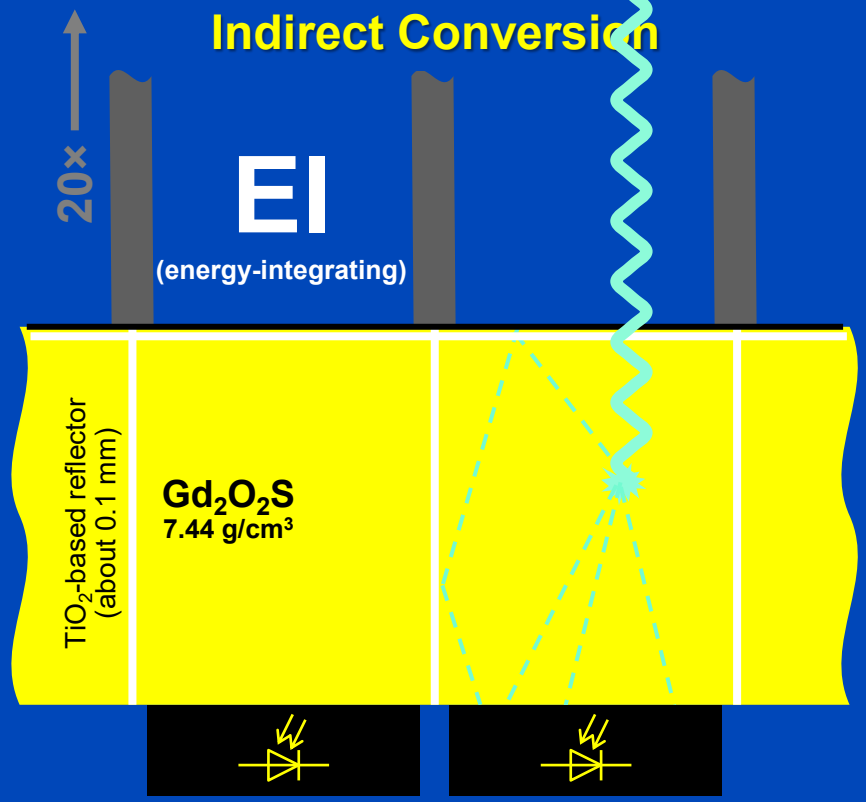

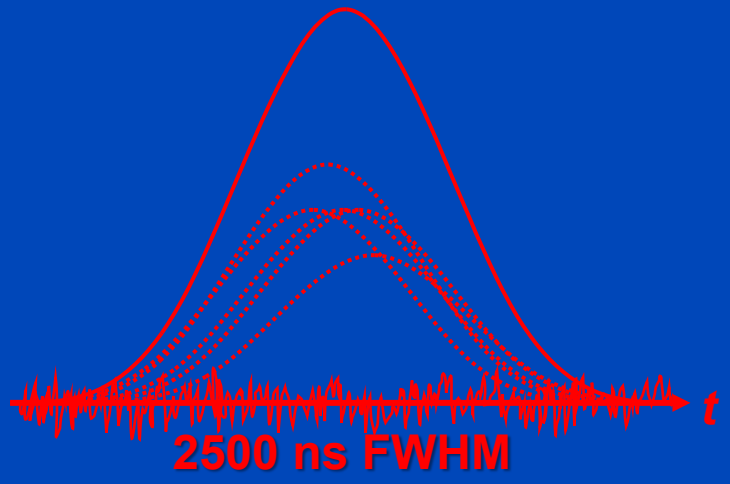

i.e. max O(40·10³) cps

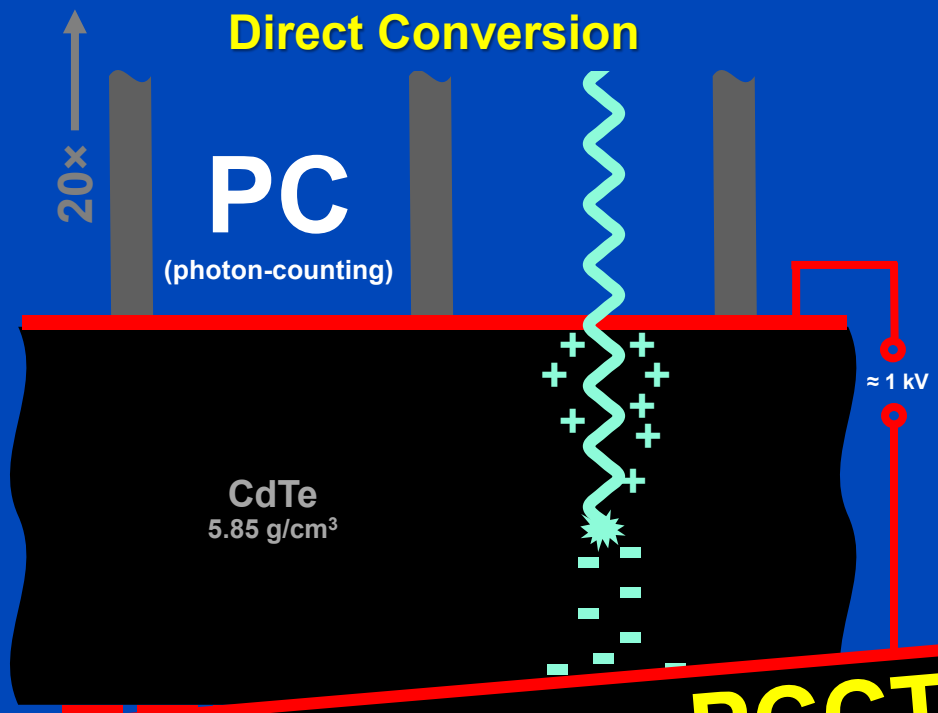

See lectures on PCCT by Peter Noël this Wednesday and Thursday

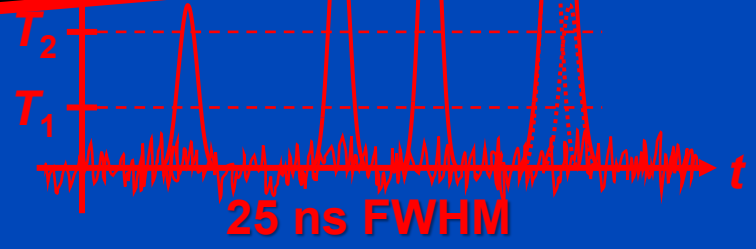

i.e. max O(40·10⁶) cps

Requirements for CT: up to 10^9 x-ray counts per second per mm^2. Hence, photon counting currently only achievable for direct converters.

Future YSO/SiPM (70 ns) or $LaBr_3$/SiPM (16 ns) indirect converters may also enable photon-counting CT.

dkfz.

Face-on and Edge-on Designs

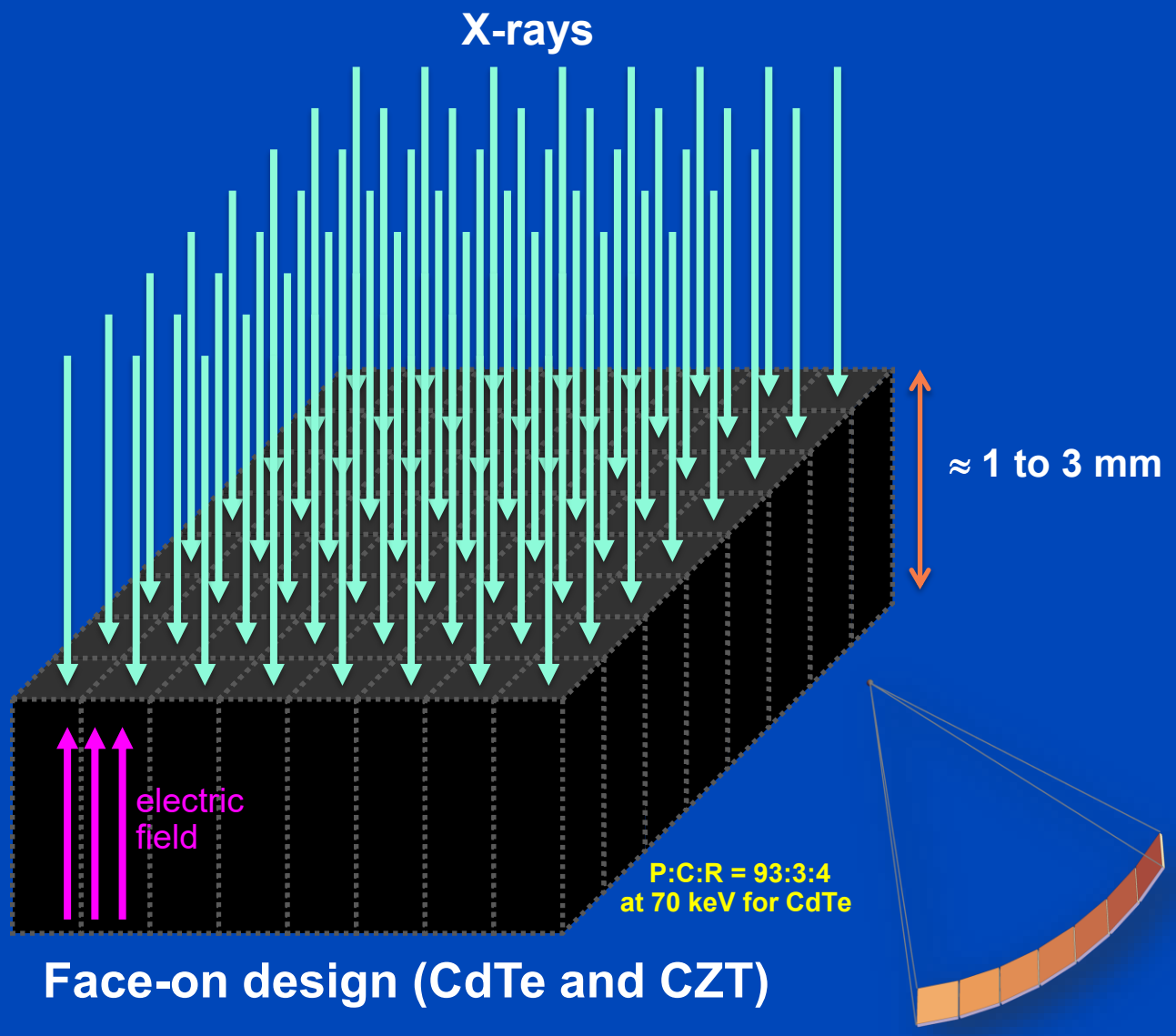

Face-on design (CdTe and CZT)

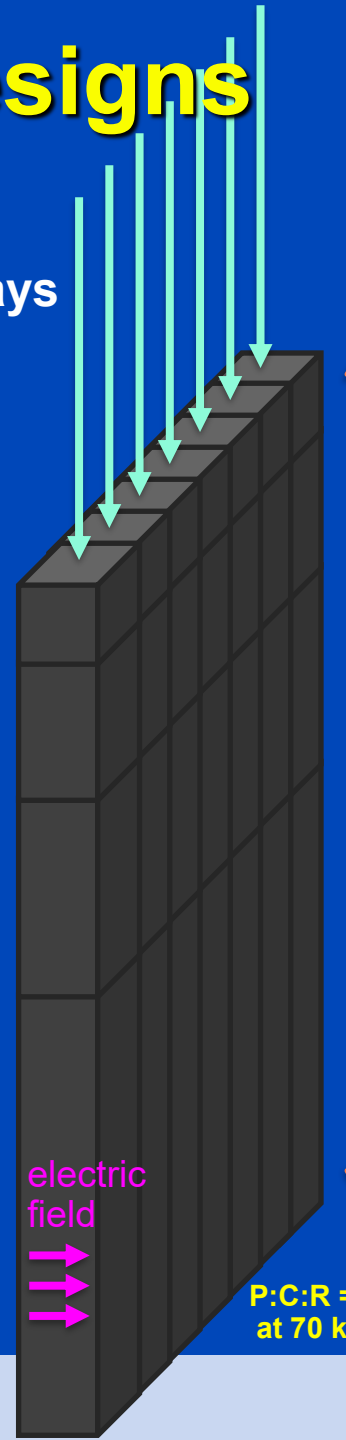

Edge-on design (Si)

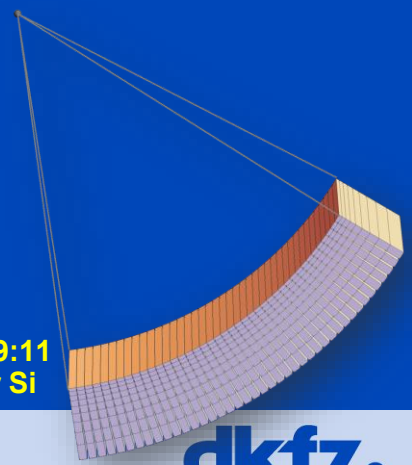

Only sensor material is shown. The electrodes are not shown. P:C:R = Photo:Compton:Rayleigh

dkfz.

Evolution of Spatial Resolution

similar to
2005: Somatom Flash (B70)

Pixel size 0.181 mm
Slice thickness 0.60 mm
Slice increment 0.30 mm
$MTF_{50\%}$ = 8.0 lp/cm
$MTF_{10\%}$ = 9.2 lp/cm

similar to
2014: Somatom CounT (U70)

Pixel size 0.181 mm
Slice thickness 0.20 mm
Slice increment 0.10 mm
$MTF_{50\%}$ = 12.1 lp/cm
$MTF_{10\%}$ = 16.0 lp/cm

scanned at
2021: Naeotom Alpha (Br98u)

10 mm

Pixel size 0.181 mm
Slice thickness 0.20 mm
Slice increment 0.10 mm
$MTF_{50\%}$ = 39.0 lp/cm
$MTF_{10\%}$ = 42.9 lp/cm

All measurements at Naeotom Alpha, Siemens Healthineers. QIR reconstructions such that the maximum spatial resolution of Flash, CounT and Alpha is demonstrated on the same sample. *C* = 1200 HU, *W* = 4000 HU

dkfz.

CT Systems 2024/2025

H = high-end, M = mid-range

CT System	Rotation, Cone, Coll.	Max. Power, Anode Angle, Name, Max. mA @ low kV	Patient-specific prefilters	Detector Configuration, Type, Name	FOM, Reconstruction Matrix	Special Reconstruction Algorithms	Spectral	
Canon Aquilion ONE Prism Edition	0.275 s, 15°, 160 mm	100 kW, 10°, MegaCool Vi, 600 mA @ 80 kV	Ag, {0, *x*} mm	320 × 0.5 mm, EI, PUREViSION	50 cm, 512	iterative (AIDR 3D), deep (AiCE, PIQE)	fast TVS with DL	H
Canon Aquilion Precision Edition	0.35 s, 3.8°, 40 mm	72 kW, 7°, MegaCool, 600 mA @ 80 kV	none	160 × 0.25 mm, EI, PUREViSION	50 cm, 512, 1024, 2048	iterative (AIDR 3D), deep (AiCE)	2 scans	H
GE Revolution Apex Elite	0.23 s, 15°, 160 mm	108 kW, 10°, Quantix 160, 1300 mA @ 70+80 kV	none	256 × 0.625 mm, EI, GemStone Clarity	50 cm, 512		fast TVS or 2 scans	H
GE Revolution Apex Plus	0.28 s, 7.6°, 80 mm	108 kW, 10°, Quantix 160, 1300 mA @ 70 kV	none	128 × 0.625 mm, EI, GemStone Clarity	50 cm, 512	deep (TrueFidelity), SnapshotFreeze	fast TVS or 2 scans	M
Philips Spectral CT 7500	0.27 s, 7.7°, 80 mm	120 kW, 8°, iMRC, 925 mA @ 80 kV	none	2 · 128 × 0.625 mm, EI, NanoPanel Prism	50 cm, 512, 768, 1024	iterative (iDose)	sandwich	H
Philips Incisive CT	0.35 s, 3.9°, 40 mm	80 kW, vMRC	none	2 · 64 × 0.625 mm, EI	50 cm, 512, 768, 1024	iterative (iDose), deep (Precise Image&Cardiac)		M
Siemens Somatom X.ceed	0.25 s, 3.7°, 38.4 mm	120 kW, 8°, Vectron, 1300 mA @ 70+80+90 kV	Sn, {0, 0.4, 0.7} mm	2 · 64 × 0.6 mm, EI, Stellar	50 cm, 512, 768, 1024	iterative (ADMIRE)	split filter (Twin Beam) or 2 scans (Twin Spiral)	M
Siemens Somatom Force	0.25 s, 5.5°, 57.6 mm	2 · 120 kW, 8°, Vectron, 2 · 1300 mA @ 70+80+90 kV	Sn, {0, 0.6} mm	2 · 2 · 96 × 0.6 mm, EI, Stellar	50 cm/35 cm, 512, 768, 1024	iterative (ADMIRE)	DSCT	H
Siemens Naeotom Alpha.Prime	0.25 s, 3.6°, 38.4 mm	1 · 120 kW, 8°, Vectron, 2 · 1300 mA @ 70+90 kV	Sn, {0, 0.4} mm	144×0.4 or 120×0.2 mm, PC, QuantaMax	50 cm, 512, 768, 1024	iterative (QIR)	PCCT	H
Siemens Naeotom Alpha.Pro	0.25 s, 5.4°, 57.6 mm	2 · 120 kW, 8°, Vectron, 2 · 1300 mA @ 70+90 kV	Sn, {0, 0.4, 0.7} mm	2 · 96×0.4 or 2 · 120×0.2 mm, PC, QuantaMax	50 cm/36 cm, 512, 768, 1024	iterative (QIR)	DSCT, PCCT	H
Siemens Naeotom Alpha.Peak	0.25 s, 5.4°, 57.6 mm	2 · 120 kW, 8°, Vectron, 2 · 1300 mA @ 70+90 kV	Sn, {0, 0.4, 0.7} mm	2 · 144×0.4 or 2 · 120×0.2 mm, PC, QuantaMax	50 cm/36 cm, 512, 768, 1024	iterative (QIR)	DSCT, PCCT	H

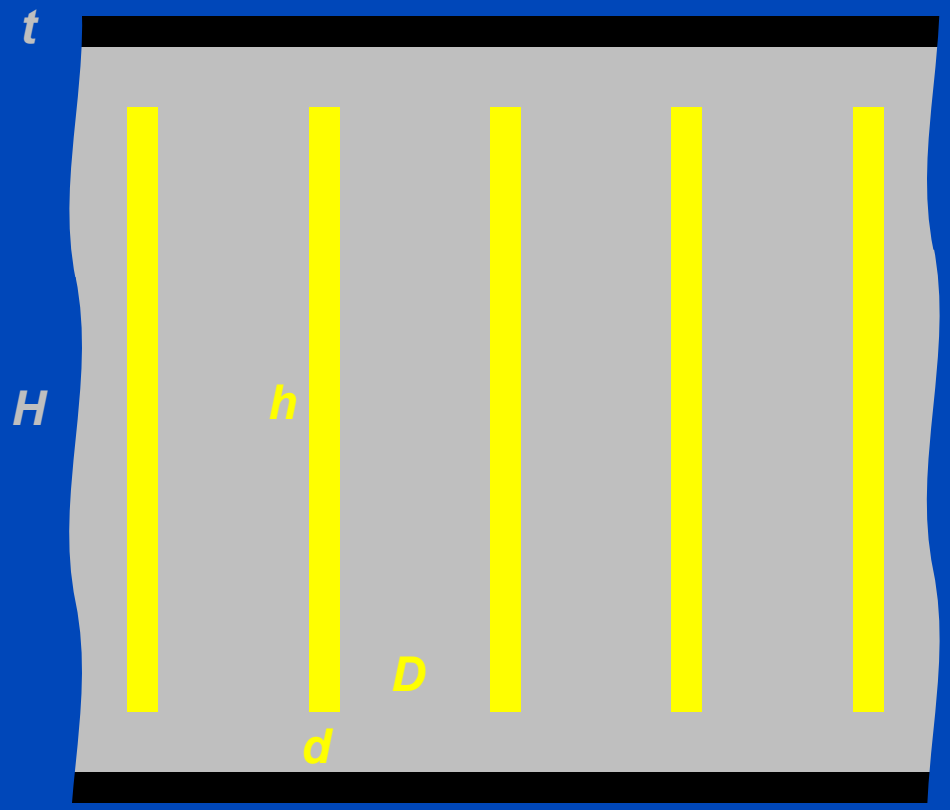

Cover thickness: *t*, e.g. 0.2 mm Al or 0.25 mm C
Height of strips: *h*
Thickness of strips: *d*, e.g. 0.04 mm Pb
Gap between strips: *D*, e.g Al or C-fiber
Grid ratio: *h*/*D*, e.g. 8 or 15
Grid frequency: 1/(*D*+*d*), e.g. 40/cm
Geometrical efficiency: *D*/(*D*+*d*)
Height of interspace material: *H*

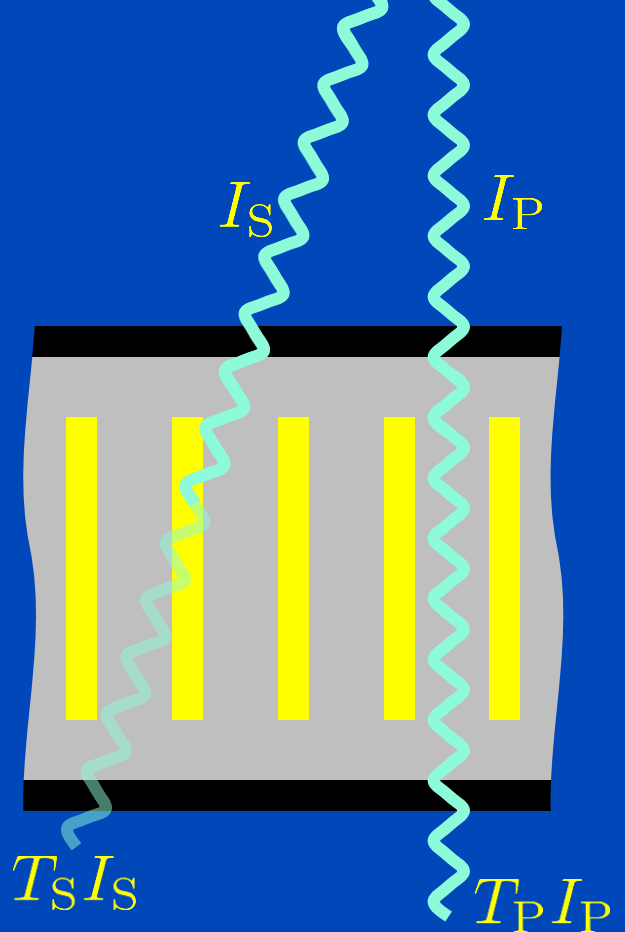

Primary intensity: I_P
Scatter intensity: I_S
Primary transmission: $T_P < 1$, e.g. 75%
Scatter transmission: $T_S > 0$, e.g. 30%

No grid: $T_P = T_S = 1$
Ideal grid: $T_P = 1$, $T_S = 0$

Drawn to grid ratio 4:1 and infinite focus distance.

dkfz.

To Grid or not to Grid?

- Only primary counts for the signal, but primary and scatter count for noise. Thus,

$$\mathrm{SNR} = \frac{T_\mathrm{P} I_\mathrm{P}}{\sqrt{T_\mathrm{P} I_\mathrm{P} + T_\mathrm{S} I_\mathrm{S}}}$$

- SNR improvement factor (SNR with grid / SNR no grid)

$$\mathrm{SNR}_\mathrm{if} = T_\mathrm{P} \frac{\sqrt{I_\mathrm{P} + I_\mathrm{S}}}{\sqrt{T_\mathrm{P} I_\mathrm{P} + T_\mathrm{S} I_\mathrm{S}}}$$

- The case $T_S = 0$ is instructive and yields

$$\mathrm{SNR}_\mathrm{if} \leq \sqrt{T_\mathrm{P}} \sqrt{1 + \mathrm{SPR}}$$

  with SPR being the scatter-to-primary ratio.

- Use a grid only for cases with $\mathrm{SNR}_\mathrm{if} \geq 1$.
- Scatter correction and noise reduction algorithms are to be used complementary and not as an alternative to grids!

Detector Technology

Clinical CT Detector Module

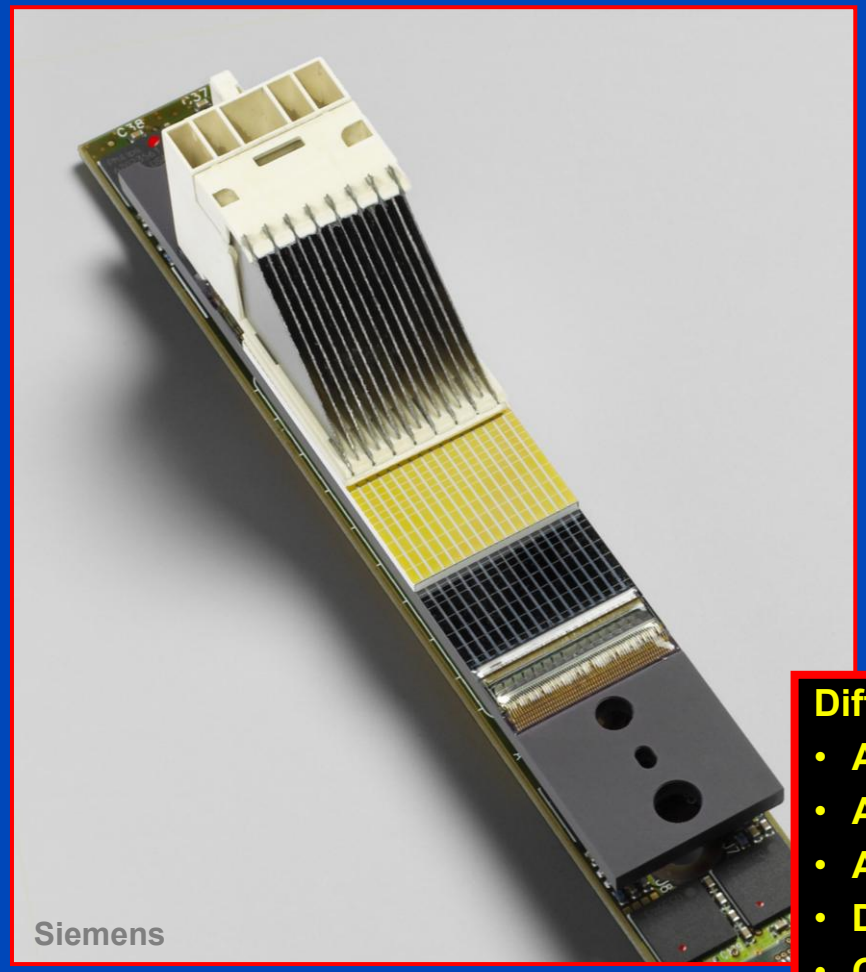

Siemens

Flat Detector (e.g. 40 × 30 cm)

Varex

Differences in:

- Absorption efficiency
- Afterglow
- Anti scatter grid
- Dynamic range
- Cross-talk
- Framerate
- …

dkfz.

Sensor Dose Efficiency

	Clinical CT (120 kV)			CBCT (120 kV)			Photon Counting CT (120 kV)		
Material	Gd_2O_2S			CsI			CdTe		
Density	7.44 g/cm^3			4.5 g/cm^3			5.85 g/cm^3		
Thickness	1.4 mm			0.6 mm			1.6 mm		
Manufacturer	Siemens			Varian			Siemens CounT + Alpha		
Water Layer	0 cm	20 cm	40 cm	0 cm	20 cm	40 cm	0 cm	20 cm	40 cm
Photons absorbed	96.2%	92.7%	89.8%	73.5%	59.2%	50.9%	94.5%	88.2%	83.1%
Energy absorbed	94.3%	90.7%	87.9%	66.4%	53.9%	46.6%	91.2%	84.8%	79.9%

Absorption values are relative to a detector of infinite thickness.

The energy absorption coefficient μ_{en} was used to estimate the absorption values.

dkfz.

X-Ray Exposure Dynamic Range *D*

- ***D*** **= saturation exposure / quantum-limited exposure**
  - **Saturation exposure N_{max}: Exposure where the detector runs into saturation**
  - **Quantum-limited exposure N_{min}: Exposure where the x-ray quantum noise equals the detector‘s electronic noise.**
- **Measurements[1]**
  - **Saturation signal: Increase exposure until you obtain $E(S_{max})$ in the offset-corrected reading.**
  - **Relation $S = k \cdot N$: Evaluate an offset-corrected medium level exposure to obtain a pair of values $Var(S_{med})$ and $E(S_{med})$. Now, use the relation $Var(N_{med}) = E(N_{med})$ with $Var(S_{med}) = k^2 \cdot Var(N_{med})$ and $E(S_{med}) = k \cdot E(N_{med})$ to find $k = Var(S_{med}) / E(S_{med})$.**
  - **Electronic noise: Determine $Var(S_{min})$ from the subtraction of two dark images.**
- **X-ray exposure dynamic range**

$$D = \frac{\mathrm{E}(N_{\max})}{\mathrm{E}(N_{\min})} = \frac{\mathrm{E}(S_{\max})/k}{\mathrm{Var}(S_{\min})/k^2} = \frac{\mathrm{E}(S_{\max})\mathrm{Var}(S_{\mathrm{med}})}{\mathrm{E}(S_{\mathrm{med}})\mathrm{Var}(S_{\min})}$$

[1]Instead of doing this very simple procedure one may want to use statistically optimal estimates. One may use many readings, and many exposure levels. One may further determine *D* on a pixel-by-pixel basis.

dkfz.

Dynamic Range Required for Diagnostic Image Quality

- Soft tissue μ = 0.0192/mm object of diameter D between D_{min} = 80 mm and D_{max} = 400 mm with a lesion of diameter d = 5 mm and contrast δ = 5 HU = 0.005.
- Number of photons to be registered at the detector:

$$I(D, \delta d) = I_0 e^{-\mu D - \mu \delta d}$$

- Minimal signal difference to be detected:

$$I(D_{\max}, \delta d) - I(D_{\max}, 0) \approx \mu \delta d I(D_{\max}, 0)$$

- Maximum signal to be detected:

$$I(D_{\min}, 0)$$

- Thus, the dynamic range required in diagnostic CT is in the order of

$$\frac{I(D_{\min}, 0)}{\mu \delta d \, I(D_{\max}, 0)} \approx 10^6 \approx 2^{20}$$

Dynamic Range in Flat Detectors

	Saturation-to-noise range			X-ray exposure range				Digital range	
	Electronic noise (ADU)	Saturation signal (ADU)	Dynamic range	Quantum limited exposure (μR)	Saturation exposure (μR)	Dynamic range	Eff. bit depth (bits)	Quantization range	Eff. bit depth (bits)
No binning, gain 2	**A1**	**B1**	**B1/A1**	**A2**	**B2**	**C2=B2/A2**	**D2=lb(C2)**	**B1:1**	**lb(B1)**
Dynamic gain switching	5.32	80500	15100	2.75	3550	**1291**	**10.3**	80500:1	16.3
0.5 pF fixed	5.32	14500	2700	2.75	595	**216**	**7.8**	14500:1	13.8
4 pF fixed	3.57	14800	4150	35.7	4200	**118**	**6.9**	14800:1	13.8
2x2 binning, gain 1									
Dual gain readout	4.33	80100	18500	1.00	1800	**1800**	**10.8**	80100:1	16.3
Dynamic gain switching	4.37	84200	19300	1.03	2062	**2002**	**11.0**	84200:1	16.4
0.5 pF fixed	4.37	14300	3300	1.03	311	**302**	**8.2**	14300:1	13.8
4 pF fixed	3.14	14800	4700	15.6	2104	**135**	**7.1**	14800:1	13.8
0.5 pF fixed, gain 2 (fluoroscopy mode)	7.25	12900	1700	0.71	125	**176**	**7.5**	12900:1	13.6

Table 2 4030CB dynamic range in available imaging modes

A2 is defined as the exposure where QuantumNoise=ElectronicNoise.

$$D = \frac{80500/k}{5.32^2/k^2} = 1291 \quad \text{if} \quad k = 0.45$$

Table taken from [Roos et al. “Multiple gain ranging readout method to extend the dynamic range of amorphous silicon flat panel imagers,” *SPIE Medical Imaging Proc.*, vol. 5368, pp. 139-149, 2004]. Additional values were added, for convenience.

dkfz.

Dynamic Range in Flat Detectors

Detector		Saturation-to-noise range				X-ray exposure range					
Type	Mode	Electronic noise	Quantum limited signal	Saturation signal	Dynamic range	Quantum limited exposure (µR)	Saturation exposure (µR)	Dynamic range	Eff. Bit depth	k	Remark
Varian 4030CB	Dynamic gain switching	5.32	**62.89**	80500	15100	2.75	3550	1291	10.3	**0.45**	
	0.5 pF fixed	5.32	**67.39**	14500	2700	2.75	595	216	7.8	**0.42**	
	4.0 pF fixed	3.57	**283.02**	14800	4150	35.7	4200	118	6.9	**0.10**	
Perkin Elmer Dexela 2923	**?**	**4.91**	**33.01**	**13600**	**2770.6**	**?**	**?**	**412.02**	**8.69**	**0.73**	**Integration time 100 ms**
	?	**6.36**	**55.37**	**13600**	**2139.6**	**?**	**?**	**245.7**	**7.94**	**0.73**	**Integration time 1000 ms**

Table 1: Dynamic range for different detectors and imaging modes. Data for Varian 4030CB taken from [1].

- **Electronic noise is measured as the pixel standard deviation of the subtraction of two dark images[1]. For the Dexela 2923 detector it was observed, that the electronic noise increases for higher integration times and thus the dynamic range decreases.**
- **Saturation signal is defined as the maximum signal in the linear signal range.**

[1] **Roos et al. – Multiple gain ranging readout method to extend the dynamic range of amorphous silicon flat panel imagers**

dkfz.

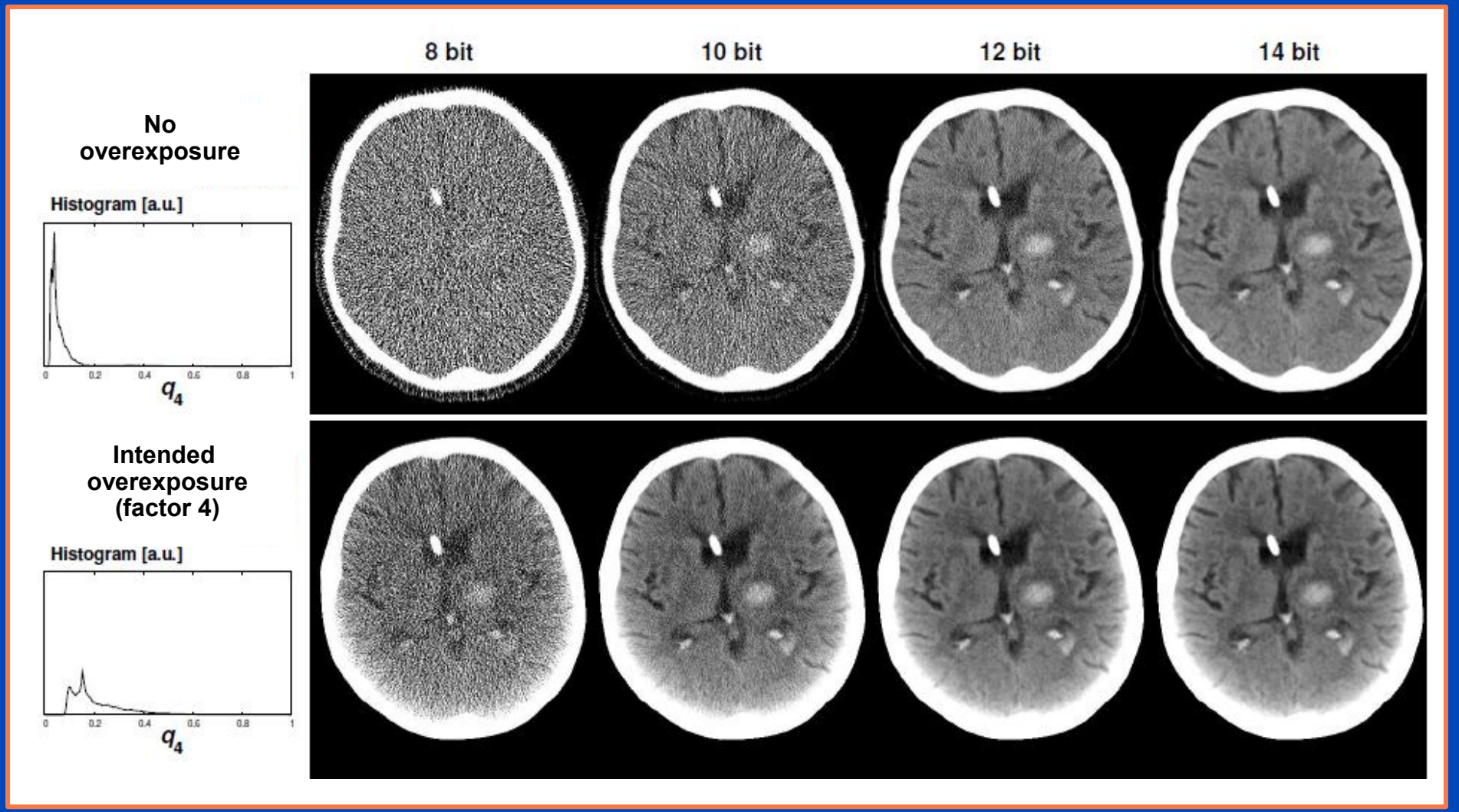
8 bit
10 bit
12 bit
14 bit
No overexposure
Histogram [a.u.]
0
0.2
0.4
0.6
0.8
1
q_4
Intended overexposure (factor 4)
Histogram [a.u.]
0
0.2
0.4
0.6
0.8
1
q_4

To Bin or not to Bin?

(the continuous view)

This nice phrase was coined by Norbert Pelc.

- We have $\mathrm{PSF}(x) = s(x) * a(x)$ and $\mathrm{MTF}(u) = S(u)A(u)$.
- From Rayleigh's theorem we find noise is

$$\sigma^2 = \int dx\, a^2(x) = \int du\, A^2(u) = \int du\, \frac{\mathrm{MTF}^2(u)}{S^2(u)}$$

- Compare small (A) with large (B) ...

Avoid binning, if possible!

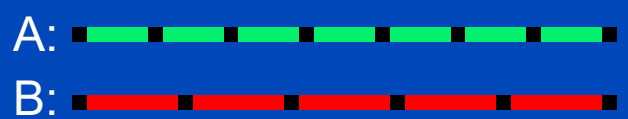

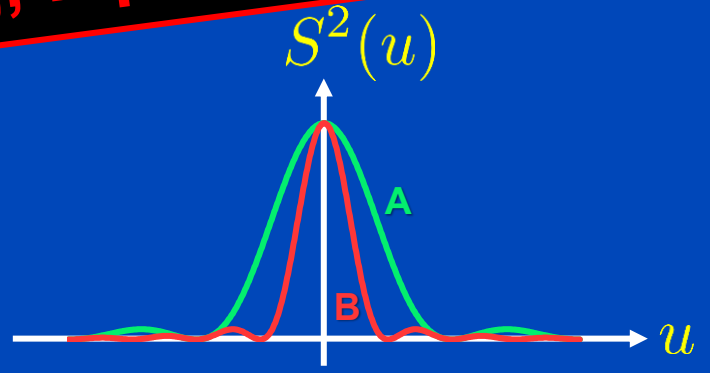

- We have $S_\mathrm{A}(u) > S_\mathrm{B}(u)$ and thus $\sigma^2_\mathrm{A} < \sigma^2_\mathrm{B}$.
- A desired MTF may be best achieved with smaller pixels.

Kachelrieß, Kalender. Med. Phys. 32(5):1321-1334, May 2005
Baek, Pineda, and Pelc. PMB 58:1433-1446, 2013

dkfz.

To Bin or not to Bin?[1]

(the discrete view, LI)

- Let detector B be the 2-binned version of detector A:

$$B_{2n} = \tfrac{1}{2}(A_{2n} + A_{2n+1}) \qquad \mathrm{Var}B = \tfrac{1}{2}\mathrm{Var}A$$

- Assume LI to be used to find in-between pixel values. Wlog we may then consider B to be upsampled with mid-point interpolation to the pixel size of detector A:

$$\hat{B} = (\ldots)$$

- To obtain t… we need to convolve A…

$$a = \tfrac{1}{2}(1,\ 1) * \tfrac{1}{4}(1,\ 2,\ 1) = \tfrac{1}{8}(1,\ 3,\ 3,\ 1)$$

20% more noise variance may be compensated by 20% more x-ray dose. Any alternative? Yes:

Avoid binning, if possible!

In 2D binning implies 44% more noise variance or dose. Again, the answer is: „not to bin“.

- Noise propagation yields 20% more noise (variance) for the binned detector[2]:

$$\mathrm{Var}\hat{A} = \tfrac{20}{64}\mathrm{Var}A = \tfrac{5}{16}\mathrm{Var}A$$

$$\mathrm{Var}\hat{B} = \tfrac{3}{8}\ \mathrm{Var}A = \tfrac{6}{5}\ \mathrm{Var}\hat{A} = 1.2\,\mathrm{Var}\hat{A}$$

[1] Kachelrieß, Kalender. Med. Phys. 32(5):1321-1334, May 2005

[2] Noise consideration valid for uncorrelated pixel noise in the unbinned detector.

dkfz.

The “Small Pixel Effect”

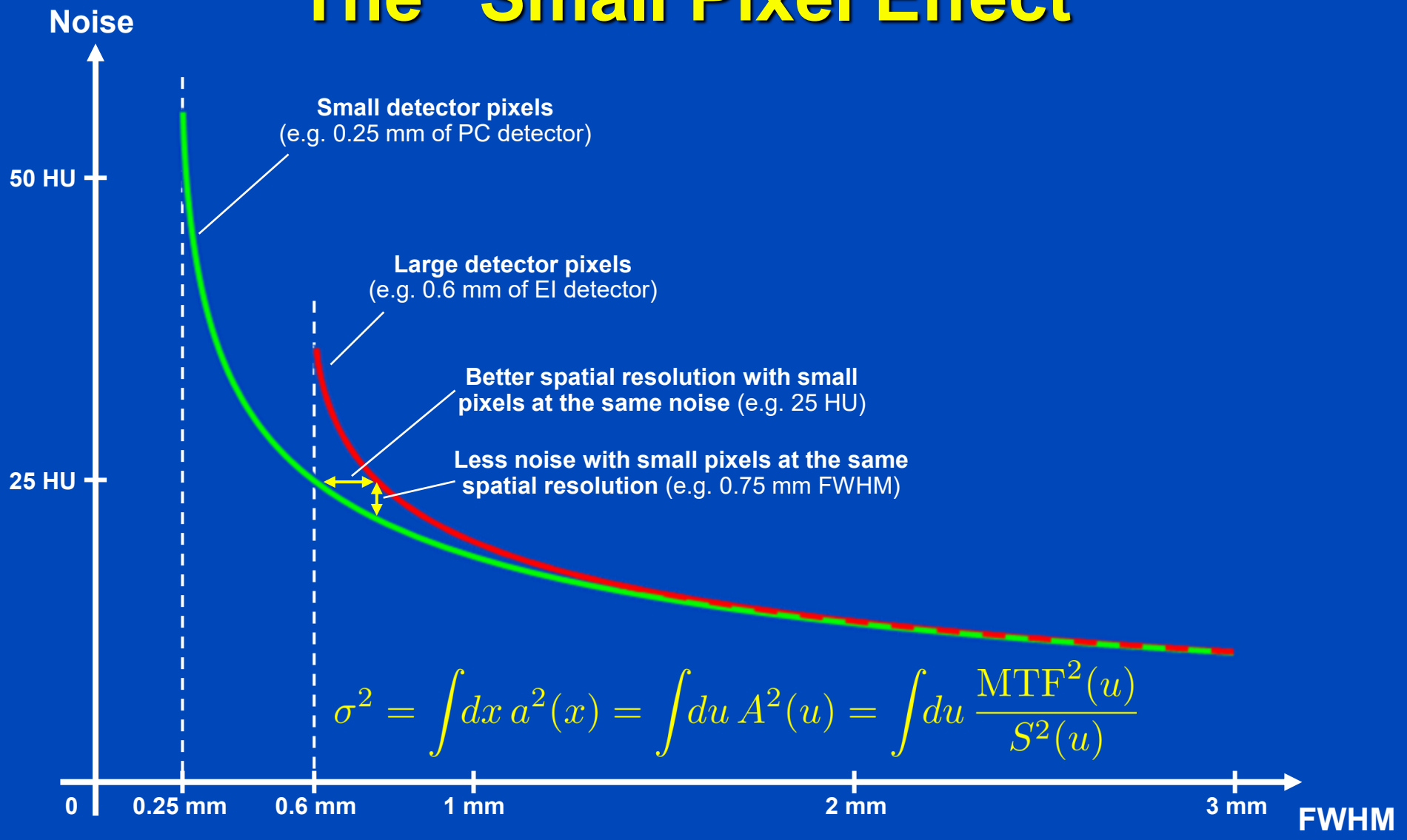

Kachelrieß, Kalender. Med. Phys. 32(5):1321-1334, May 2005

dkfz.

Detector Pixel Force vs. Alpha

Force
920 × 96 detector pixels
pixel size 0.52 × 0.56 mm at iso
avg. sampling 0.56 × 0.6 mm at iso
57.6 mm z-coverage

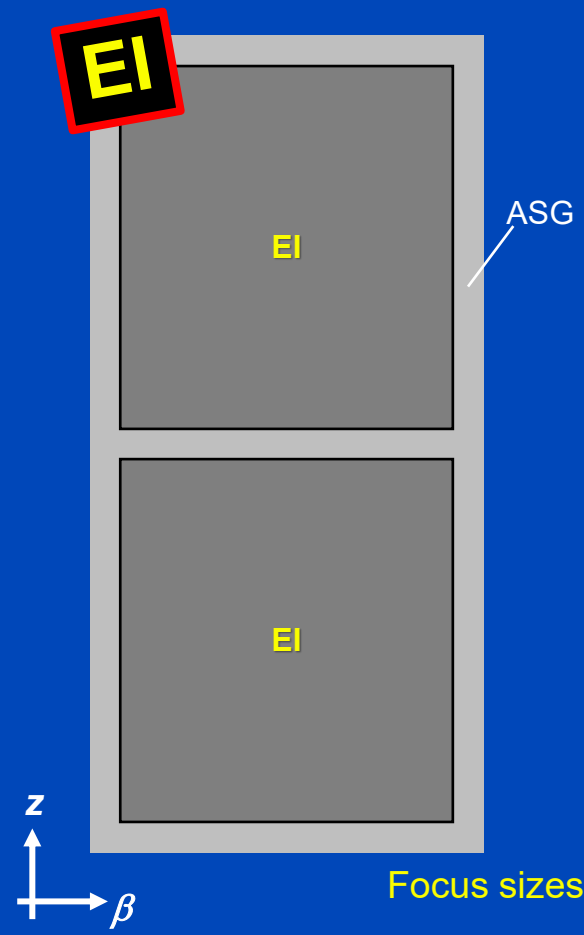

Alpha (Std, Quantum Plus)
1376 × 144 macro pixels
pixel size 0.3 × 0.352 mm at iso
avg. sampling 0.344 × 0.4 mm at iso
57.6 mm z-coverage

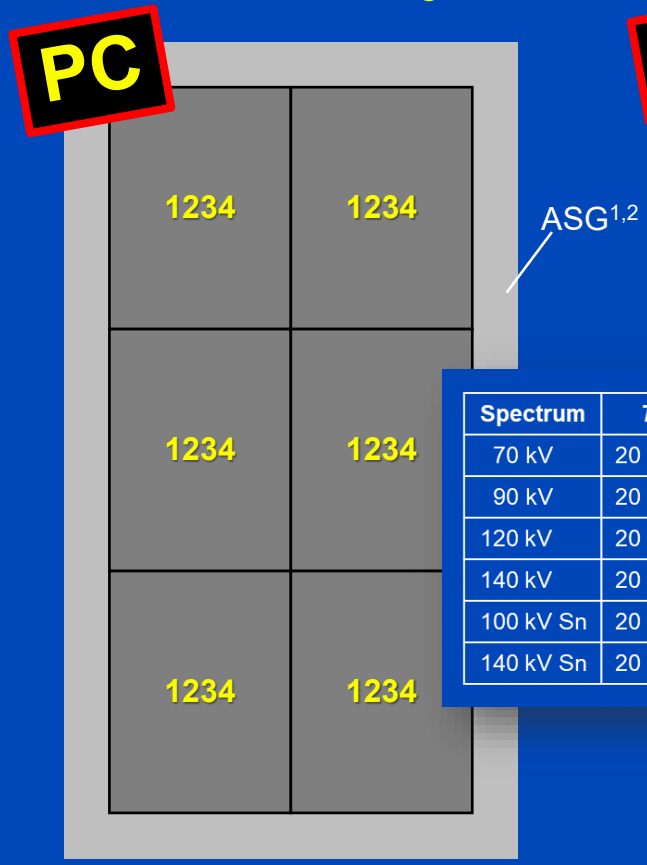

Spectrum	T_1	T_2
70 kV	20 keV	50 keV
90 kV	20 keV	60 keV
120 kV	20 keV	65 keV
140 kV	20 keV	70 keV
100 kV Sn	20 keV	65 keV
140 kV Sn	20 keV	80 keV

Alpha (UHR, QuantumHD)
2752 × 120 pixels
pixel size 0.151 × 0.176 mm at iso
avg. sampling 0.172 × 0.2 mm at iso
24 mm z-coverage

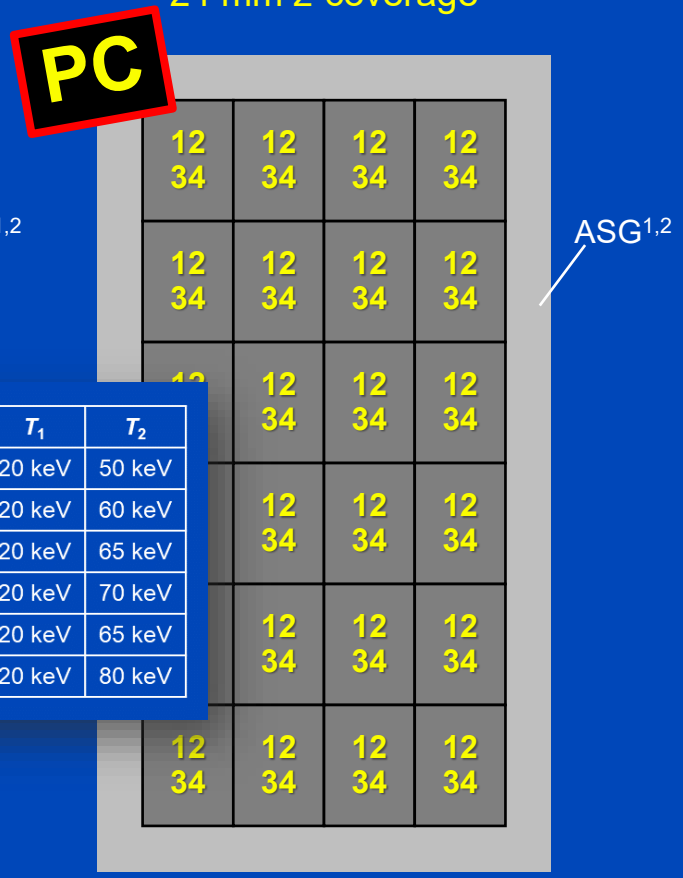

Focus sizes (Vectron): 0.181×0.226 mm, 0.271×0.7316 mm, 0.362×0.497 mm at iso
which are 0.4×0.5 mm, 0.6×0.7 mm, 0.8×1.1 mm at focal spot

[1]J. Ferda et al. Computed tomography with a full FOV photon-counting detector in a clinical setting, the first experience. European Journal of Radiology 137:109614, 2021
[2]Rajendran et al. Full field-of-view, high-resolution, photon-counting detector CT: technical assessment and initial patient experience. Phys. Med. Biol. 66:205019, 2021

dkfz.

Small Pixel Effect at Naeotom Alpha

Medium Phantom, 4 mGy $CTDI_{32}$

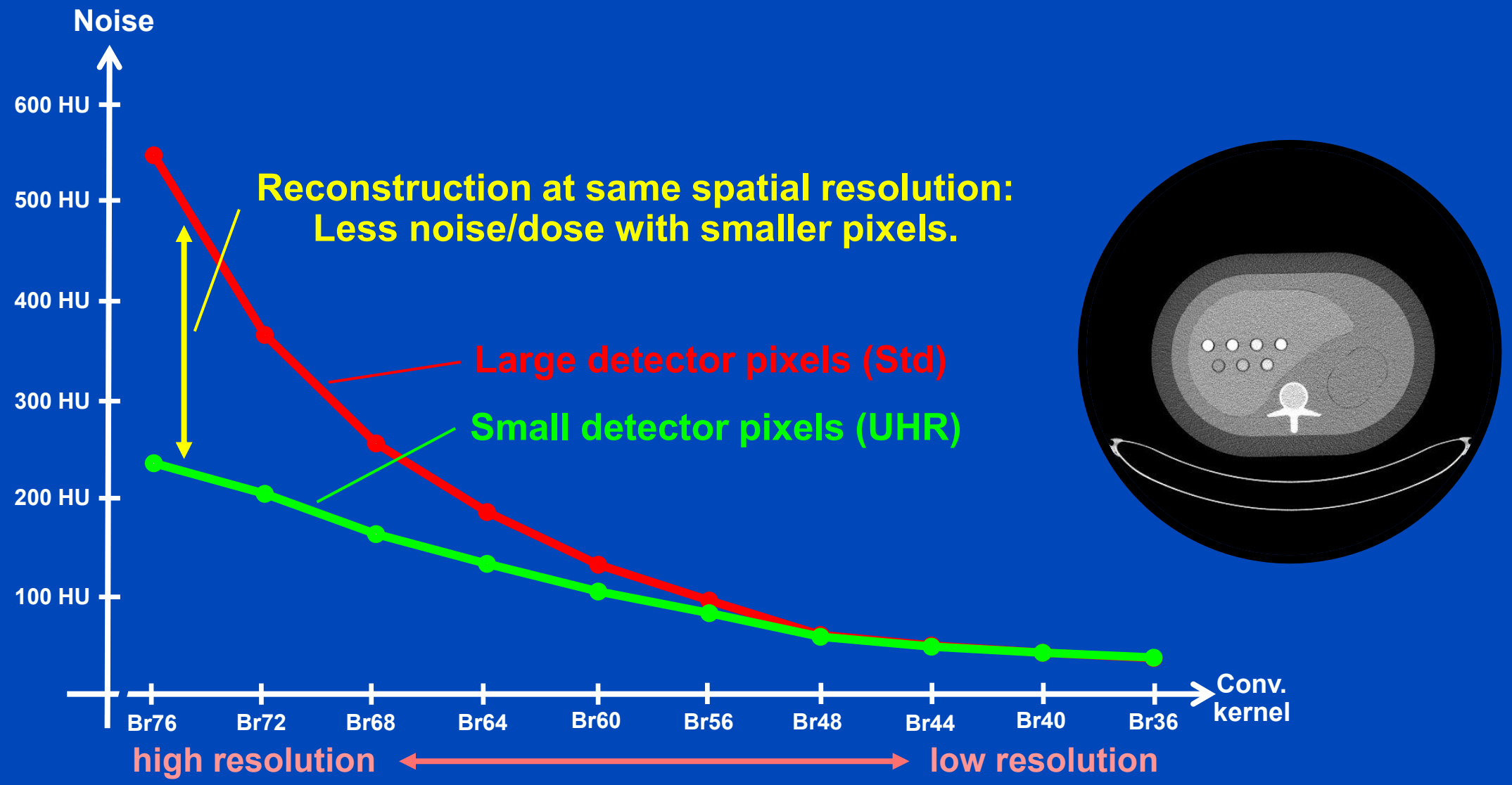

To disable the longitudinal small pixel effect, we reconstructed rather thick slices (1 mm thickness).

dkfz.

All images reconstructed with 1024^2 matrix and 0.15 mm slice increment.

C = 1000 HU, *W* = 3500 HU

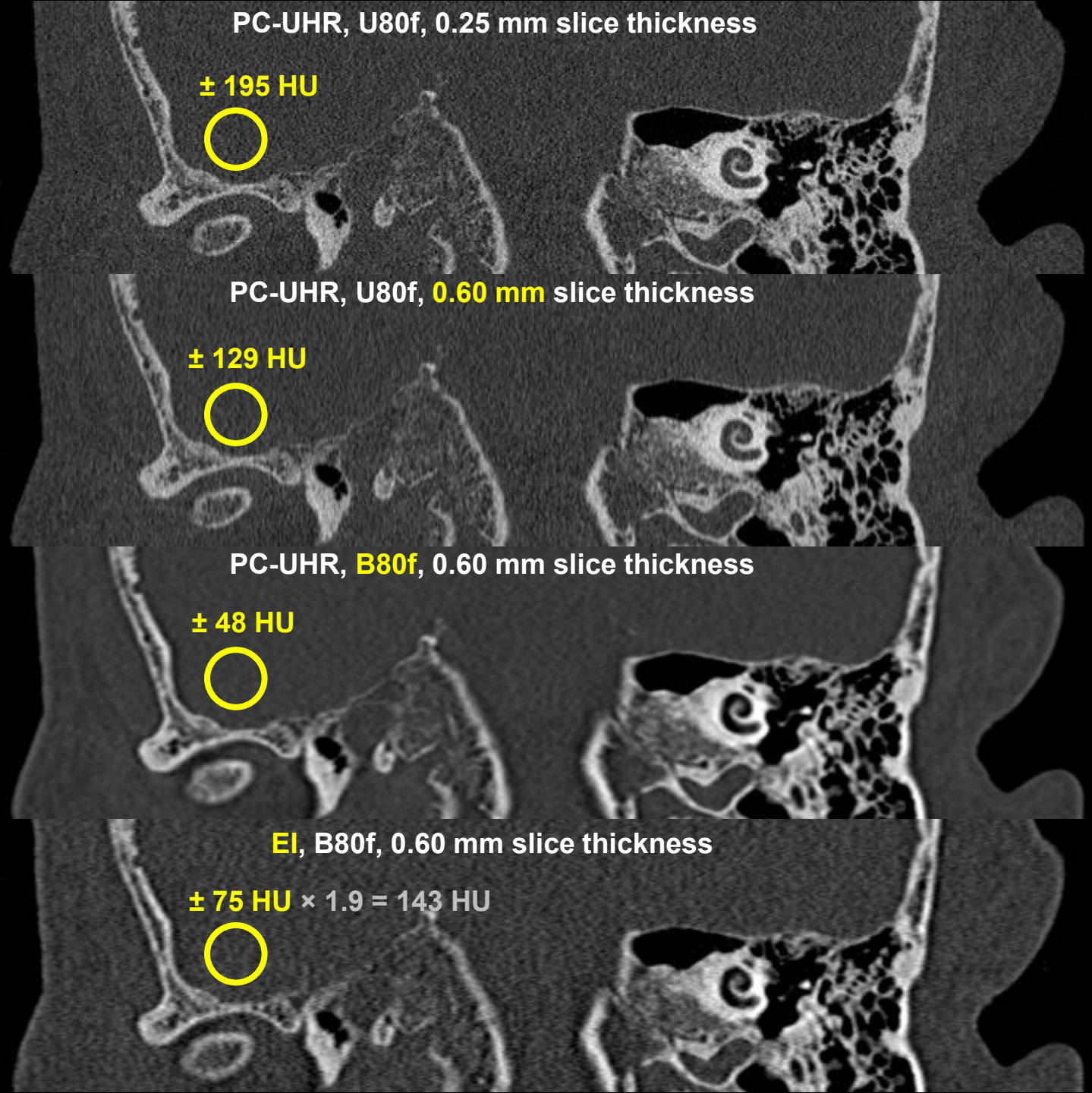

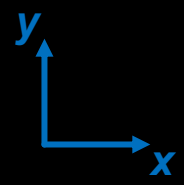

Courtesy of the Institute of Forensic Medicine of the Heidelberg University and of the Division of Radiology of the German Cancer Research Center (DKFZ)

dkfz.

L. Klein, C. Amato, S. Heinze, M. Uhrig, H.-P. Schlemmer, M. Kachelrieß, and S. Sawall.
Effects of Detector Sampling on Noise Reduction in a Clinical Photon-Counting Whole-Body CT. Investigative Radiology, vol. 55(2):111-119, February 2020.

Energy-Integrating Detector (B70f)

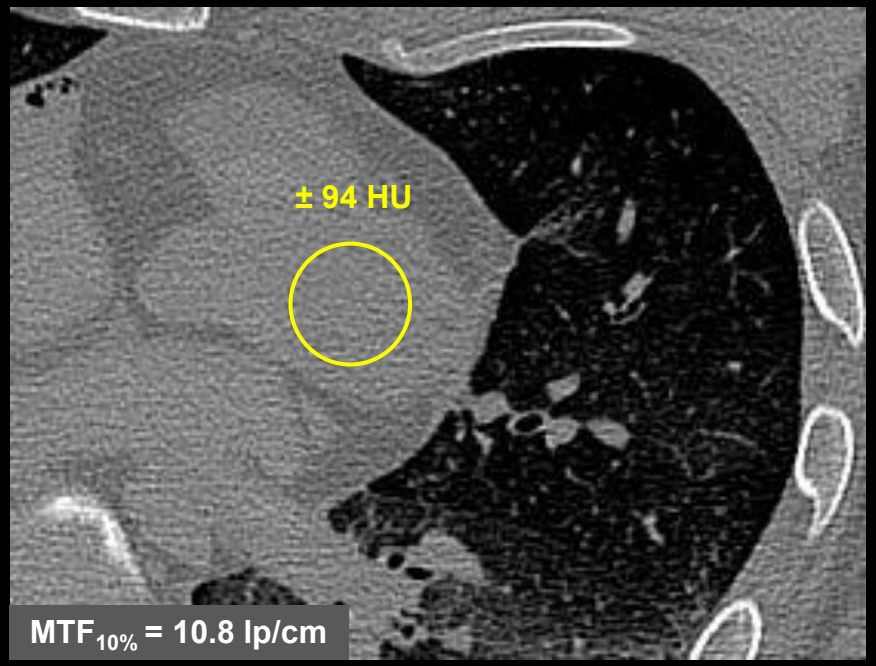

Photon-Counting Detector (B70f)

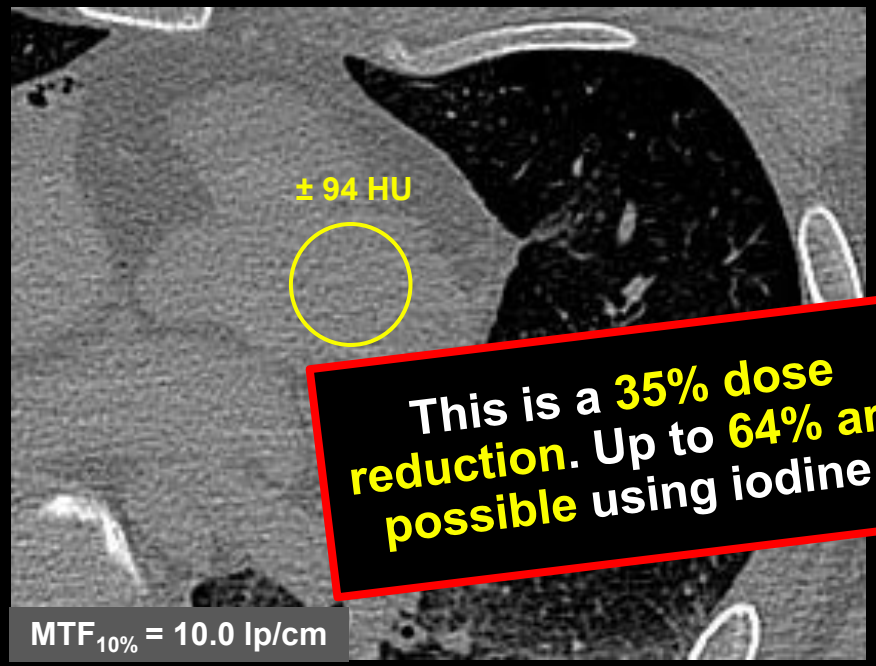

This is a **35% dose reduction**. Up to **64% are possible** using iodine.

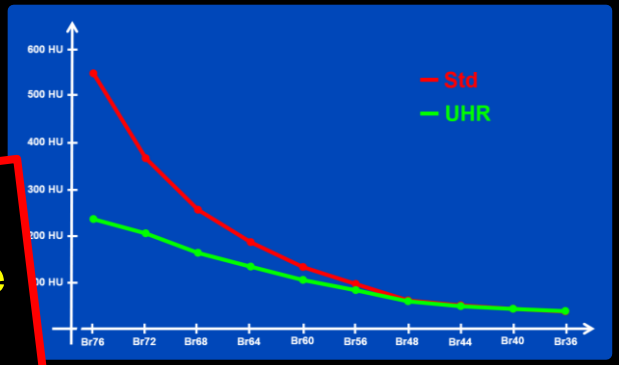

Acquisition with EI:
- Tube voltage of 120 kV
- Tube current of 300 mAs
- Resulting dose of $CTDI_{vol\ 32\ cm}$ = **22.6 mGy**

Acquisition with UHR:
- Tube voltage of 120 kV
- Tube current of 180 mAs
- Resulting dose of $CTDI_{vol\ 32\ cm}$ = **14.6 mGy**

C = 50 HU, *W* = 1500 HU

dkfz.

Scan Trajectories

Circle

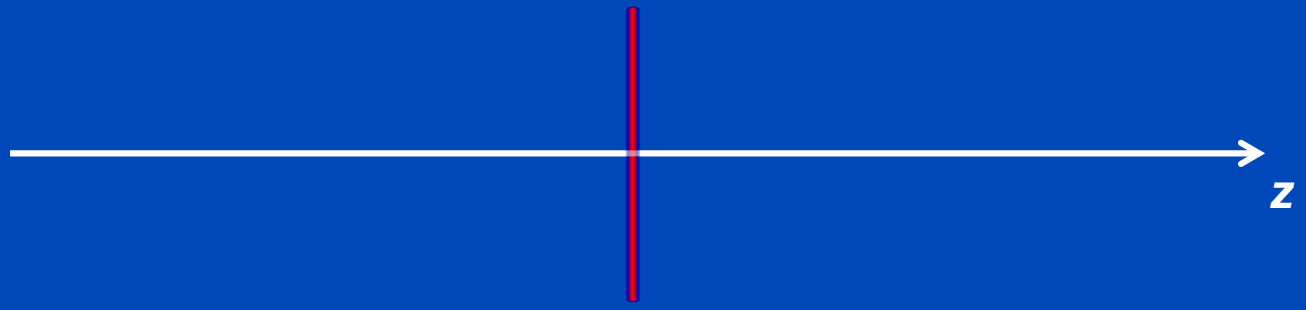

Sequence

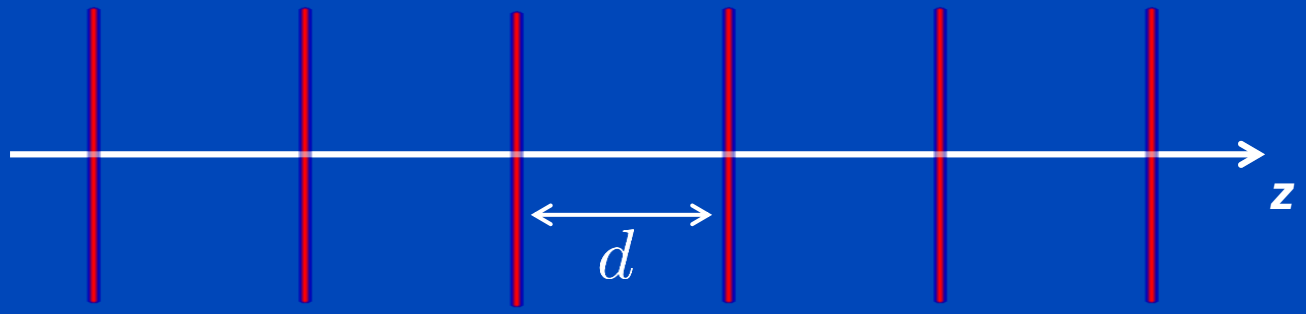

$$p = \frac{d}{MS} \leq 0.9$$

Spiral

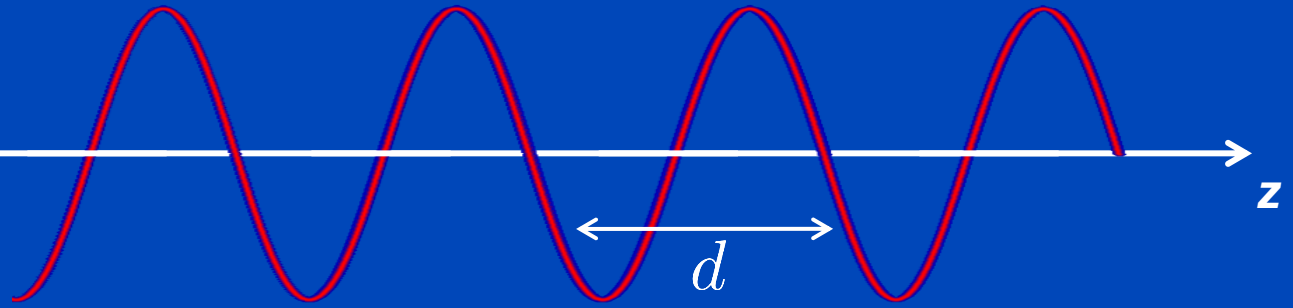

$$p = \frac{d}{MS} \leq 1.5$$

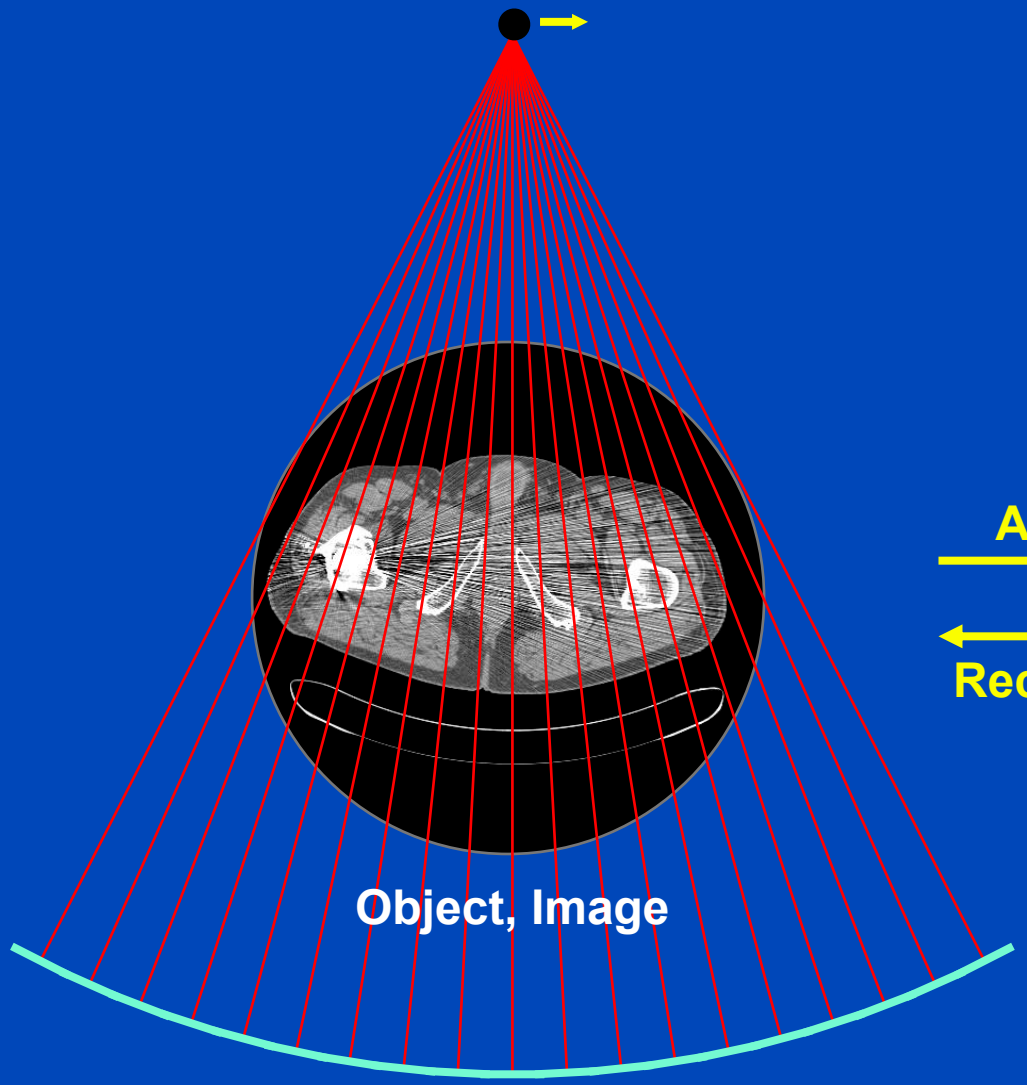

Acquisition

Reconstruction

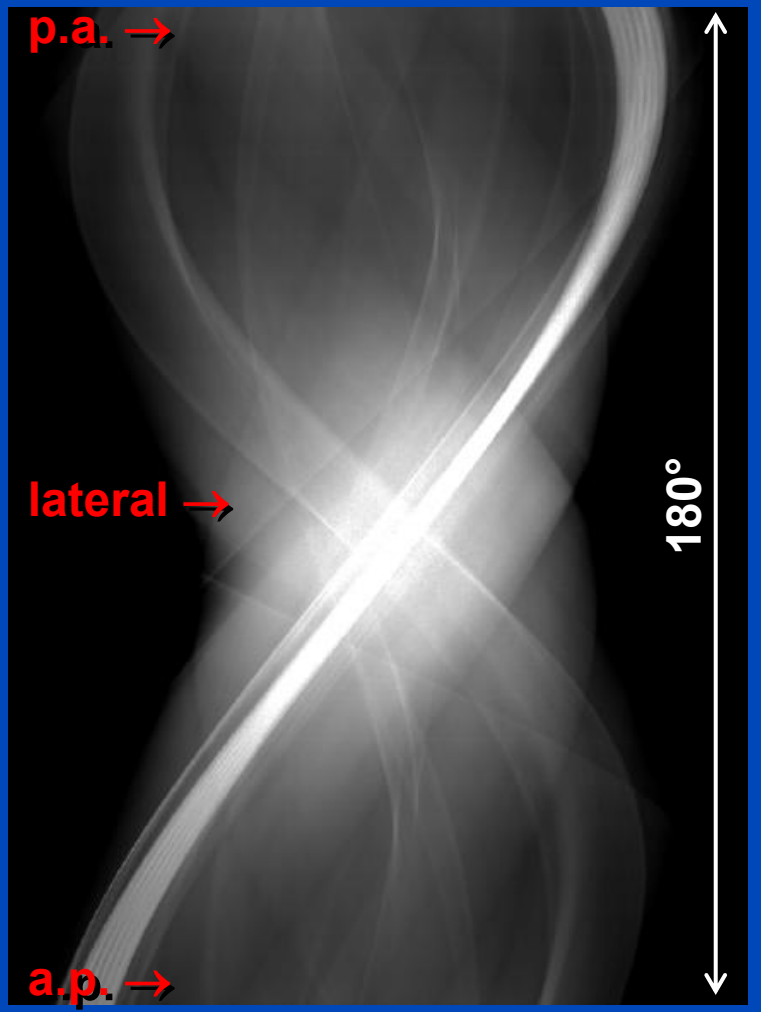

Sinogram, Rawdata

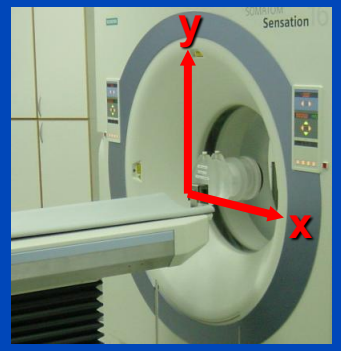

Data Completeness

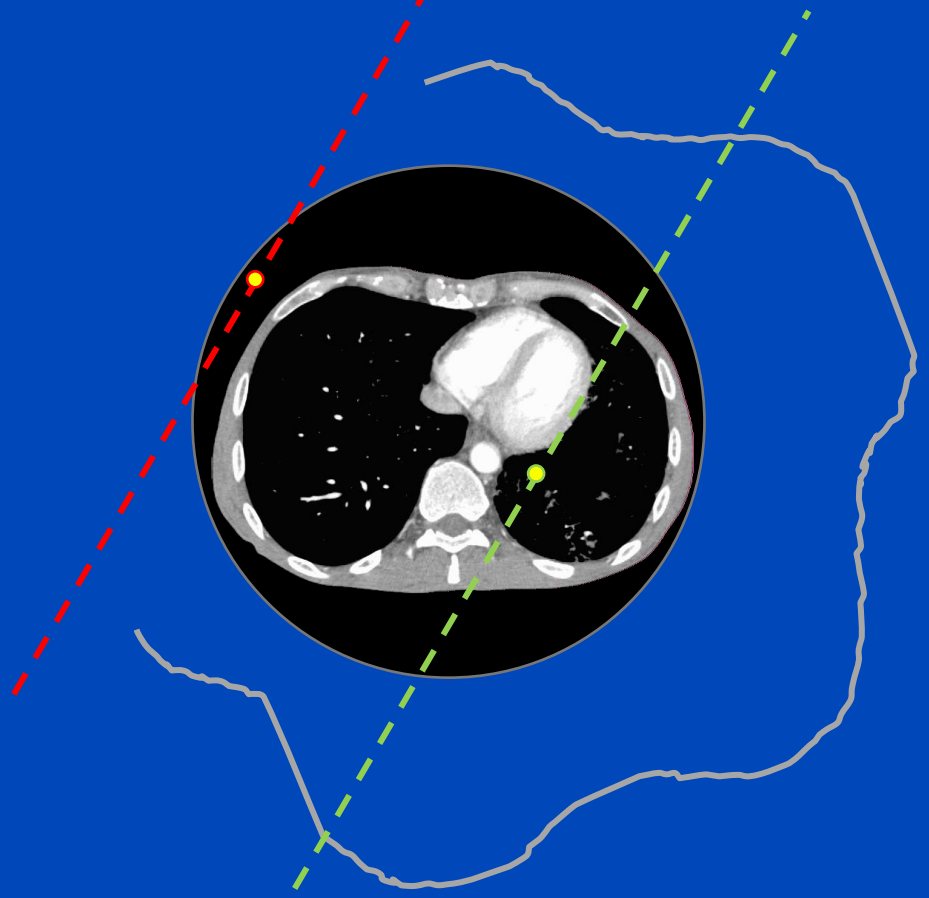

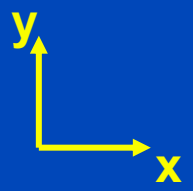

Any straight line through a voxel must be intersected by the source trajectory at least once.

ANALYTICAL IMAGE RECONSTRUCTION

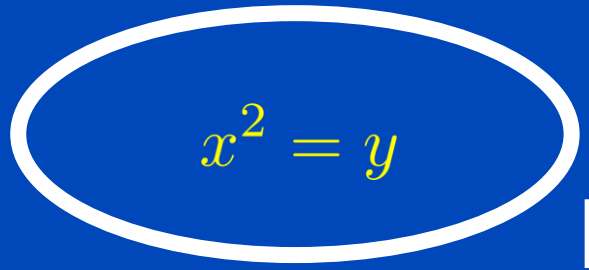

Model

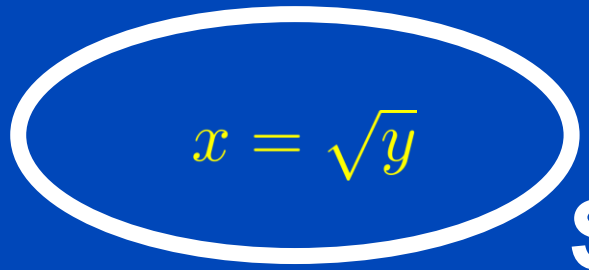

Solution

Filtered Backprojection (FBP)

Measurement: $$p(\vartheta,\xi) = \int dxdy\, f(x,y)\delta(x\cos\vartheta + y\sin\vartheta - \xi)$$

Fourier transform:

$$\int d\xi\, p(\vartheta,\xi)e^{-2\pi i\xi u} = \int dxdy\, f(x,y)e^{-2\pi iu(x\cos\vartheta + y\sin\vartheta)}$$

This is the central slice theorem: $$P(\vartheta,u) = F(u\cos\vartheta, u\sin\vartheta)$$

Inversion:

$$f(x,y) = \int_0^\pi d\vartheta \int_{-\infty}^{\infty} du\, |u| P(\vartheta,u) e^{2\pi iu(x\cos\vartheta + y\sin\vartheta)}$$

$$= \int_0^\pi d\vartheta\, p(\vartheta,\xi) * k(\xi)\Big|_{\xi = x\cos\vartheta + y\sin\vartheta}$$

Filtered Backprojection (FBP)

1. Filter projection data with the reconstruction kernel.
2. Backproject the filtered data into the image:

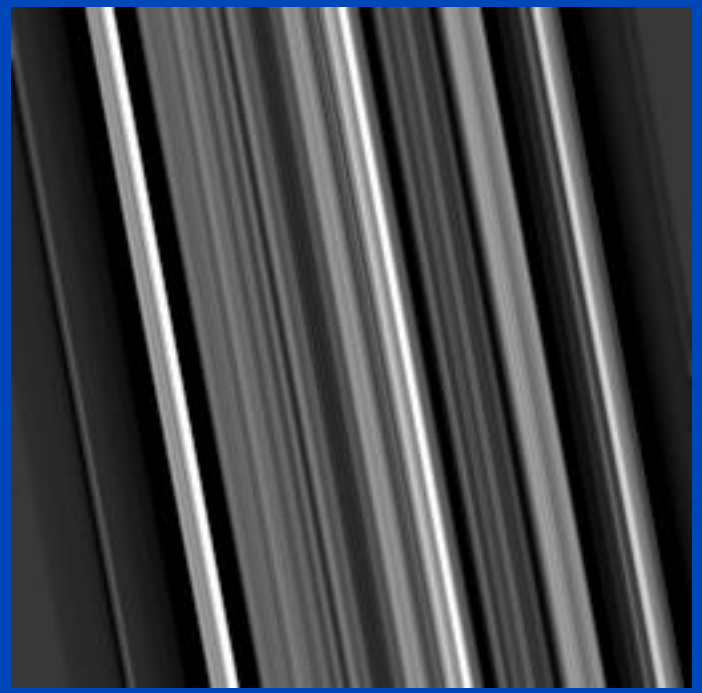

Smooth kernel (e.g. B30)

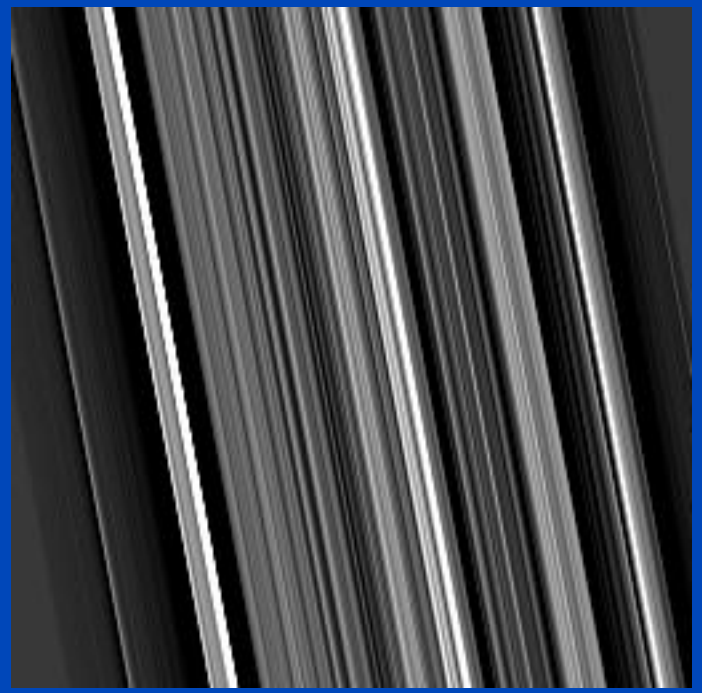

Sharp kernel (e.g. B70)

Reconstruction kernels balance between spatial resolution and image noise.

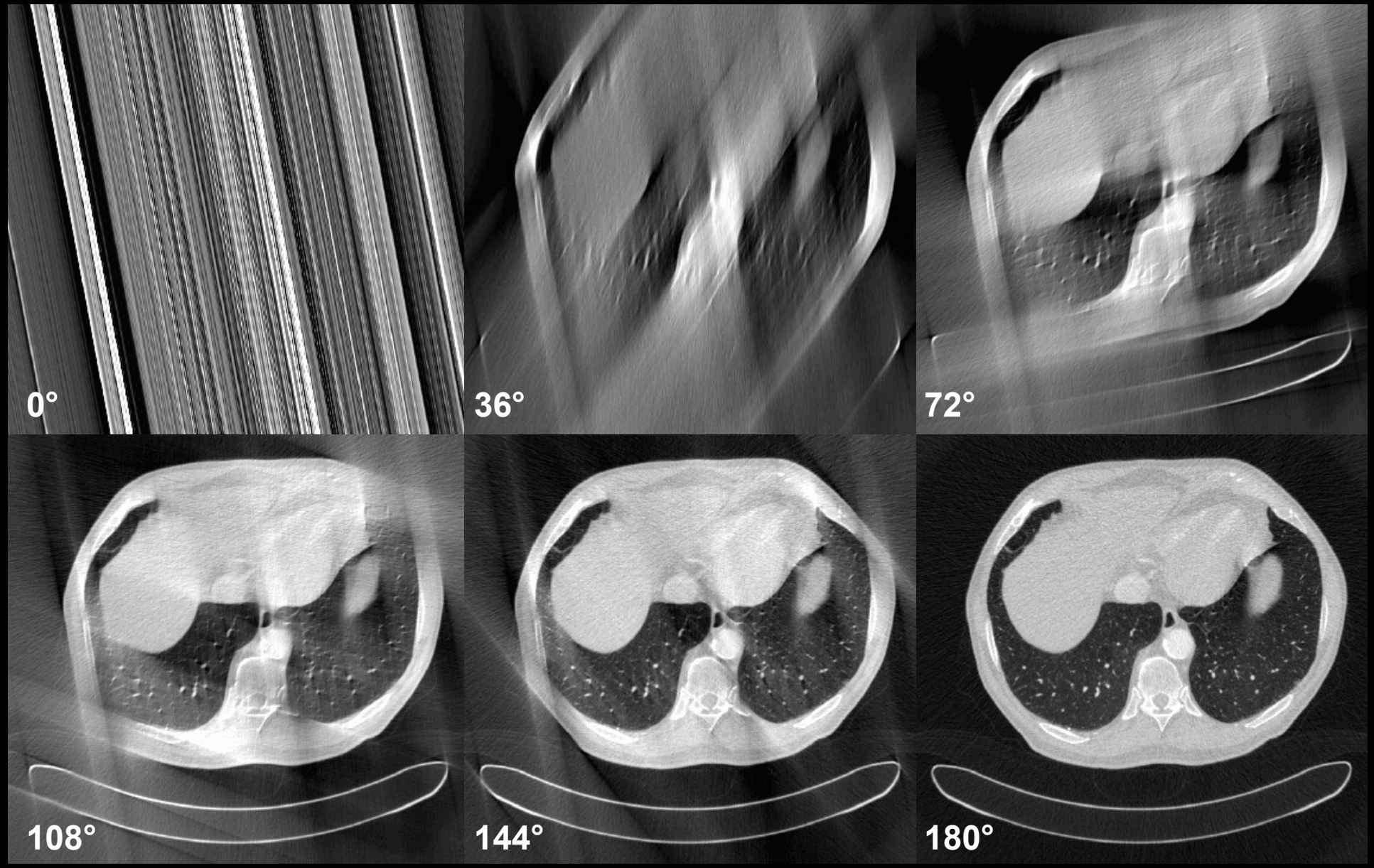
0°
36°
72°
108°
144°
180°

Sinogram domain

normalized

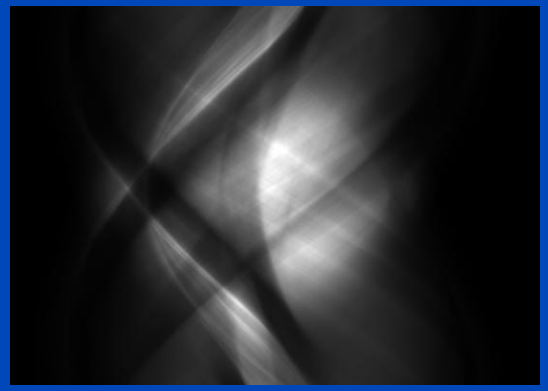

log normalized

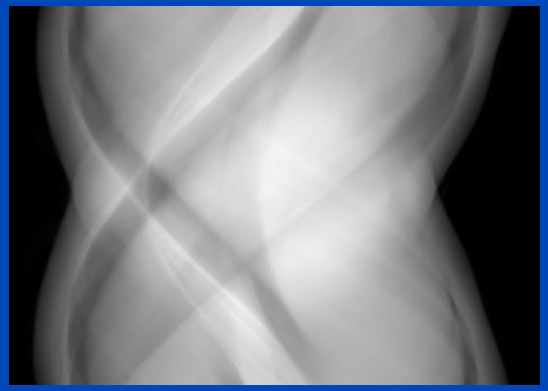

log normalized and convolved

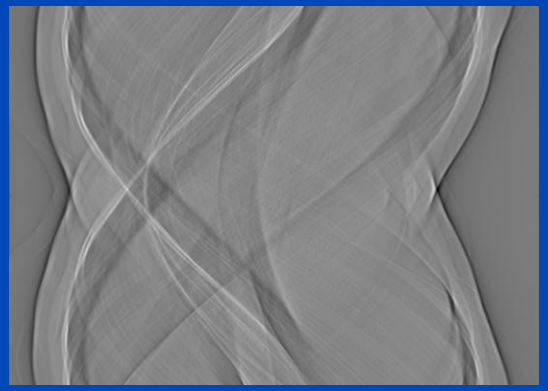

Image domain

after 36°

after 72°

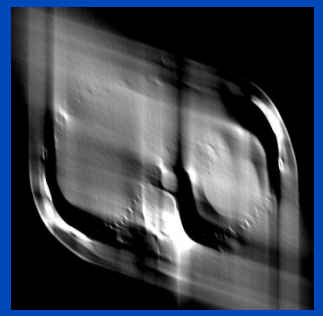

after 108°

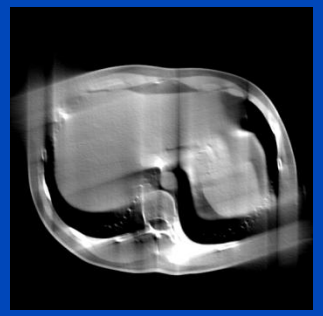

after 144°

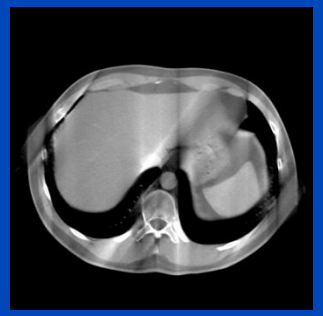

after 180°

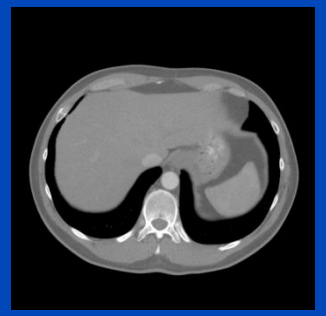

1 projection

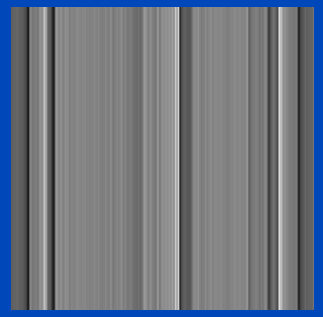

2 projections

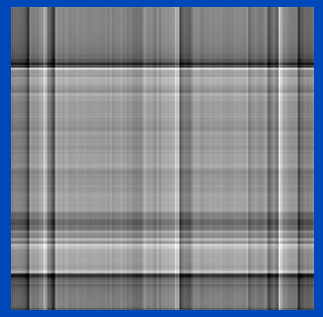

4 projections

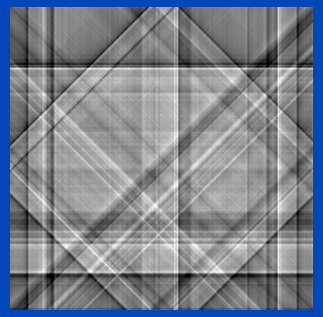

8 projections

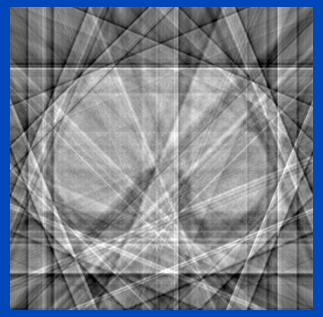

all projections

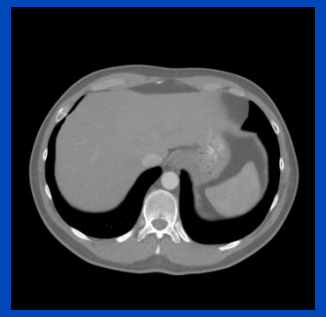

dkfz.

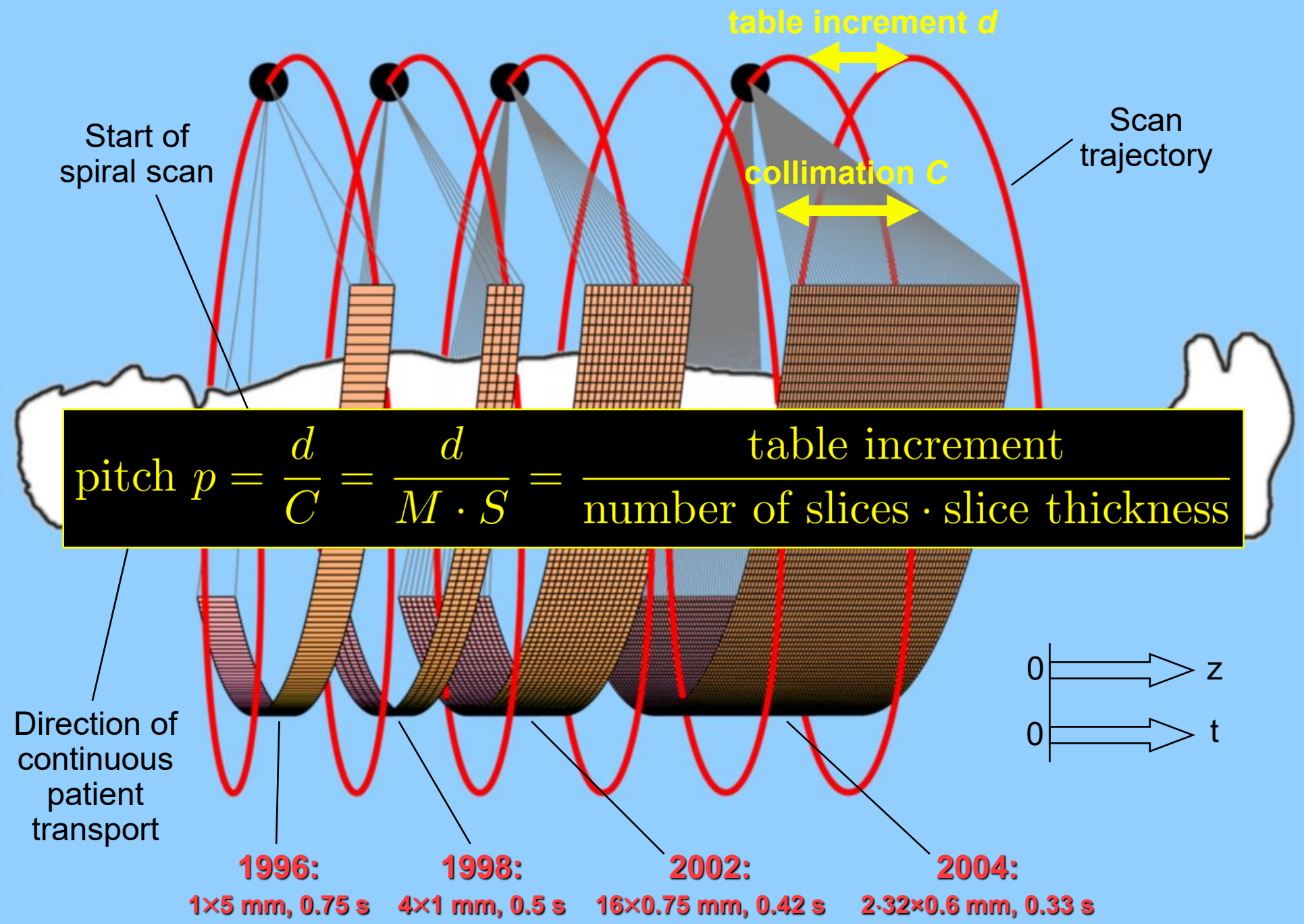

Kalender et al., Radiology 173(P):414 (1989) and 176:181-183 (1990)

360° LI Spiral z-Interpolation for Single-Slice CT (*M*=1)

$$p = \frac{d}{MS} \leq 2$$

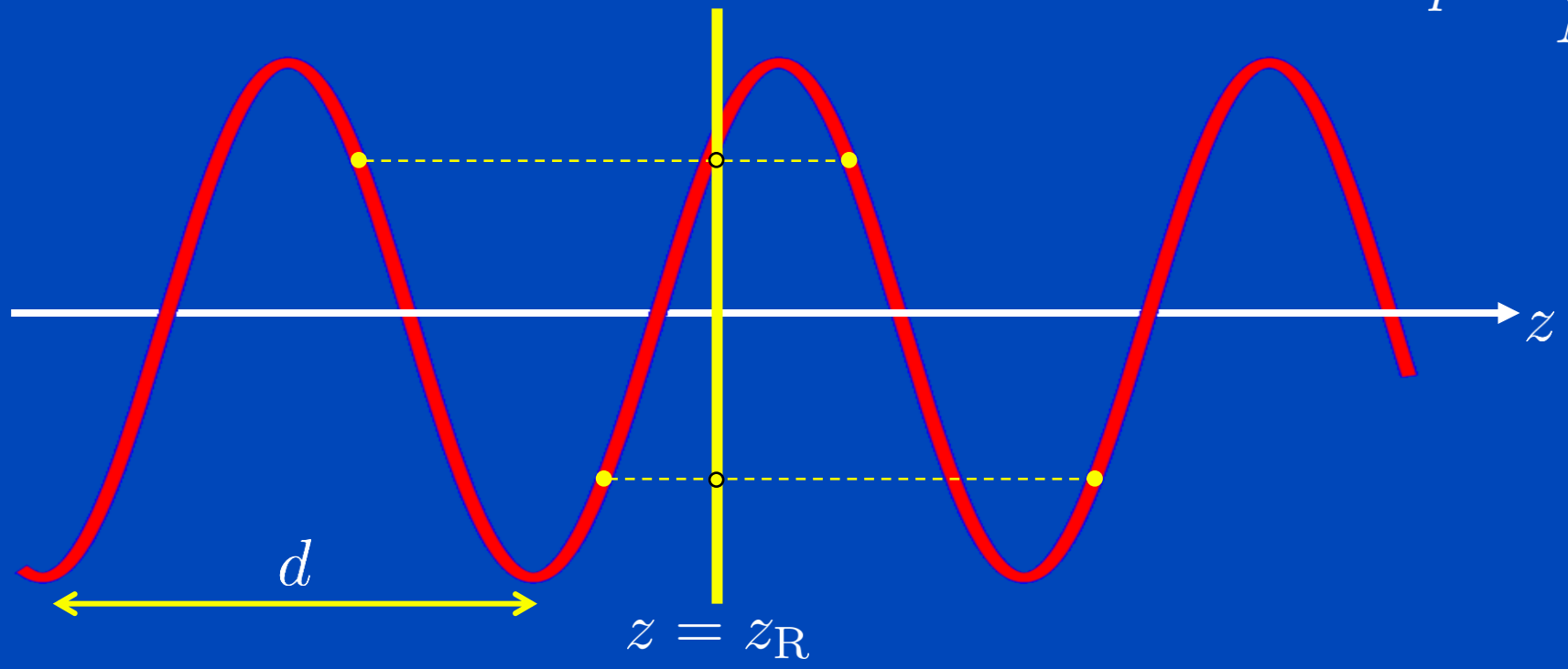

Spiral z-interpolation is typically a linear interpolation between points adjacent to the reconstruction position to obtain circular scan data.

without *z*-interpolation

with *z*-interpolation

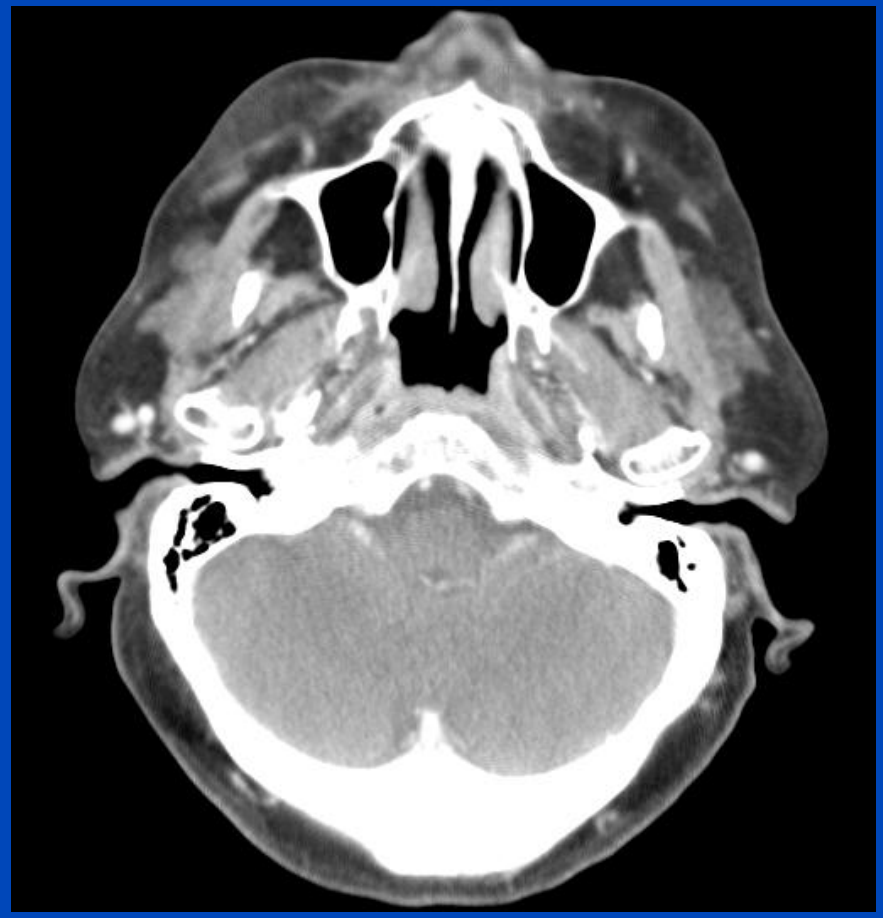

RSNA 1989
SSCT (*M* = 1)

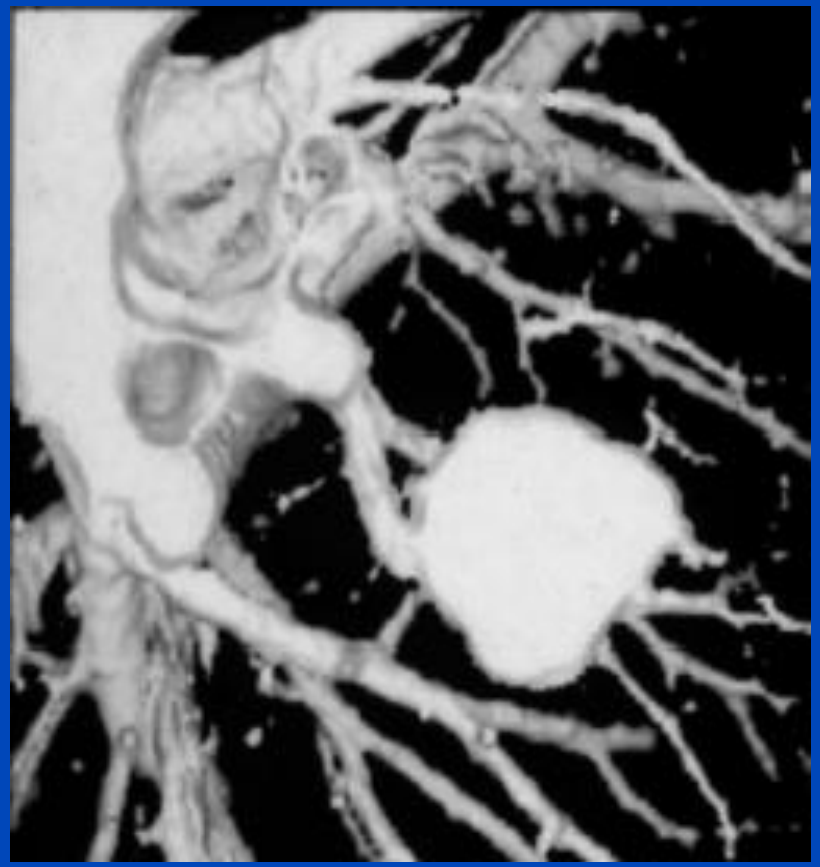

RSNA 2001
MSCT (*M* = 16)

What's so Nice about Spiral CT?

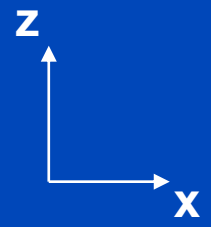

S = 3 mm, *RI* = 3 mm

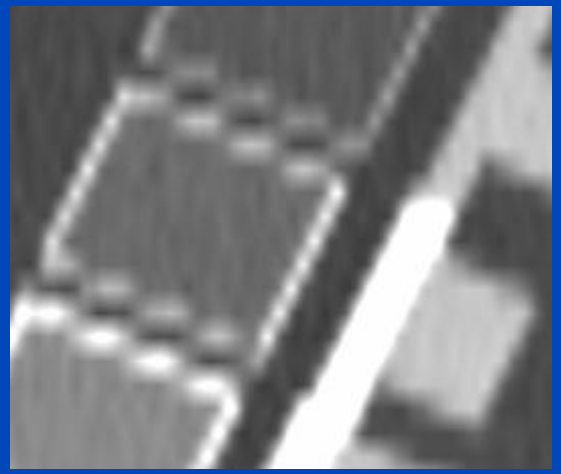

S = 3 mm, *RI* = 1 mm

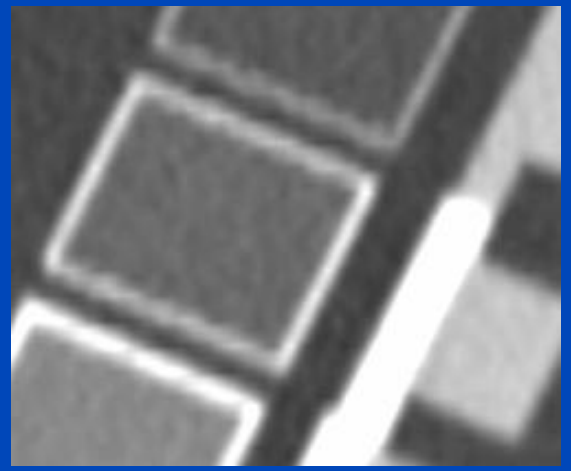

MPR images of the European Spine Phantom (inclined at 25°).

Sampling Artifact

S_{eff} = 3 mm, *RI* = 3 mm

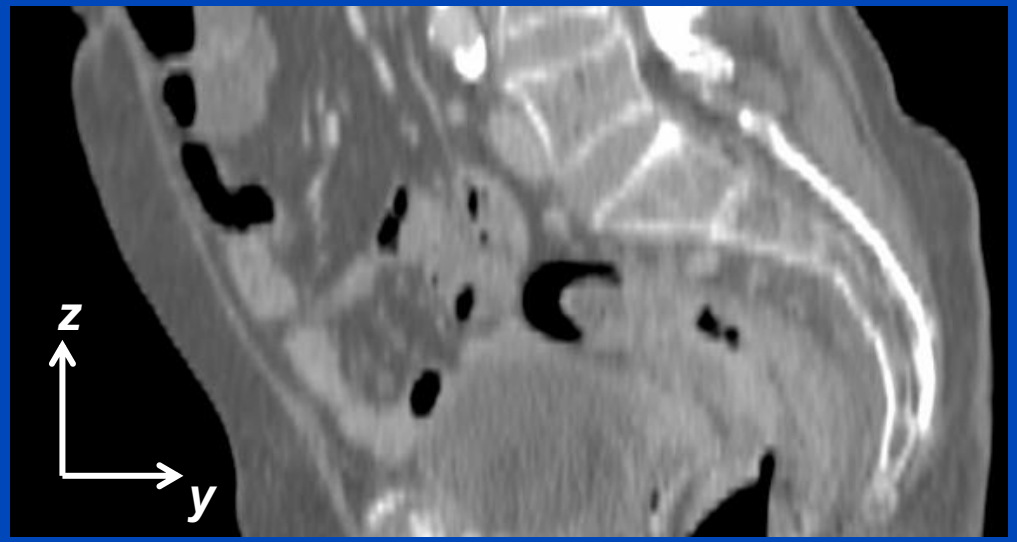

S_{eff} = 3 mm, *RI* = 1 mm

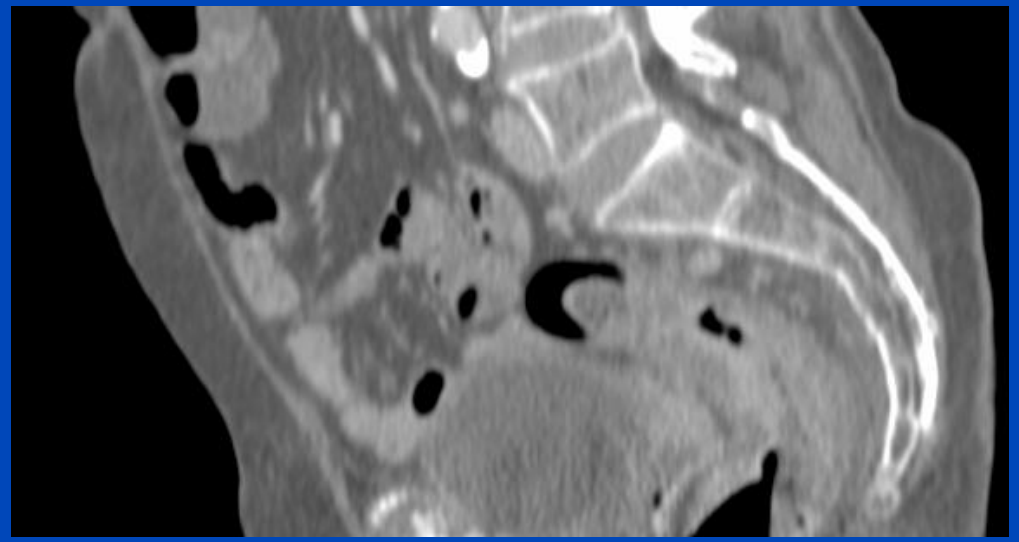

Always perform overlapping recons!

C = 0 HU, *W* = 800 HU

dkfz.

The ASSR Algorithm

AMERICAN ASSOCIATION of PHYSICISTS IN MEDICINE

Congratulations

This paper received the Sylvia Sorkin Greenfield Award for the best scientific paper on imaging in Medical Physics in 2000.

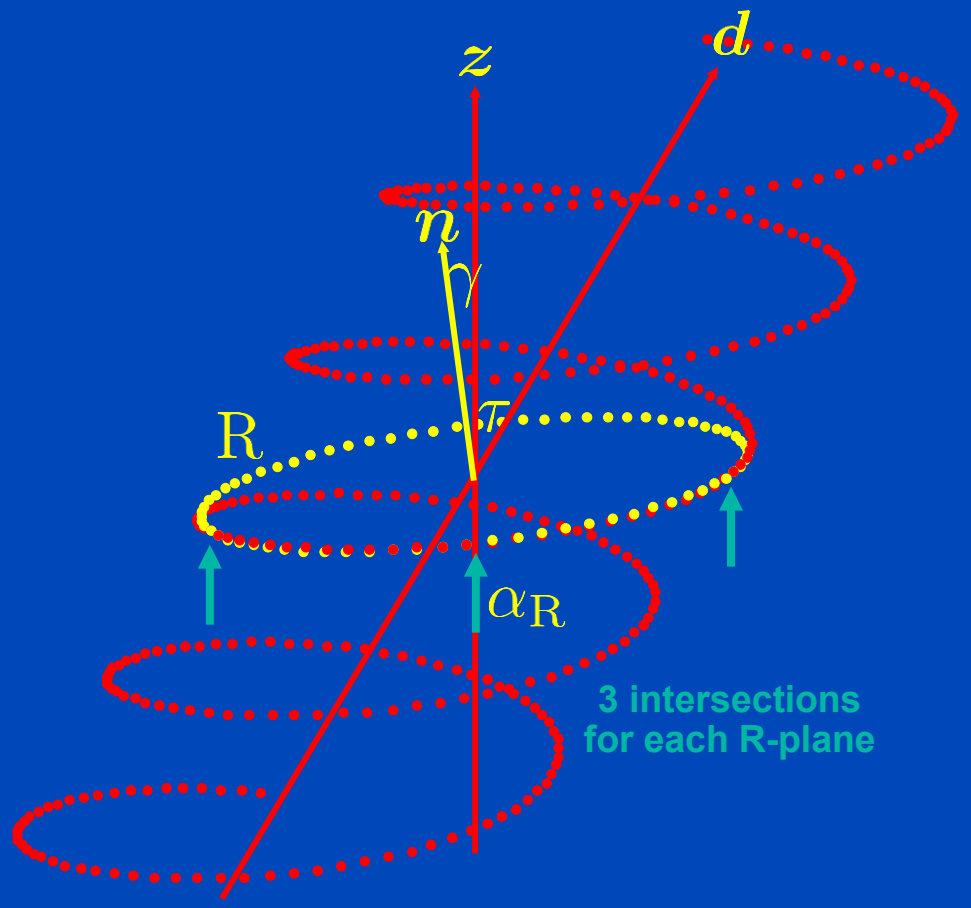

$$p = \frac{d}{MS} \leq 1.5$$

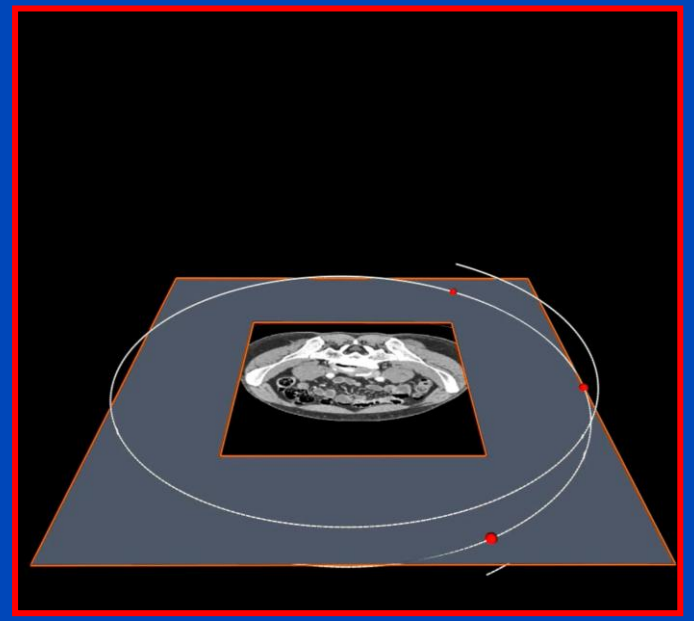

Mean deviation at distance R_M: $\Delta \approx 0.007 \cdot d$

at distance R_F: $\Delta \approx 0.014 \cdot d$

ITERATIVE IMAGE RECONSTRUCTION

$$x^2 = y$$

$$x = \sqrt{y}$$

Model

$$(x_n + \Delta x_n)^2 = y$$

$$x_n^2 + 2x_n\Delta x_n + \Delta x_n^2 = y$$

$$x_n^2 + 2x_n\Delta x_n \approx y$$

$$\Delta x_n = \tfrac{1}{2}(y - x_n^2)/x_n$$

$$x_{n+1} = x_n + \Delta x_n$$

Update equation

This is an iterative solution.

dkfz.

Influence of Update Equation and Model

$0.5\,(3 - x_n^2)/x_n$	$0.4\,(3 - x_n^2)/x_n$	$0.5\,(3 - x_n^{2.1})/x_n$
$x_0 = 1.$	$x_0 = 1.$	$x_0 = 1.$
$x_1 = 2.$	$x_1 = 1.8$	$x_1 = 2.$
$x_2 = 1.75$	$x_2 = 1.74667$	$x_2 = 1.67823$
$x_3 = 1.73214$	$x_3 = 1.73502$	$x_3 = 1.68833$
$x_4 = 1.73205$	$x_4 = 1.73265$	$x_4 = 1.68723$
$x_5 = 1.73205$	$x_5 = 1.73217$	$x_5 = 1.68734$
$x_6 = 1.73205$	$x_6 = 1.73207$	$x_6 = 1.68733$
$x_7 = 1.73205$	$x_7 = 1.73206$	$x_7 = 1.68733$
$x_8 = 1.73205$	$x_8 = 1.73205$	$x_8 = 1.68733$

$$x^2 = 3, \quad x_0 = 1, \quad x_{n+1} = x_n + \Delta x_n$$

dkfz.

Iterative Reconstruction

- Aim: less artifacts, lower noise, lower dose
- Iterative reconstruction
  - Reconstruct an image.
  - Does the image correspond to the rawdata?
  - If not, reconstruct a correction image and continue.
- CT product implementations
  - AIDR 3D (adaptive iterative dose reduction, Canon)
  - ASIR (adaptive statistical iterative reconstruction, GE)
  - iDose (Philips)
  - IRIS (image reconstruction in image space, Siemens)
  - FIRST (forward projected model-based iterative reconstruction solution, Canon)
  - VEO, MBIR (model-based iterative reconstruction, GE)
  - IMR (iterative model reconstruction, Philips)
  - SAFIRE, ADMIRE, QIR (quantum iterative reconstruction, Siemens)

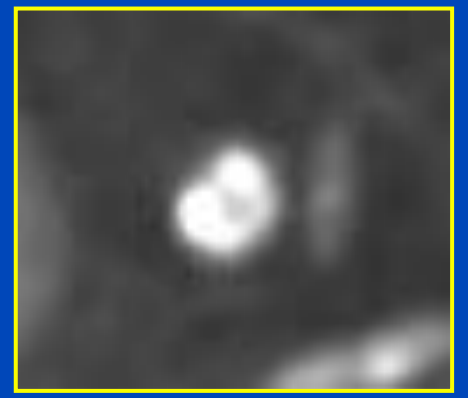

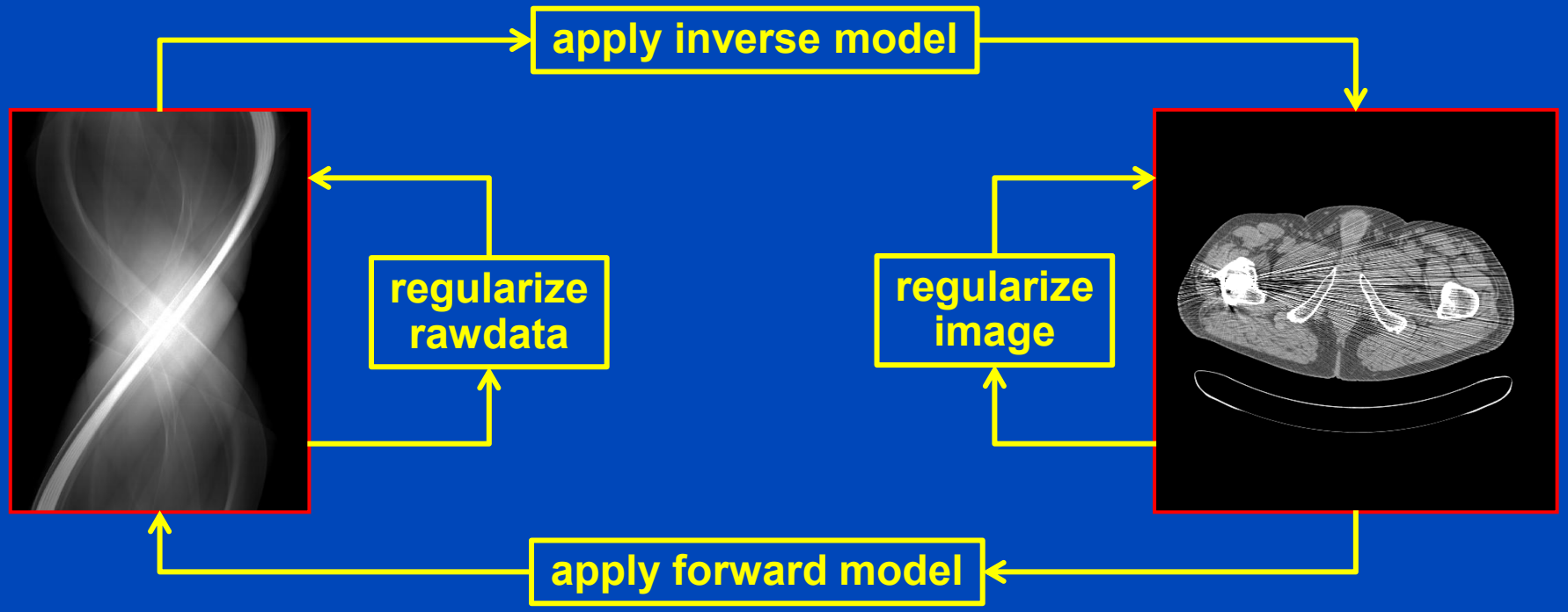

- Rawdata regularization: adaptive filtering[1], precorrections, filtering of update sinograms...
- Inverse model: backprojection (R^T) or filtered backprojection (R^{-1}). In clinical CT, where the data are of high fidelity and nearly complete, one would prefer FBP to increase convergence speed.
- Image regularization: edge-preserving filtering. It may model physical noise effects (amplitude, direction, correlations, …). It may reduce noise while preserving edges. It may include empirical corrections.
- Forward model (R_{phys}): Models physical effects. It can reduce beam hardening artifacts, scatter artifacts, cone-beam artifacts, noise, …

[1]M. Kachelrieß et al., Generalized Multi-Dimensional Adaptive Filtering, MedPhys 28(4), 2001

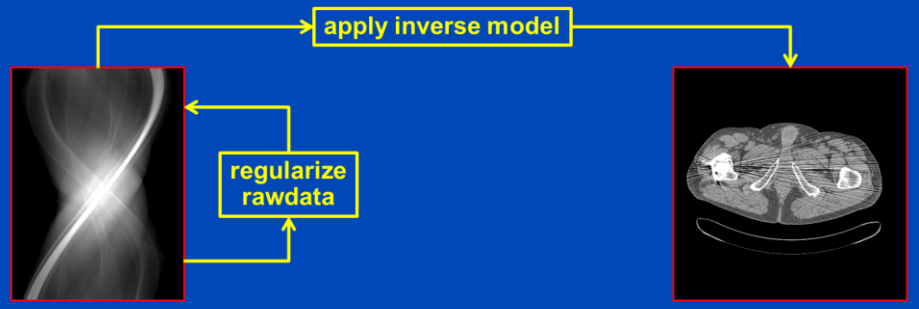

Conventional FBP with rawdata denoising (all vendors)

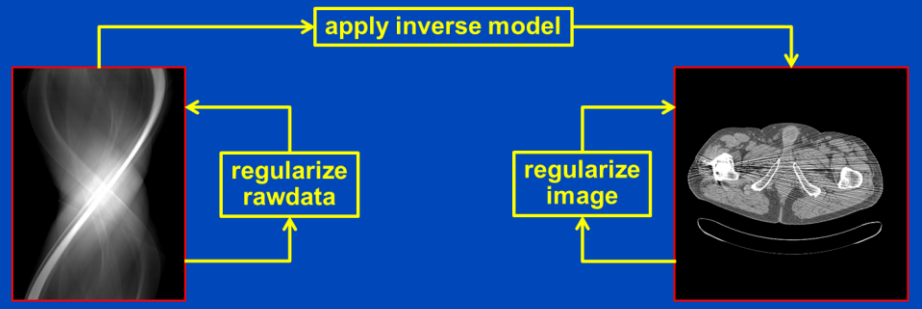

AIDR3D (Canon), ASIR, ASIR-V (Ge), IRIS (Siemens), iDose (Philips), SnapShot Freeze (GE), iTRIM (Siemens)

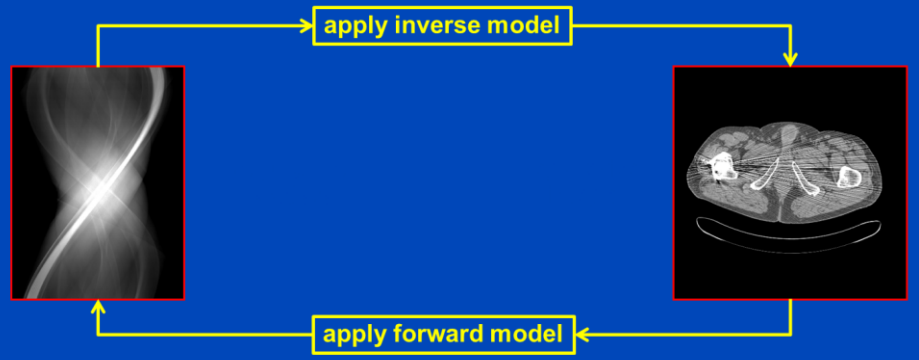

Veo123/MBIR (Ge)

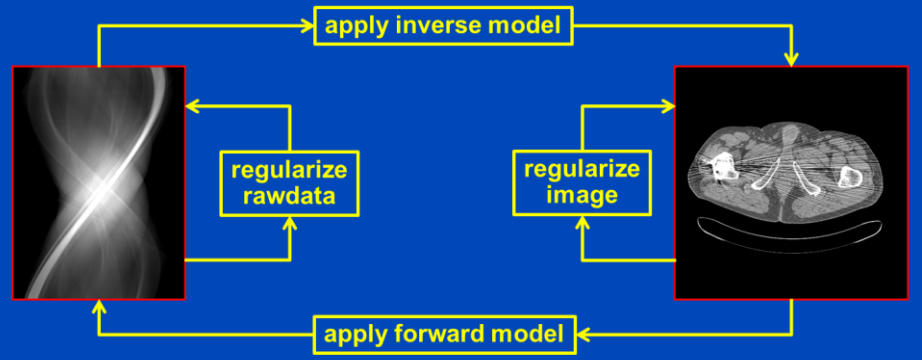

FIRST (Canon), IMR (Philips), SAFIRE, ADMIRE, QIR (Siemens)

M. Kachelrieß. Current Cardiovascular Imaging Reports 6:268–281, 2013

dkfz.

FBP

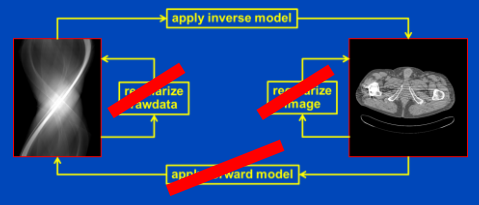

ASIR

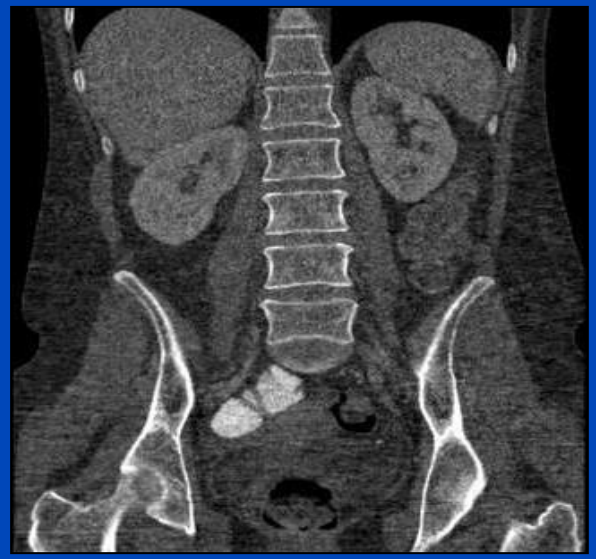

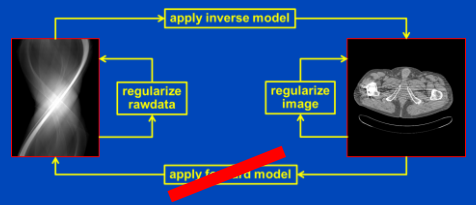

Veo

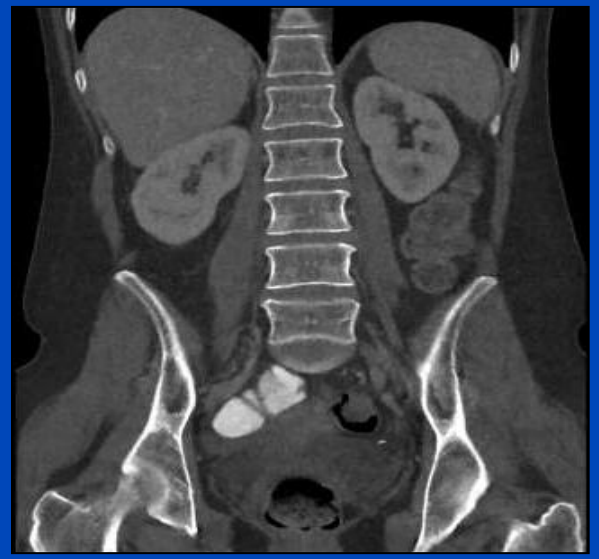

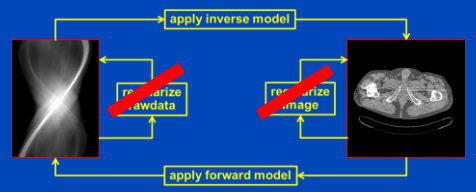

Courtesy of Dr. Jiang Hsieh, GE Healthcare Technologies, WI, USA.

Usual Assumption: CT is Linear and Translation Invariant

- PSF and MTF are well-defined
- Noise is well-defined
- Noise and spatial r
- Parameters are v
- Simple phantom
- …

This is valid only for analytical reconstruction!

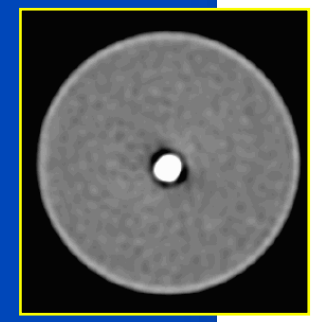

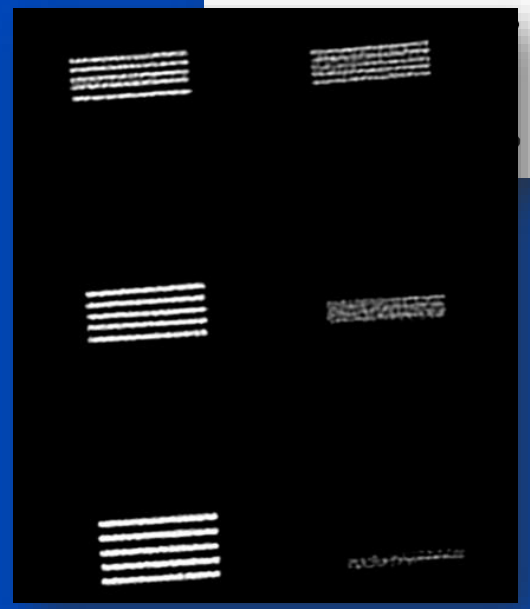

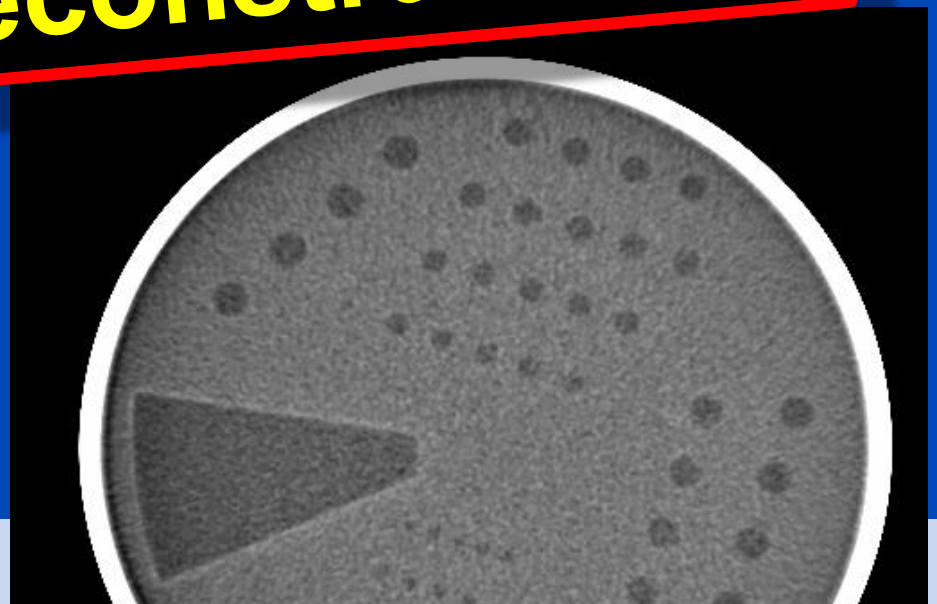

Analysis of Siemens' SAFIRE Algorithm
(Taken at the Siemens Somatom Flash DSCT Scanner)

- **Semiantropomorphic phantom**
  - 20 cm × 30 cm thorax phantom of 20 cm length with 2.5 cm water extension ring, totalling to 25 cm × 35 cm size
  - 10 cm QRM 3D medium contrast insert with 40 HU background and 20 HU lesions (at 120 kV)
- **Scan and recon parameters**
  - 128 × 0.6 mm collimation
  - U = 120 kV
  - p = 0.6
  - t_{rot} = 1.0 s
  - S_{eff} = 0.6 mm
  - 1 high dose scan with 1100 mAs_{eff}
  - 25 low dose scans with 44 mAs_{eff} each
  - FBP (= analytical): B30s, B50s
  - SAFIRE (= iterative): I30s and I50s, strengths 3 and 5
  - Averaging of 25 low dose scans after reconstruction
  - Mean±StdDev in large medium contrast lesion
  - Display at C = 50 HU and W = 100 HU

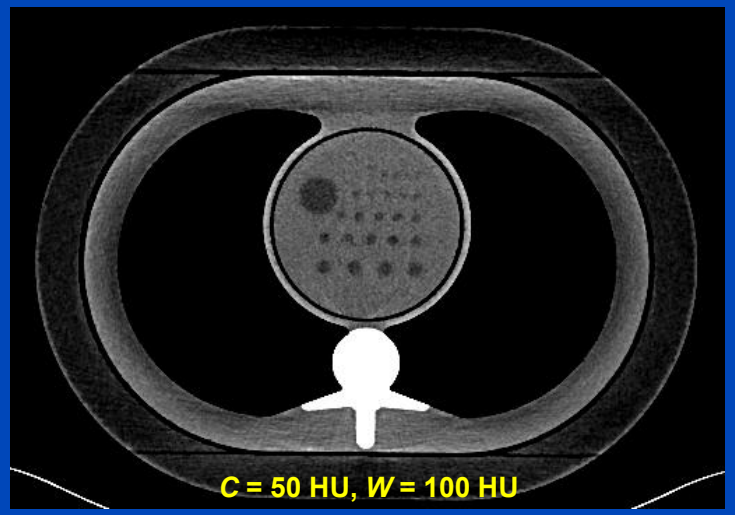

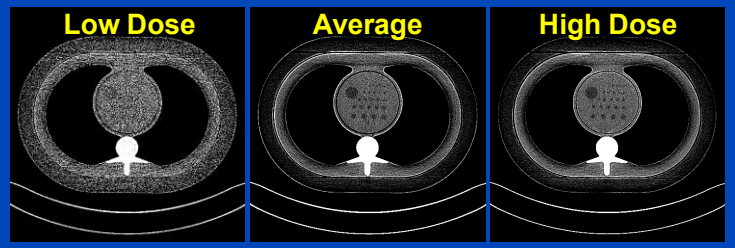

Average of 25 Low Dose Scans

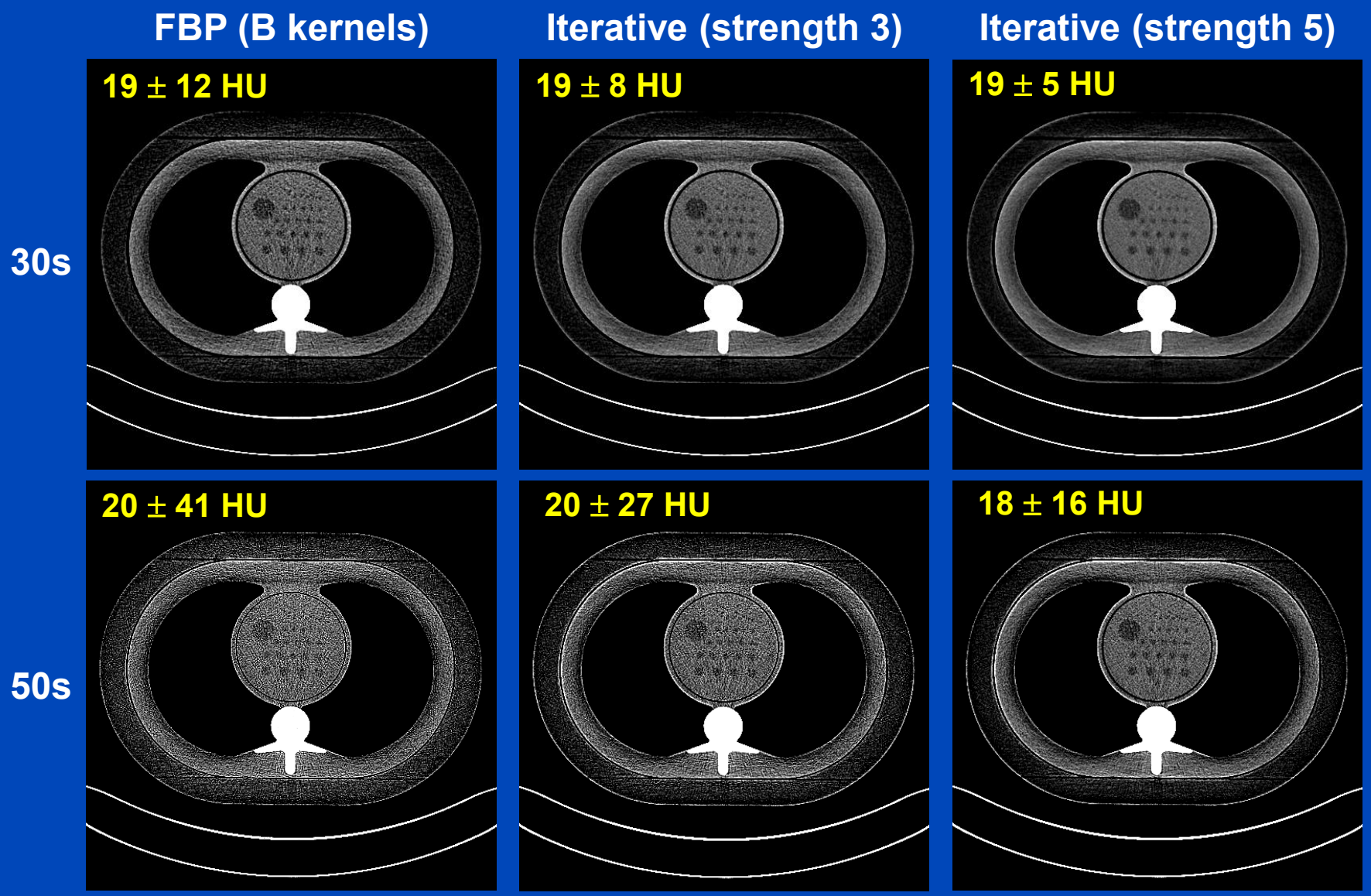

High Dose Scan

	FBP (B kernels)	Iterative (strength 3)	Iterative (strength 5)
30s	18 ± 10 HU	18 ± 6 HU	19 ± 4 HU
50s	17 ± 40 HU	19 ± 25 HU	18 ± 13 HU

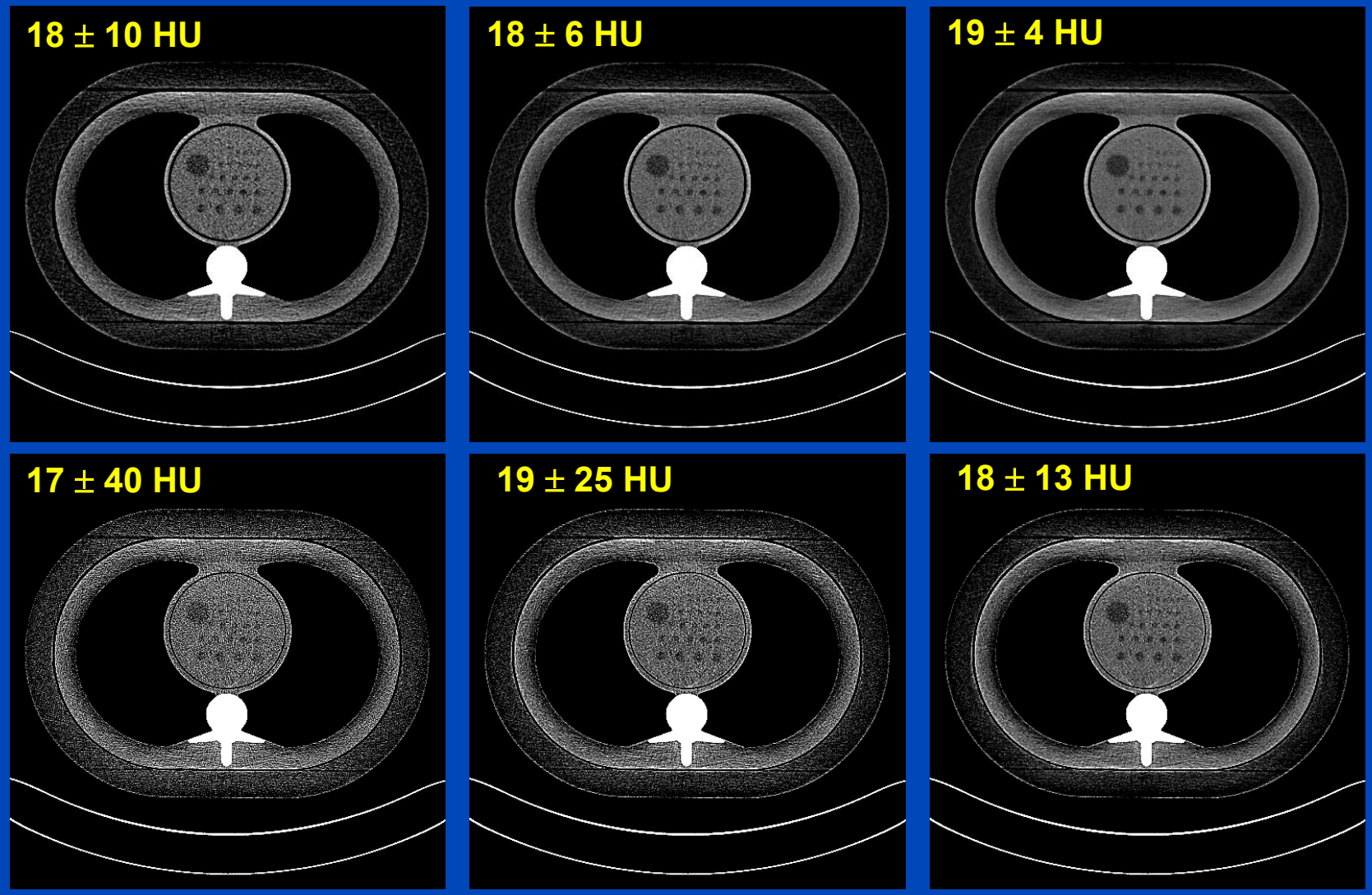

dkfz.

Analysis of GE‘s MBIR (Veo) Iterative Reconstruction Algorithm

Statistical model based iterative reconstruction (MBIR) in clinical CT systems. Part II. Experimental assessment of spatial resolution performance

Ke Li
Department of Medical Physics, University of Wisconsin-Madison, 1111 Highland Avenue, Madison, Wisconsin 53705 and Department of Radiology, University of Wisconsin-Madison, 600 Highland Avenue, Madison, Wisconsin 53792

John Garrett and Yongshuai Ge
Department of Medical Physics, University of Wisconsin-Madison, 1111 Highland Avenue, Madison, Wisconsin 53705

Guang-Hong Chen[a)]
Department of Medical Physics, University of Wisconsin-Madison, 1111 Highland Avenue, Madison, Wisconsin 53705 and Department of Radiology, University of Wisconsin-Madison, 600 Highland Avenue, Madison, Wisconsin 53792

(Received 8 March 2014; revised 9 May 2014; accepted for publication 2 June 2014; published 23 June 2014)

Li et al., MedPhys 41(7), July 2014

dkfz.

Contrast Dependency of the PSF
(of GE's FBP and Veo Algorithms)

	Contrast (HU)
Object 1	13
Object 2	33
Object 3	62
Object 4	120
Object 5	224
Object 6	346
Object 7	814
Object 8	1710

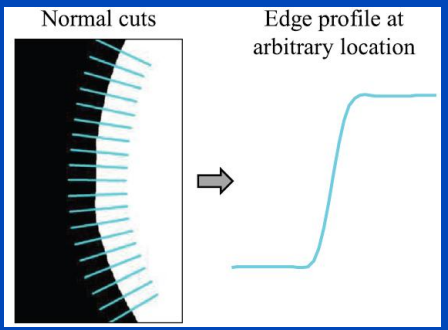

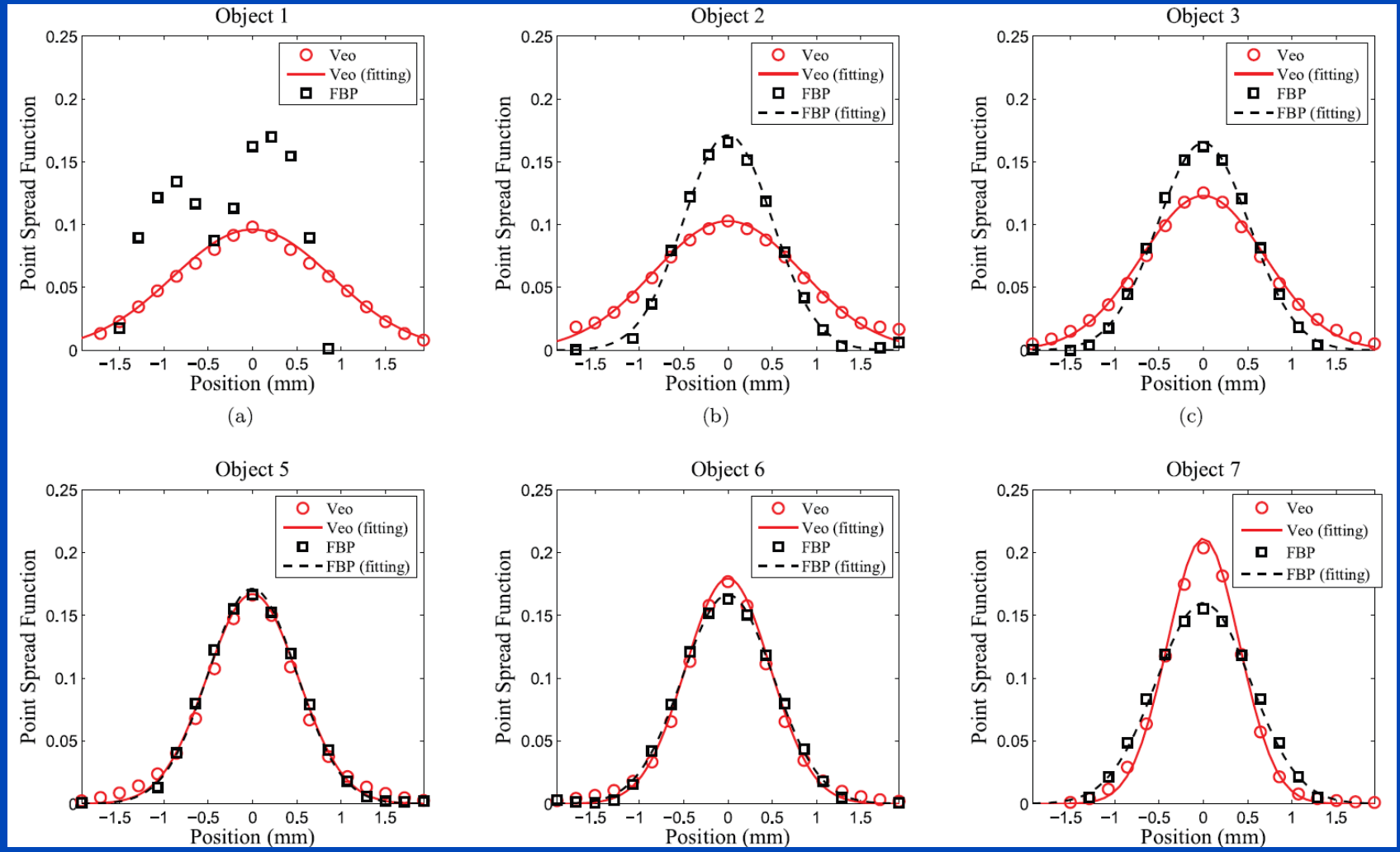

Li et al., MedPhys 41(7), July 2014

Dose Dependency of the PSF
(of GE's FBP and Veo Algorithms)

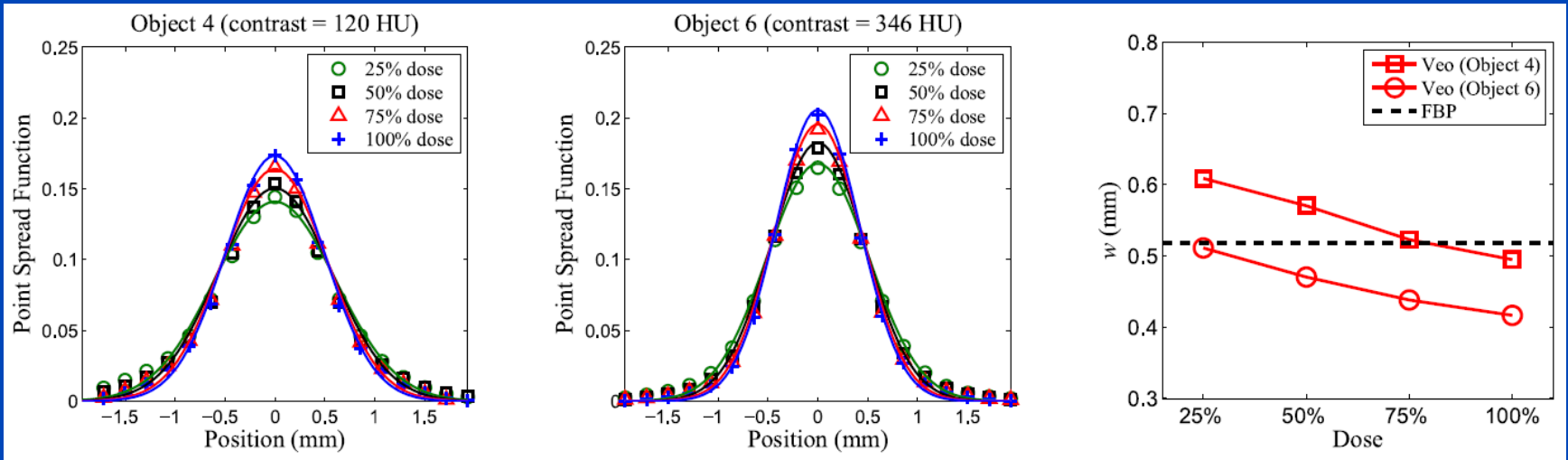

dkfz.

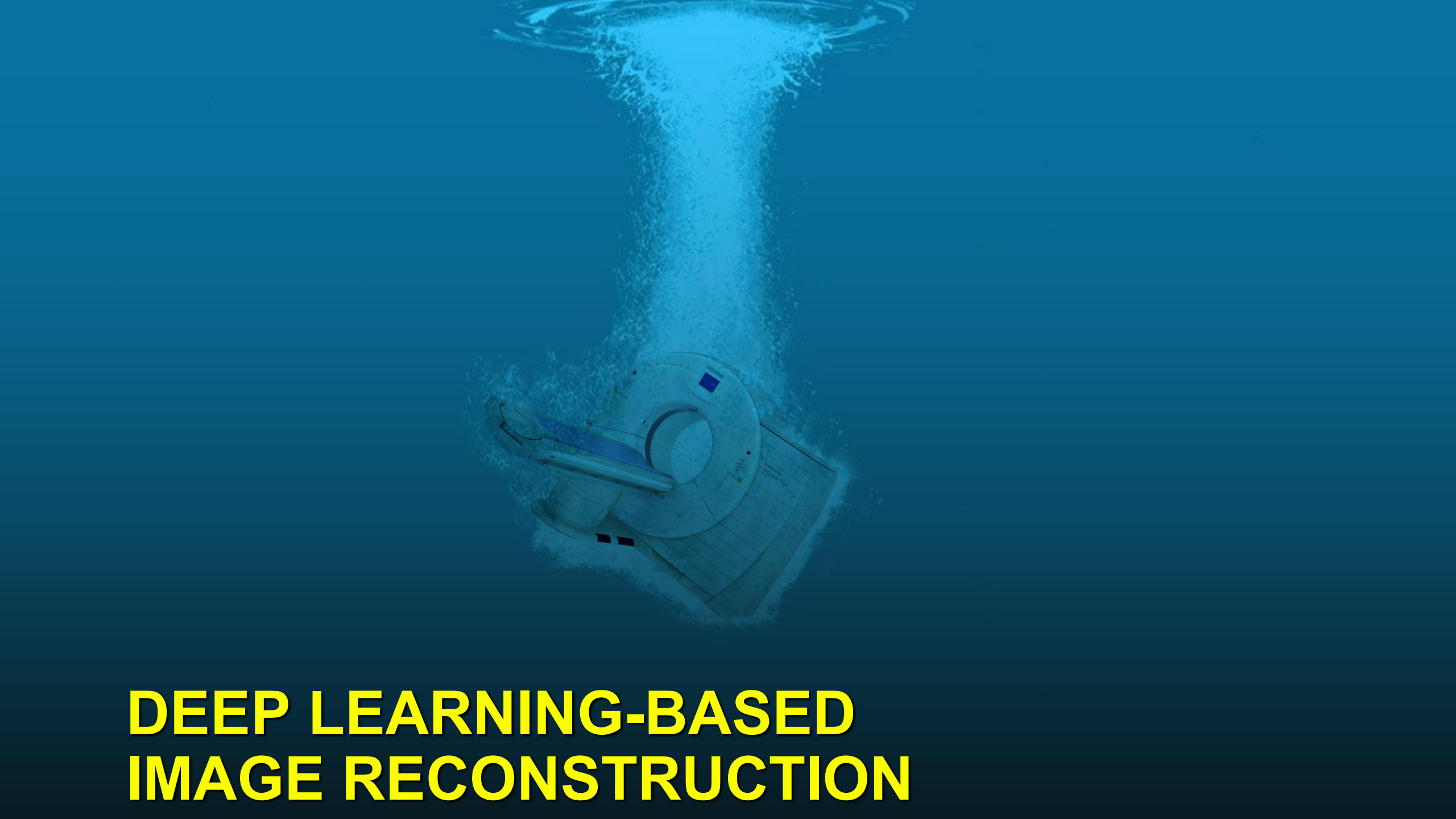

DEEP LEARNING-BASED IMAGE RECONSTRUCTION

$x^2 = y$

$x = \sqrt{y}$

$\Delta x_n = \frac{1}{2}(y - x_n^2)/x_n$

$x_{n+1} = x_n + \Delta x_n$

$\{(y^{(d)}, x^{(d)}) \mid d = 1 \quad D \text{ with } D$

$f_{c_1,c_2,\ldots c_P}(y)$ with P being large

See tomorrow's lecture!

Data

Model

$$\boldsymbol{c} = \arg\min_{\boldsymbol{c}} \sum_d \left(f_{\boldsymbol{c}}(y^{(d)}) - x^{(d)}\right)^2$$

Loss

$$x = f_{c_1,c_2,\ldots c_P}(y)$$

Inference

This is a data-driven solution.

dkfz.

Thank You!

This presentation will soon be available at www.dkfz.de/ct.

Job opportunities through DKFZ's international PhD or Postdoctoral Fellowship programs (www.dkfz.de), or directly through marc.kachelriess@dkfz.de.

Parts of the reconstruction software were provided by RayConStruct® GmbH, Nürnberg, Germany.